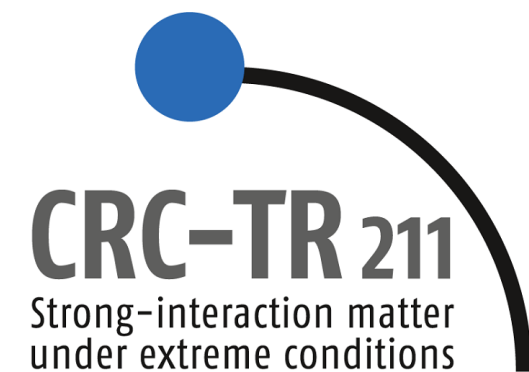


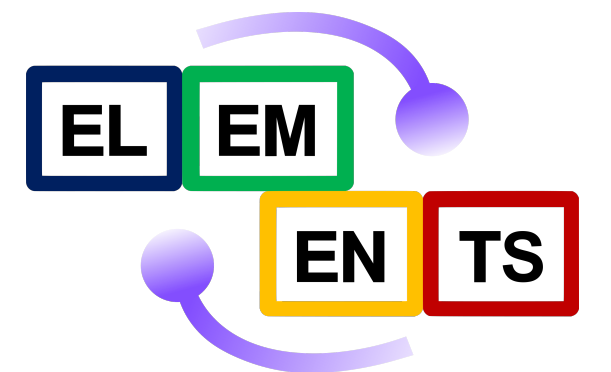
QCD thermodynamics: An overview of recent progress

Francesca Cuteri

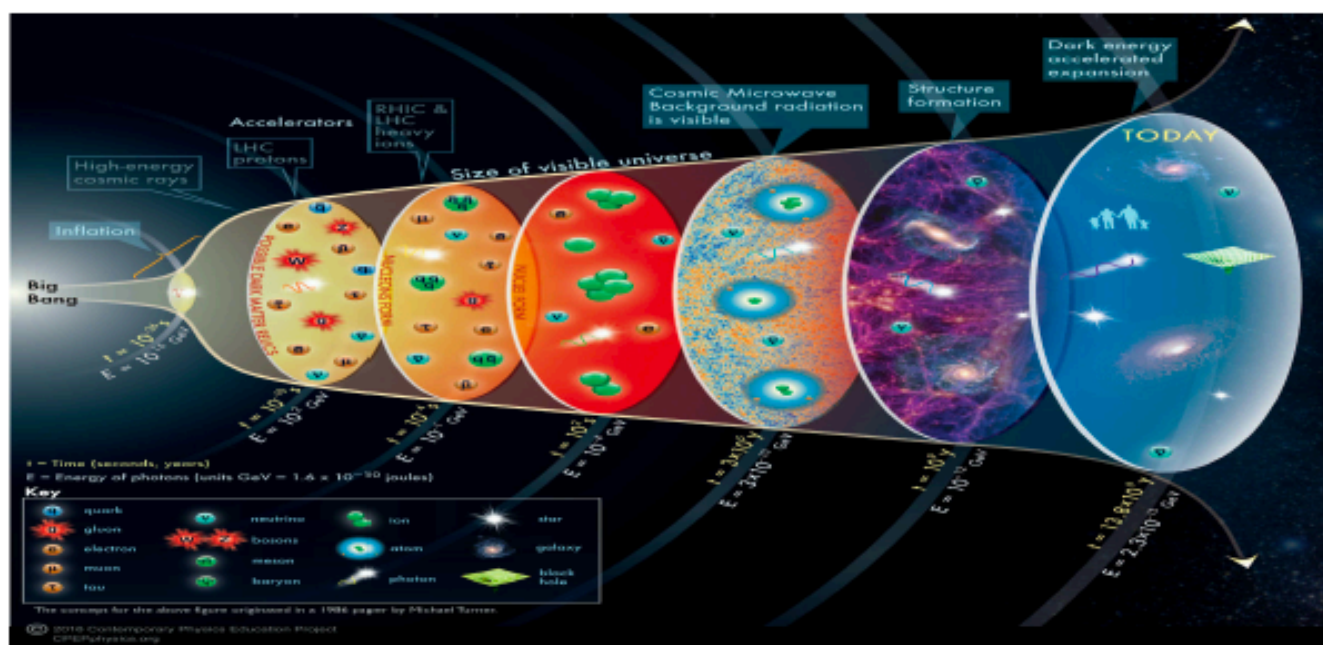
Goethe Universität - Frankfurt am Main



The 39th International Symposium on Lattice Field Theory
August 08, 2022



Hot/dense/magnetized states of QCD matter - The sketch



Early Universe (QCD epoch)

$$100\text{MeV} \lesssim T \lesssim 200\text{MeV}$$

$$b = (8.60 \pm 0.06) \times 10^{-11}, \quad q = 0$$

$$|I| = |I_e + I_\mu + I_\tau| < 0.012$$

$$B? \longrightarrow 10^{-16} \lesssim B \lesssim 10^{-9} \text{ Gauss (EGMFs)}$$

Hotter
“diluter”

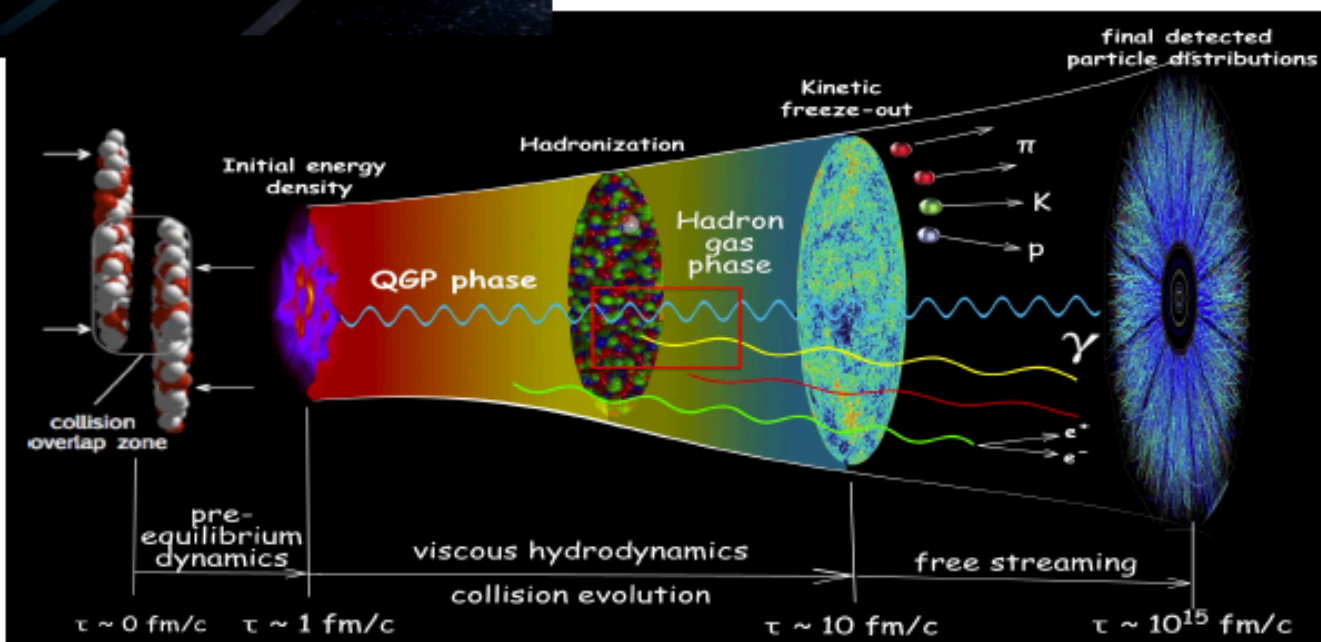
Heavy ion collisions (HIC)

$$50\text{MeV} \lesssim T \lesssim 200\text{MeV}$$

$$n \lesssim 0.12 \text{ fm}^{-3}$$

$$\delta = N - Z / (N + Z) \lesssim 0.25$$

$$B \lesssim 10^{19} \text{ Gauss} \sim 10^{20} B_{\text{Earth}}$$



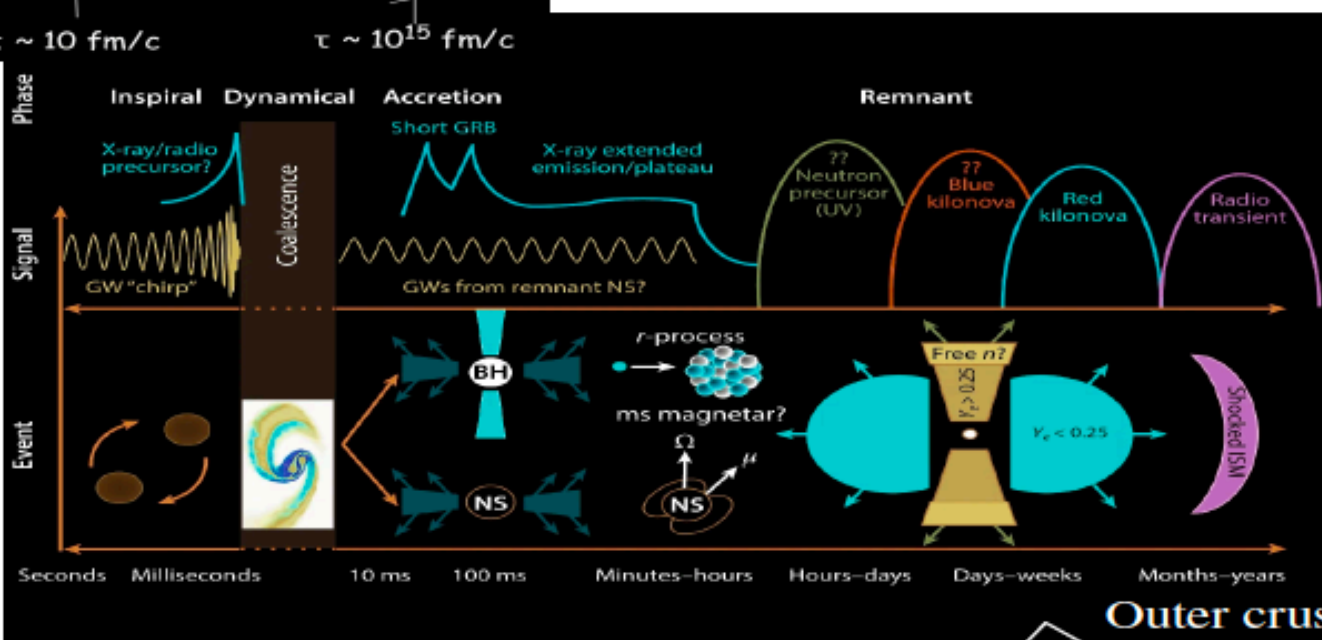
$$T \in [50, 80] \text{ MeV}$$

$$n \sim 2n_0, \quad n_0 = 0.16 \text{ fm}^{-3}$$

$$n_{\text{quark}} \neq 0$$

$$10^{10} \lesssim B \lesssim 10^{12} \text{ Gauss} \rightarrow B \gtrsim 10^{16} \text{ Gauss}$$

Binary Neutron Star (BNS) mergers



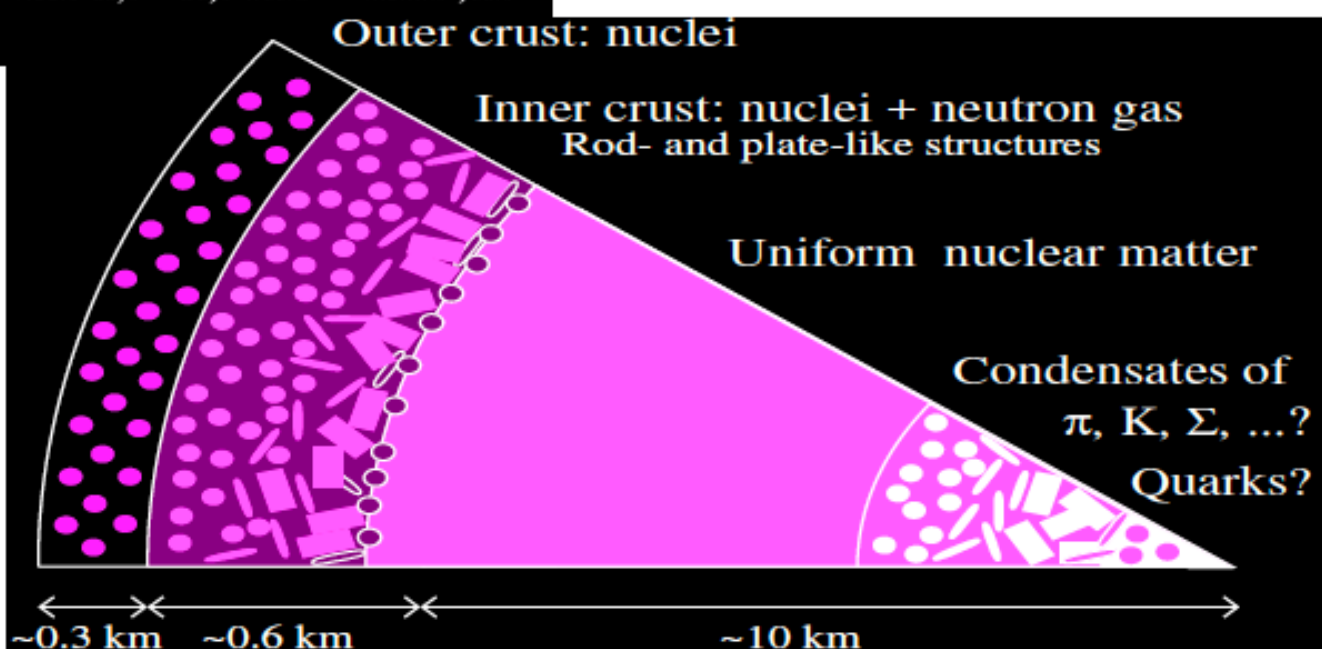
$$T \lesssim 1 \text{ KeV}$$

$$0.3n_0 \lesssim n \lesssim 15n_0, \quad n_0 = 0.16 \text{ fm}^{-3}$$

$$n_p/n \sim 0.04, \quad \text{at } n_0$$

$$10^8 \lesssim B \lesssim 10^{15} \text{ Gauss}$$

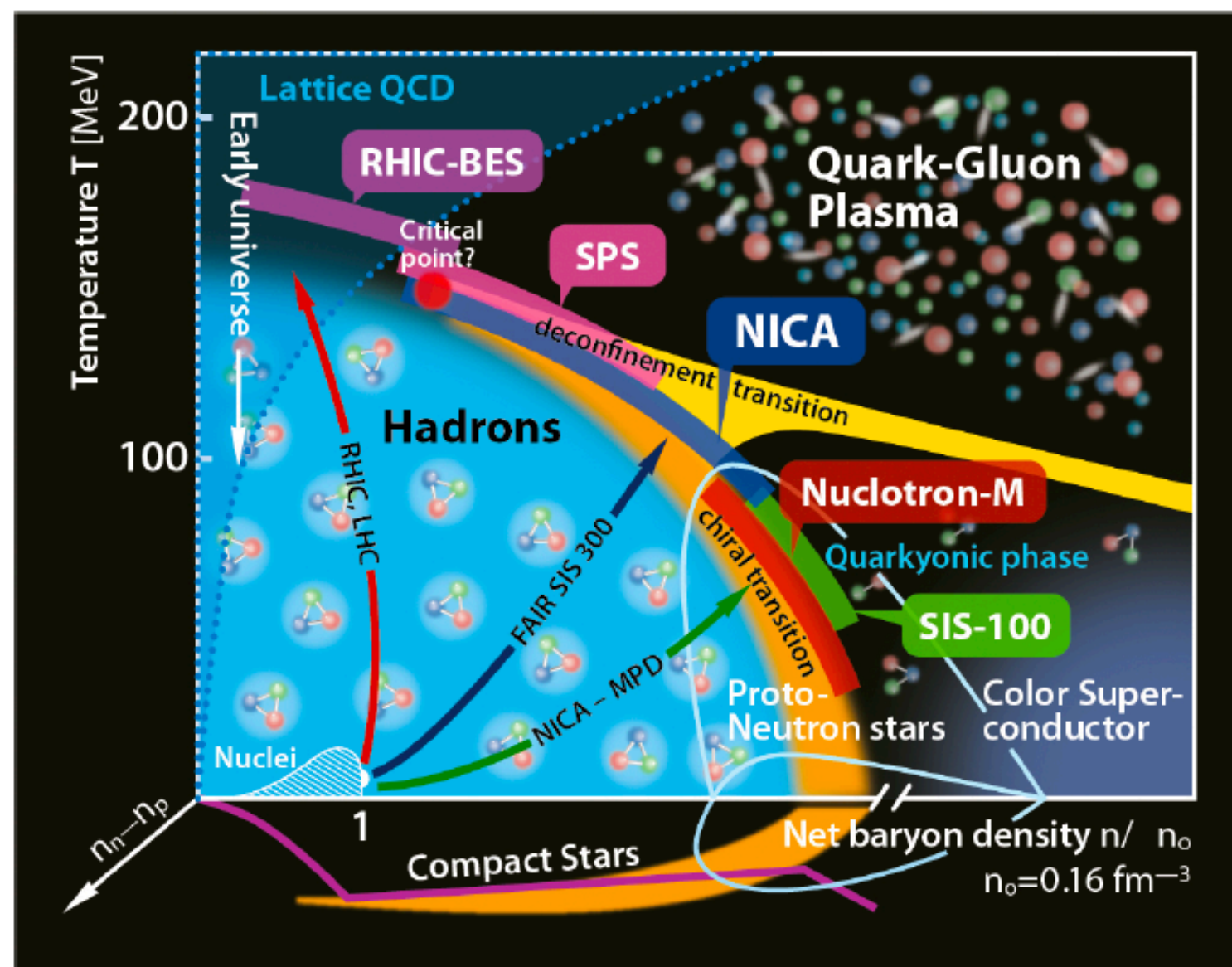
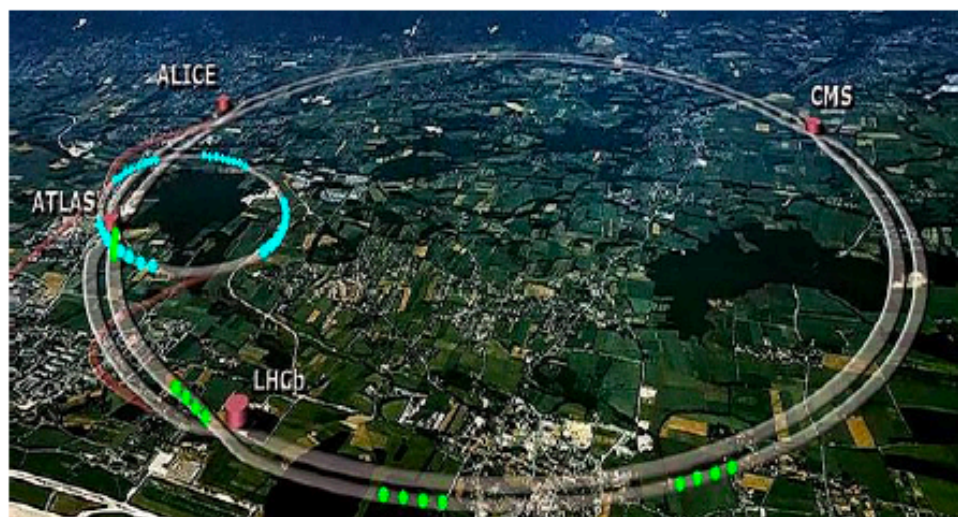
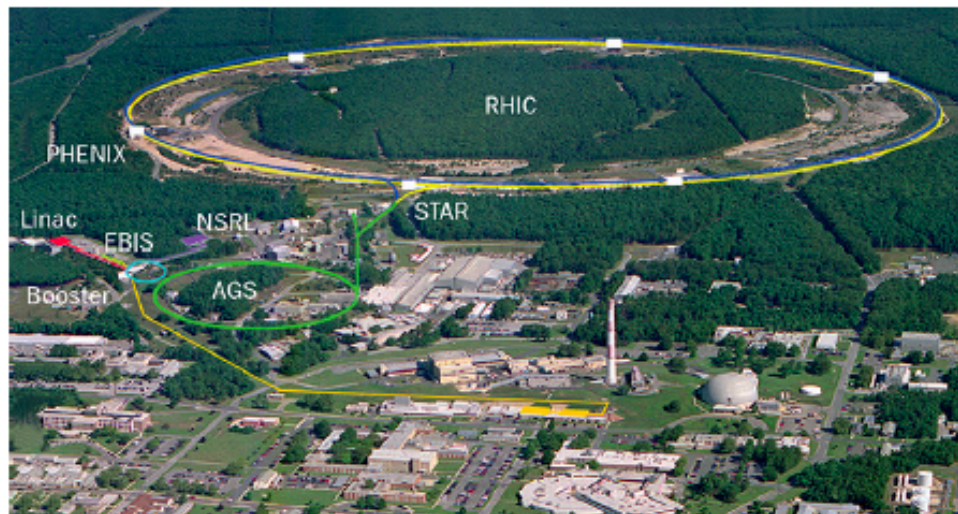
Neutron star interior



Colder
denser

$$1\text{eV} \approx 12 \times 10^3 \text{ K}; \quad B_{\text{Earth}} \approx 0.5 \text{ Gauss}$$

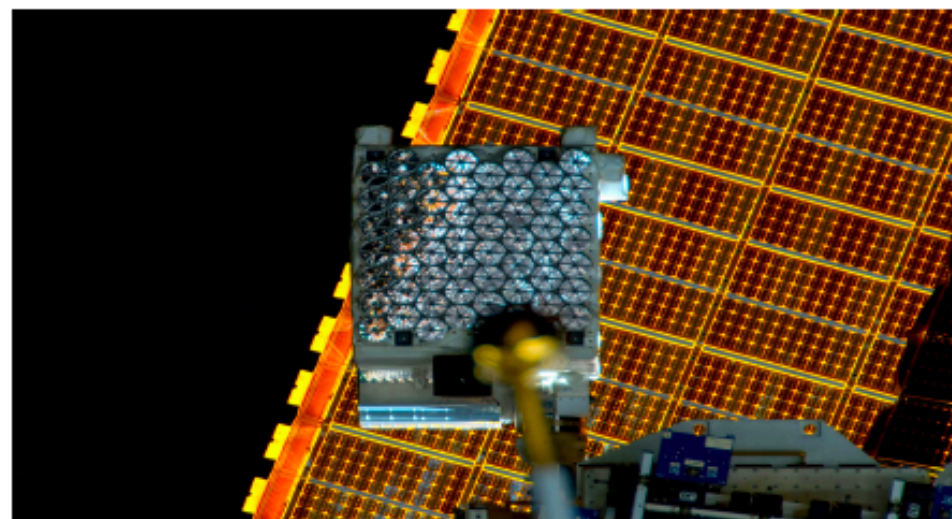
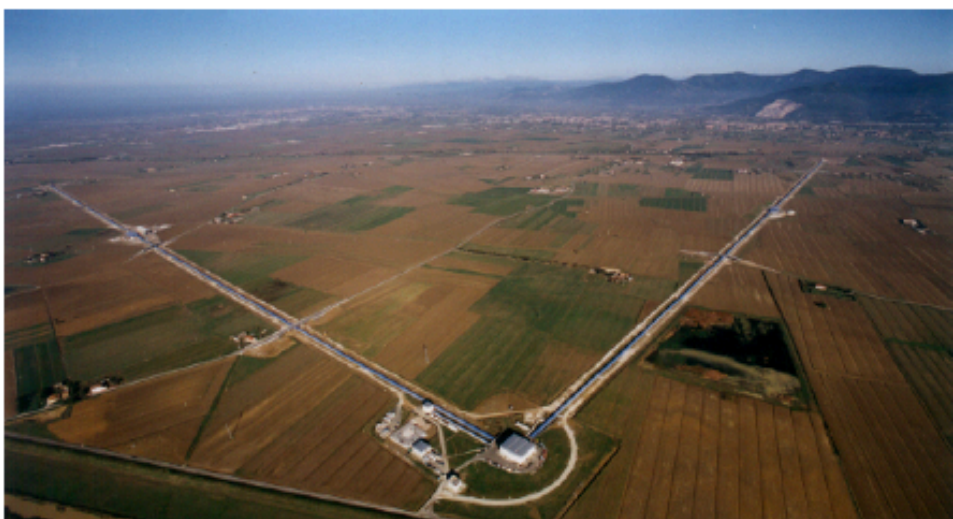
Major experimental and observational campaigns, besides theoretical motivations



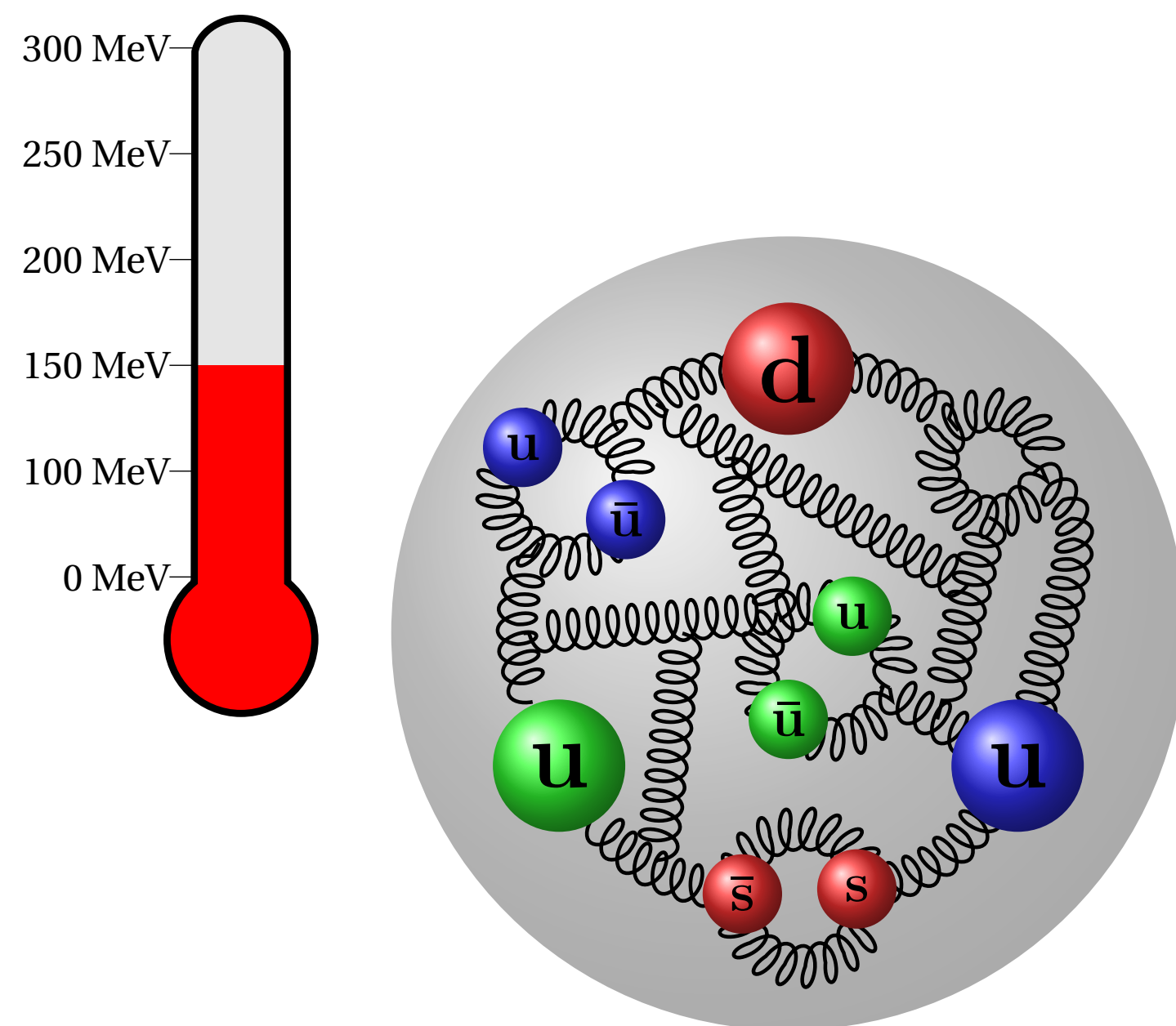
Observational astronomy



Heavy ion collisions



Nonzero temperature

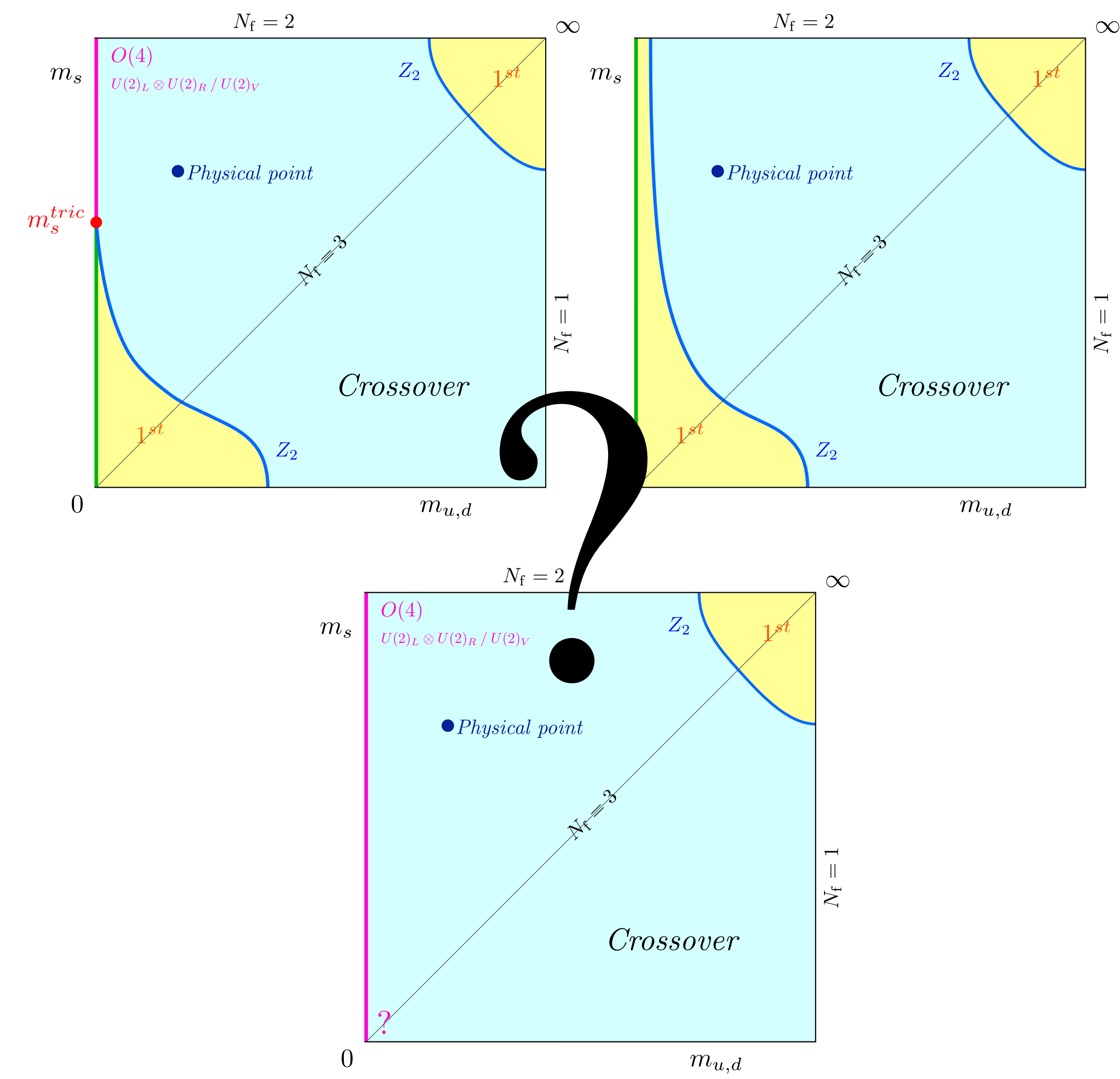


- ▶ The thermal crossover/transition
- ▶ Thermal effects on hadrons
- ▶ From the hadronic to the QGP phase: correlators, screening masses, spectral functions
- ▶ Transport properties
- ▶ Topological features

Reka Agnes Vig, Tue 15:40

Tamas G. Kovacs, Wed 17:30

The thermal crossover/transition as a function of the flavor content (light masses)

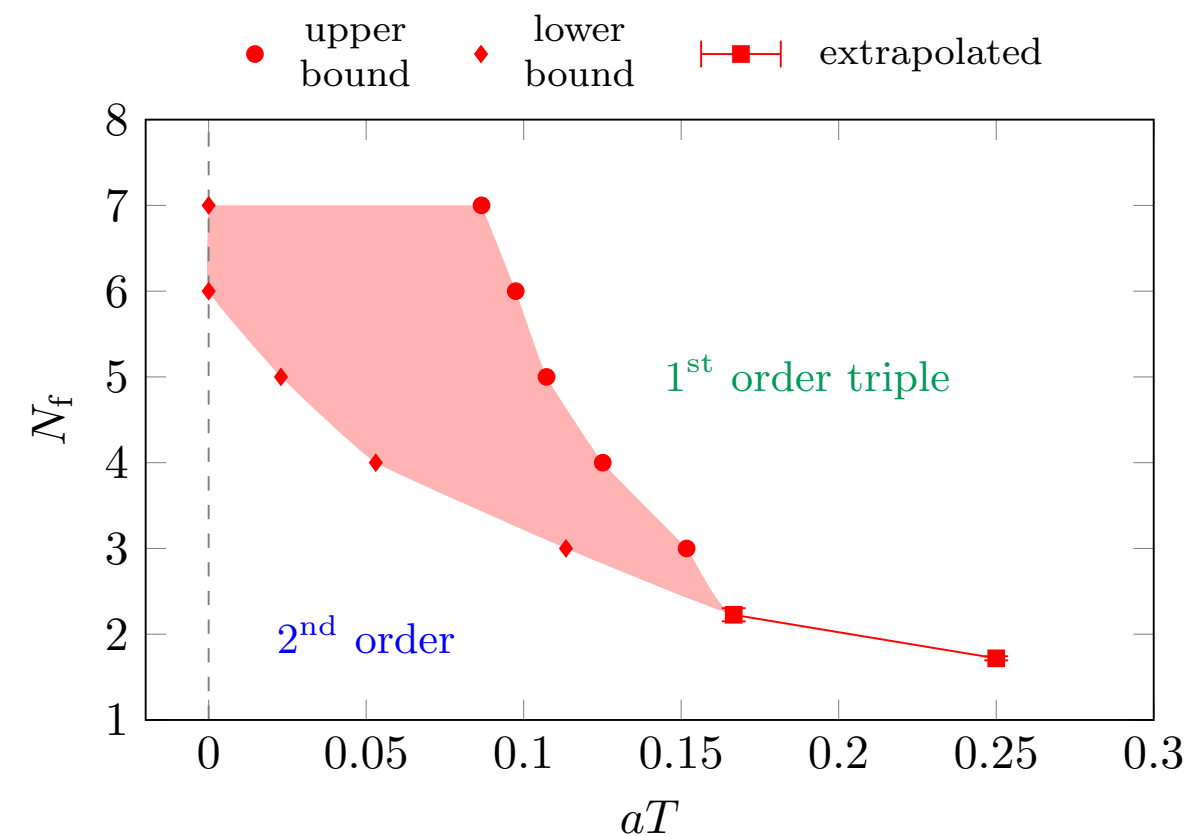
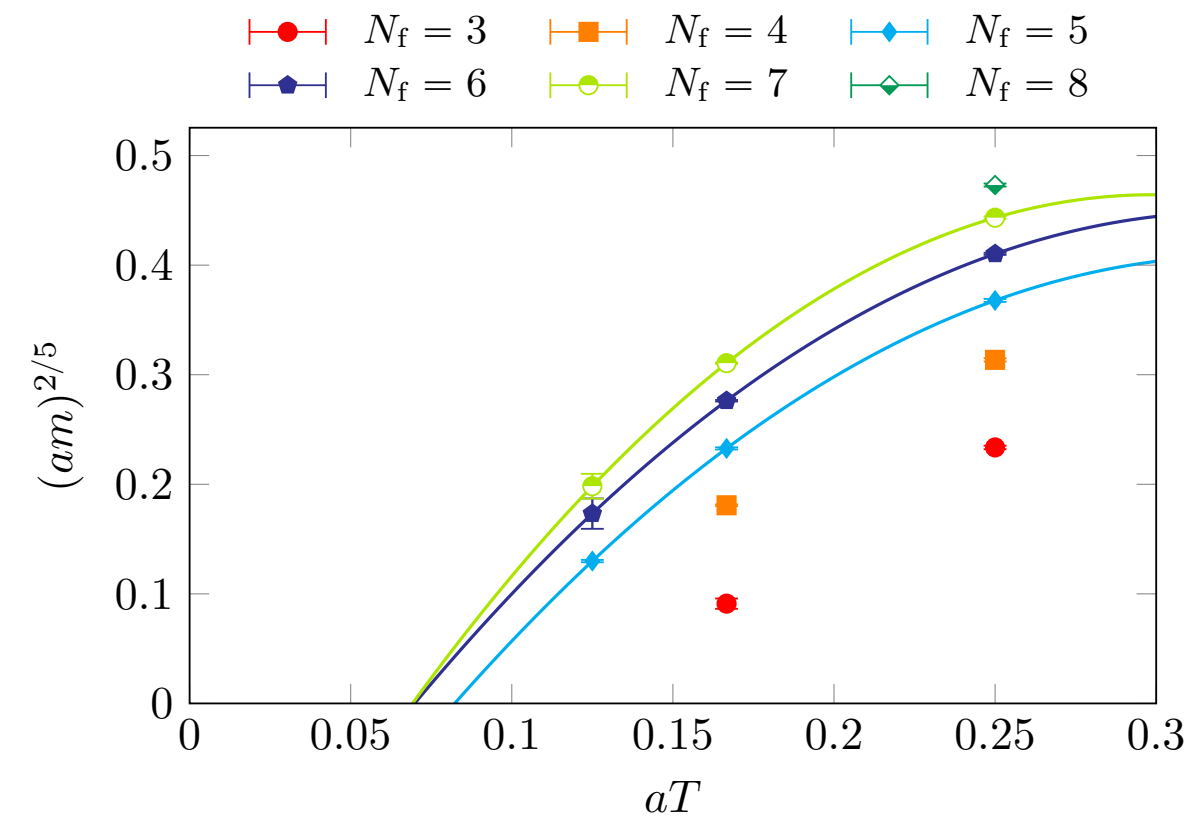
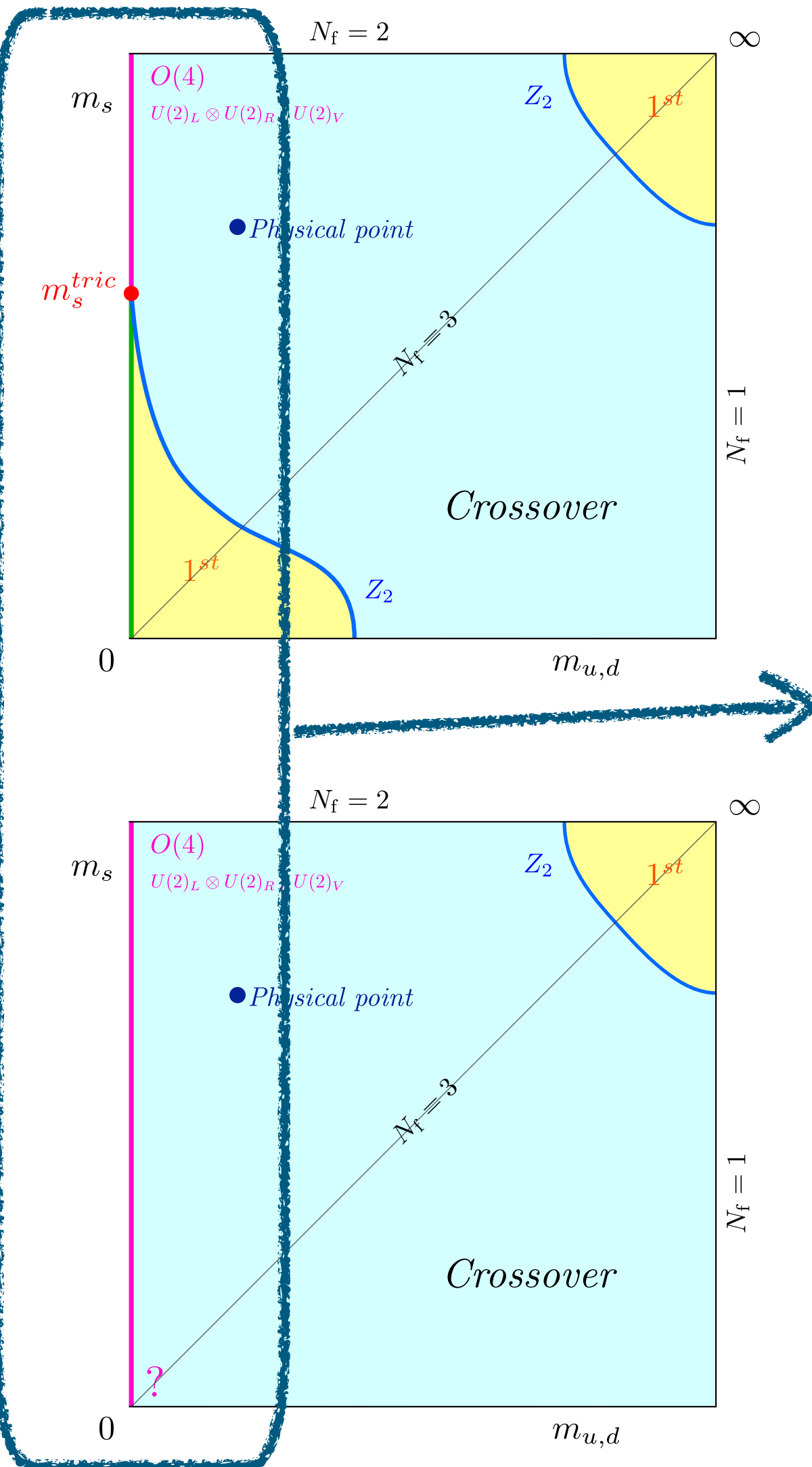


N_f	Action	N_τ	$m_\pi^{Z_2}$ [MeV] at $\mu = 0$	Ref.
3	clover	6-8		Jin et al. (2015)
	clover	8-10		Jin et al. (2017)
	clover	10-12		Kuramashi et al. (2020)
2	std	4		Philipsen, Pinke (2016)
	tm	12		tftM coll. (2013)
	clover	16		Brandt et al. (2017)

N_f	Action	N_τ	$m_\pi^{Z_2}$ [MeV] at $\mu = 0$	Ref.
3	std	4		Karsch, Laermann, Schmidt (2001)
	std	4		Christ, Liao (2003)
	std	6		de Forcrand, Kim, Philipsen (2007)
	p4	4		Karsch et al. (2004)
2	HISQ	6		Bazavov et al. (2017)
	std- μ_i	4		Bonati et al. (2014)

The thermal crossover/transition as a function of the flavor content

Columbia plot: Light masses



[Cuteri, Philipsen, Sciarra '21 \(JHEP\)](#)

Evidence for continuum chiral limit to feature 2^{nd} order transitions for $N_f \in [2 - 7]$

staggered unimproved $N_\tau \in [4 - 8]$ & reanalysis of $N_f = 3$ clover Wilson at $N_\tau \in [4 - 12]$

Thermal transition with Möbius domain wall fermions

- ▶ $N_f = 3$, to locate Z_2 boundary
 - Crossover at $m_q^{\overline{MS}}(2 \text{ GeV}) \sim 40 \text{ MeV}$, for $T_{pc} \sim 196 \text{ MeV}$
 - Transition at $m_q^{\overline{MS}}(2 \text{ GeV}) \sim 4 \text{ MeV}$, for $T_{pc} \sim 131 \text{ MeV} ??$
- ▶ $N_f = 2 + 1$, near the physical point
 - Dealing with residual chiral symmetry breaking by $m_{res} > \bar{m}_{ud}$
 - First results at $N_\tau \in \{12, 16\}$

... Yu Zhang, Tue 14:20, ... Yasumichi Aoki, Fri 16.40

... Issaku Kanamori, Fri 17.00

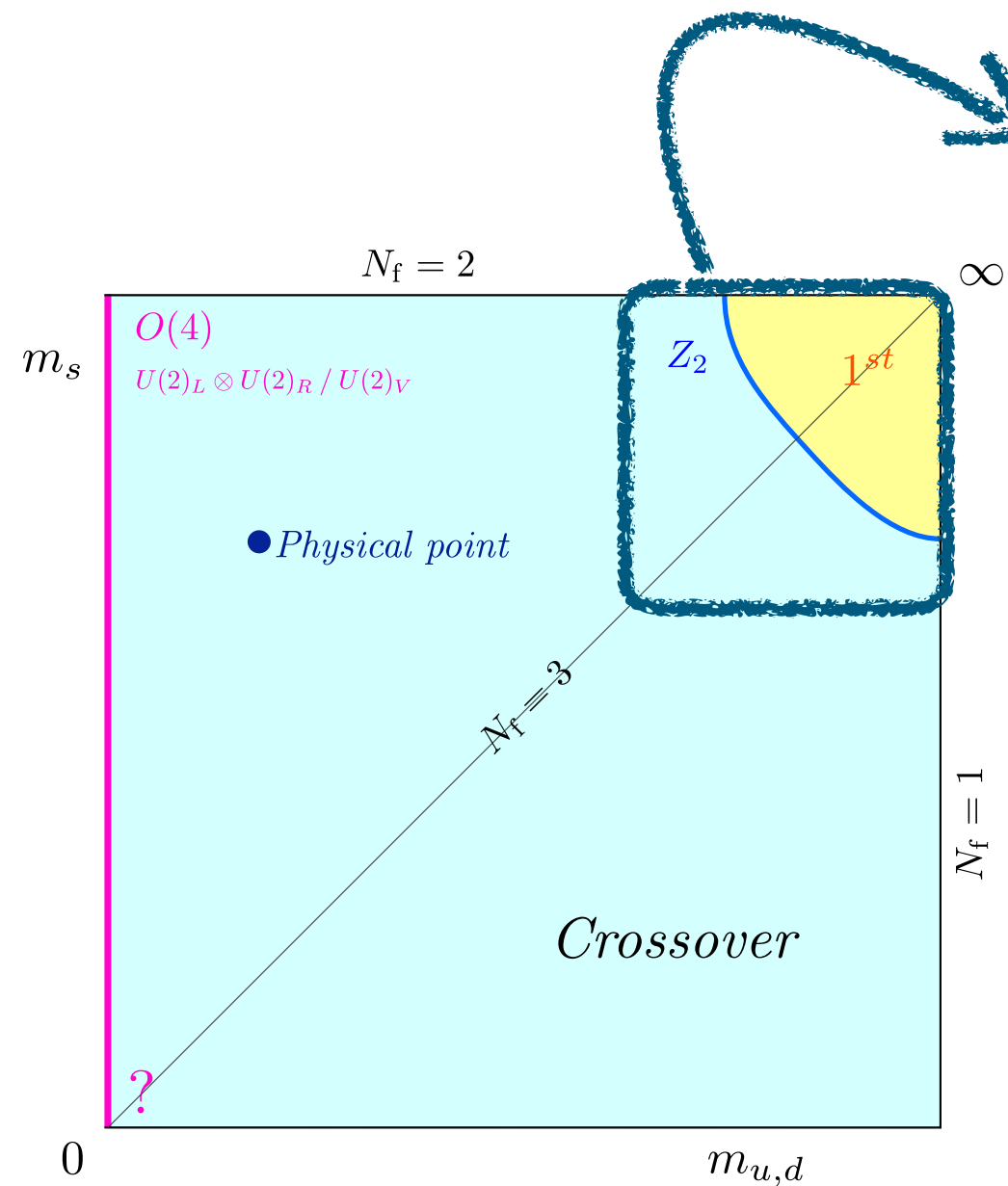
[Nakamura et al '22 \(PoSLAT21\)](#)

Larger 1^{st} order triple regions in the Roberge-Weiss plane

- ▶ HISQ fermions with $N_\tau = 4$ [Cuteri et al '22 \(PRD\)](#)
 - RW endpoint 2^{nd} order for $m_{ud} \geq m_s/320$
 - In the chiral limit $T_\chi = T_{RW} = 195(1) \text{ MeV}$
- ▶ Unimproved staggered with $N_\tau = 4$ at nonzero imaginary μ_I, μ_B
 - Even larger 1^{st} order region at $N_f = 2$ [Brandt et al '22](#)
- ▶ Localization properties of Dirac modes [Cardinali et al '22 \(PRD\)](#)
- ▶ Larger N_f values [Alfredo D'Ambrosio, Tue 15:00](#)

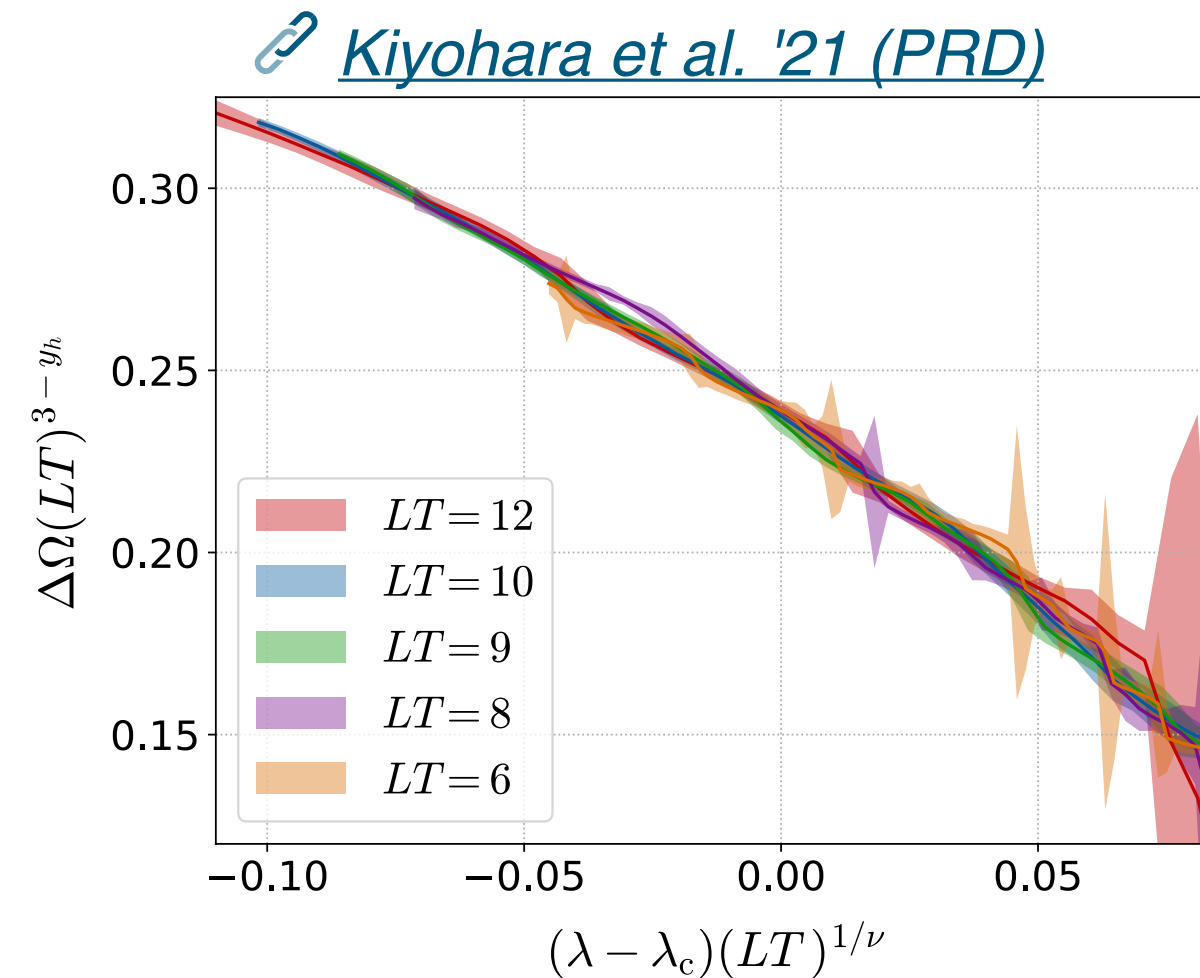
The thermal crossover/transition as a function of the flavor content

Columbia plot: Heavy masses



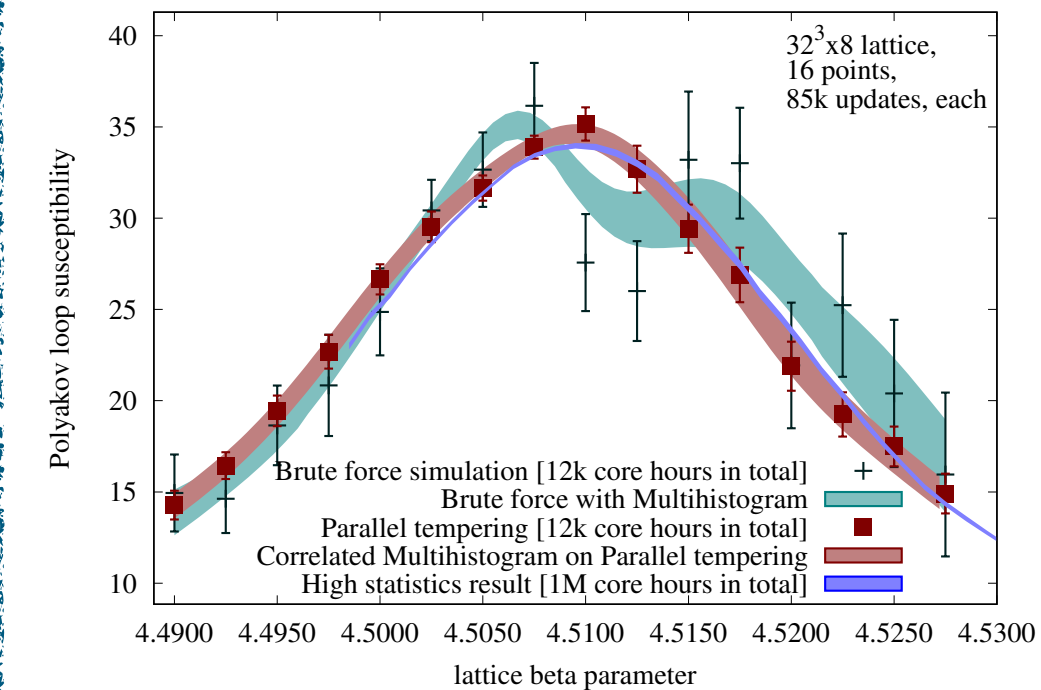
Deconfinement Z_2 boundary

- ▶ $N_f = 2$ unimproved staggered at $N_\tau \in \{8, 10\}$
[Kaiser, Philipsen, Sciarra '22 \(PoSLAT21\)](#)
 - Exploring possibility to develop a Ginzburg-Landau effective theory around the Z_2 -critical point
Reinhold Kaiser, Tue 14:40
- ▶ $N_f \in \{1, 2, 3\}$ Wilson with hopping parameter expansion
 - LO reliable for $N_\tau = 4$, method to include needed higher-order terms for $N_\tau \geq 6$
 - Distribution function of the real part of the Polyakov loop consistent with Z_2 FSS at smaller N_σ/N_τ than B_4
Kazuyuki Kanaya, Wed 14:00



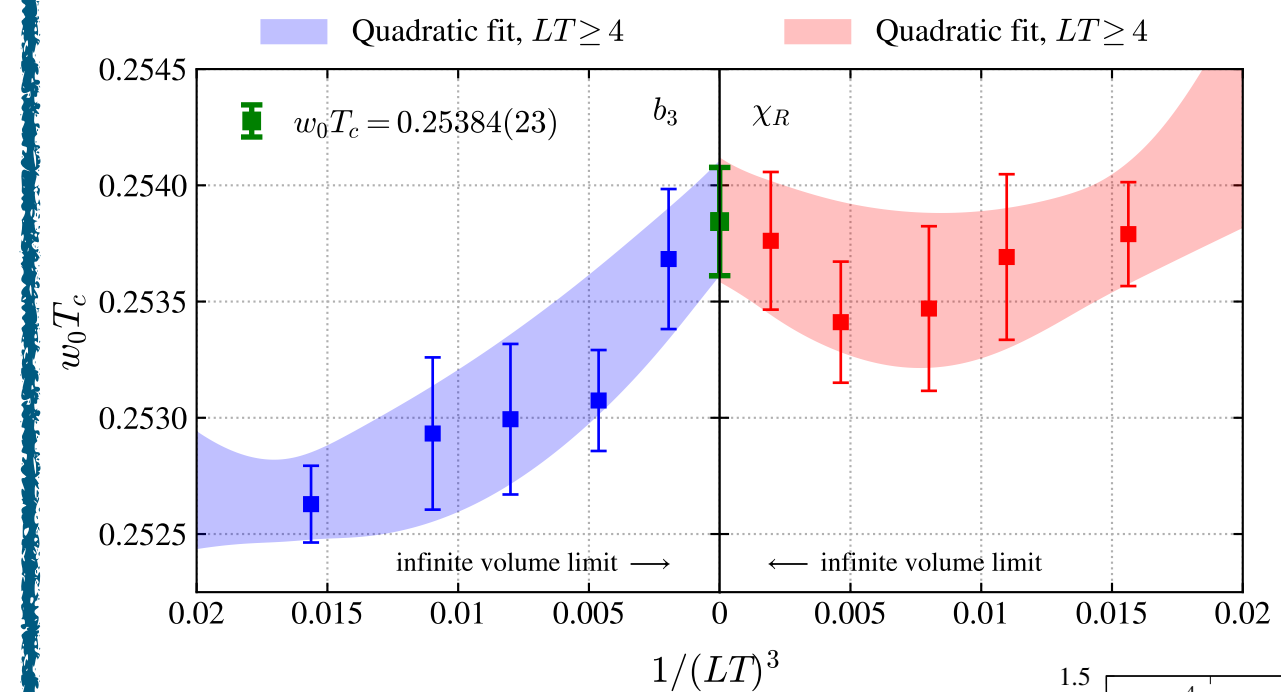
Reducing autocorrelations with parallel tempering

[Borsanyi et. al '22 \(PRD\)](#)



- ▶ Allows swap updates between simultaneous calculations at different T
- ▶ Can be extended to m , μ or other parameters of the fermionic action
- ▶ Employed for ergodic sampling of Q_{top} using the density of states
[Cossu et. al '21 \(EPJc\)](#)

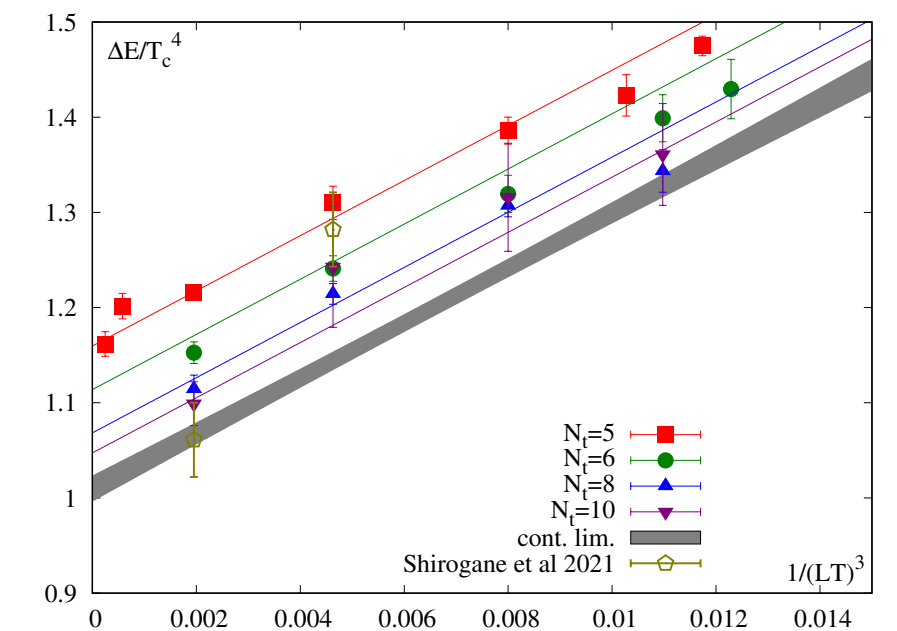
Quenched QCD: 1st order transition in the continuum



- $w_0 T_c = 0.25384(23)$ first per-mille accurate result in thermodynamics

- latent heat understood as the discontinuity of the trace anomaly, $(\epsilon - 3p)/T^4$, as the transition is crossed

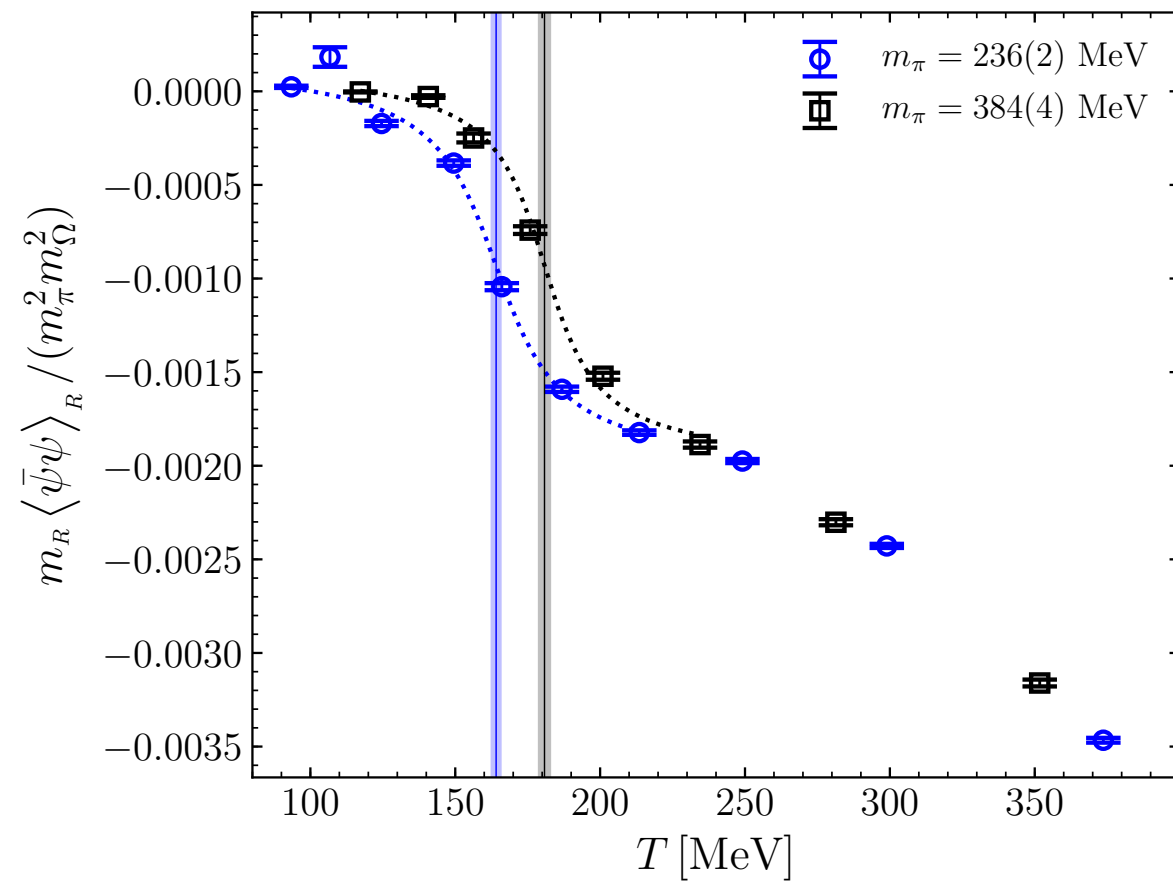
[Ruben Kara, Tue 15:20](#)



Thermal effects on hadrons

“Generation 2L” FASTSUM anisotropic, clover $N_f = 2 + 1$

a_τ [fm]	a_τ^{-1} [GeV]	$\xi = a_s/a_\tau$	a_s [fm]	m_π [MeV]	$T_{pc}^{\psi\psi}$ [MeV]
0.03246(7)	6.079(13)	3.453(6)	0.1121(3)	239(1)	167(2)(1)



- ▶ T varied in fixed-scale approach
- ▶ T_c shifted by ~ 20 MeV when m_π goes from 390 to 240 MeV

[Aarts et al. '22 \(PRD\)](#)

Bottomonium & interquark bottomonium potential

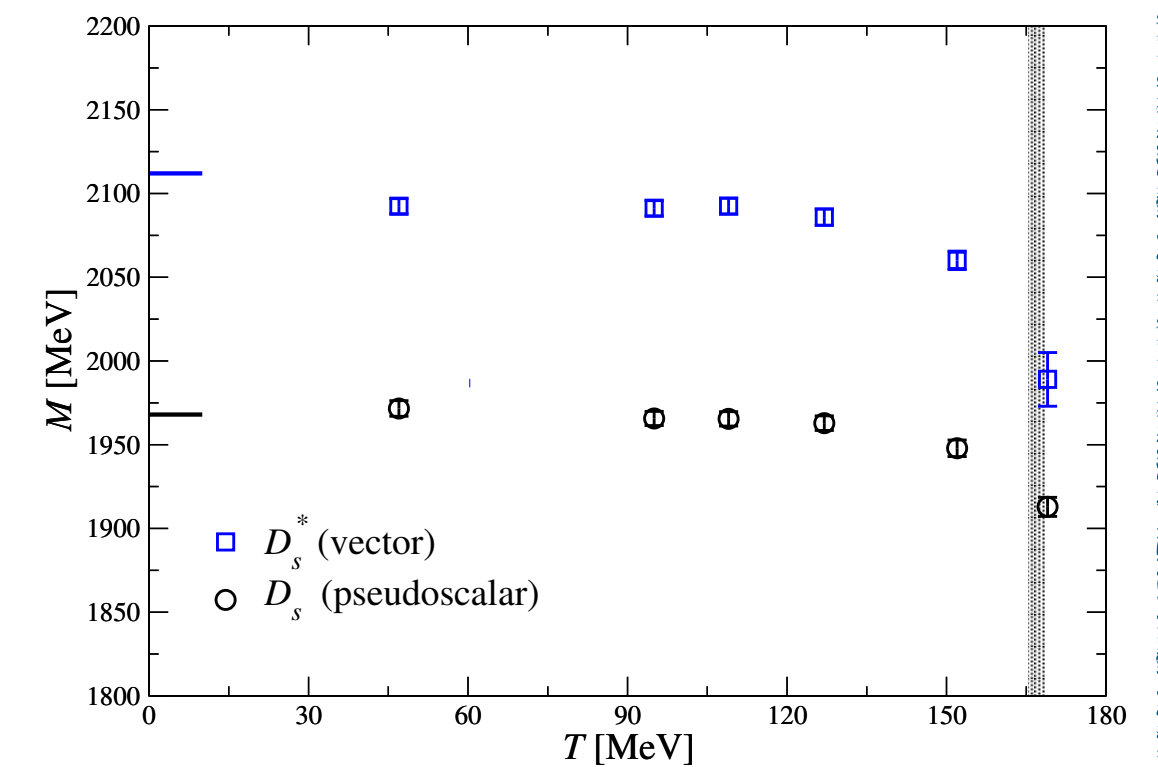
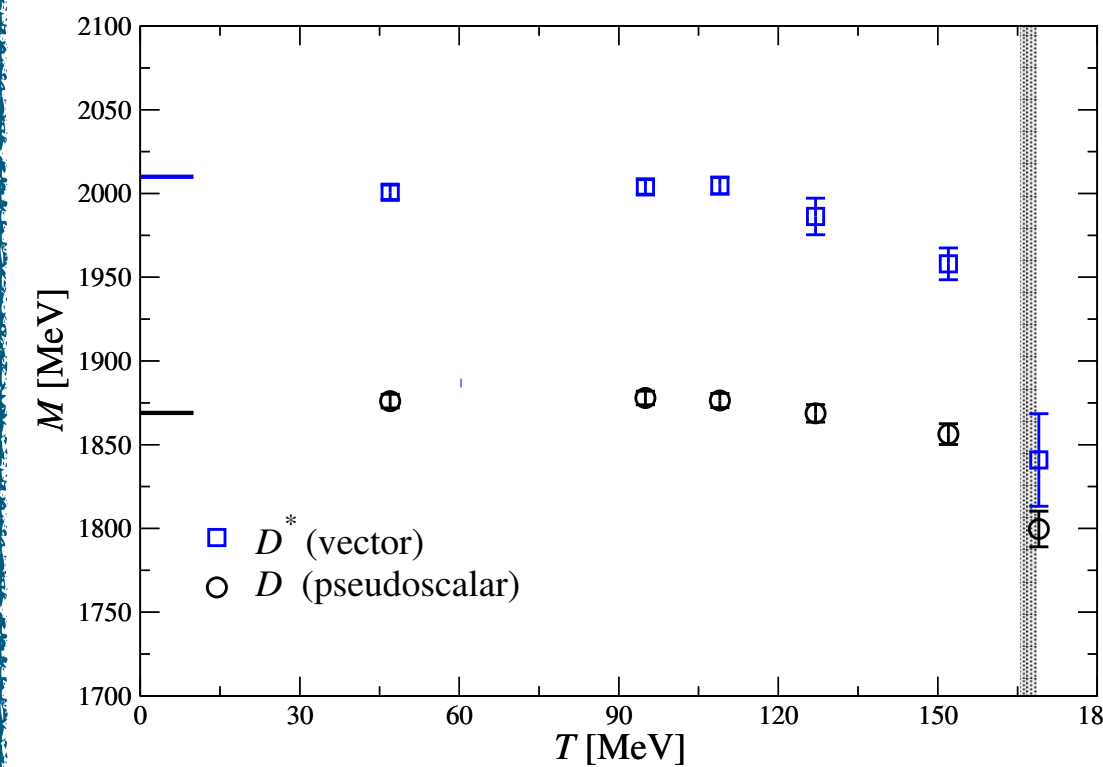
- ▶ Backus-Gilbert method for reconstructing spectra of NRQCD bottomonia
 - Results for the η_b , Υ and χ_{b1} generated from Tikhonov-regularized Backus-Gilbert coefficient sets.
- ▶ Thermal interquark potential of bottomonium using the HAL QCD method with NRQCD quarks

[Spriggs et al. '22 \(PoS LAT21\)](#)

Ben Page, Wed 14:20, Thomas Spriggs, Wed 14:40

Charmed baryons & mesons at $T > 0$ in the hadronic phase

- ▶ First systematic study throughout hadronic phase of D and D_s masses (PS & V channels)
 - Groundstate mass at T_{\min}
 - T effects, by ratios of correlators (no fitting/spectral reconstruction), at the percentage level



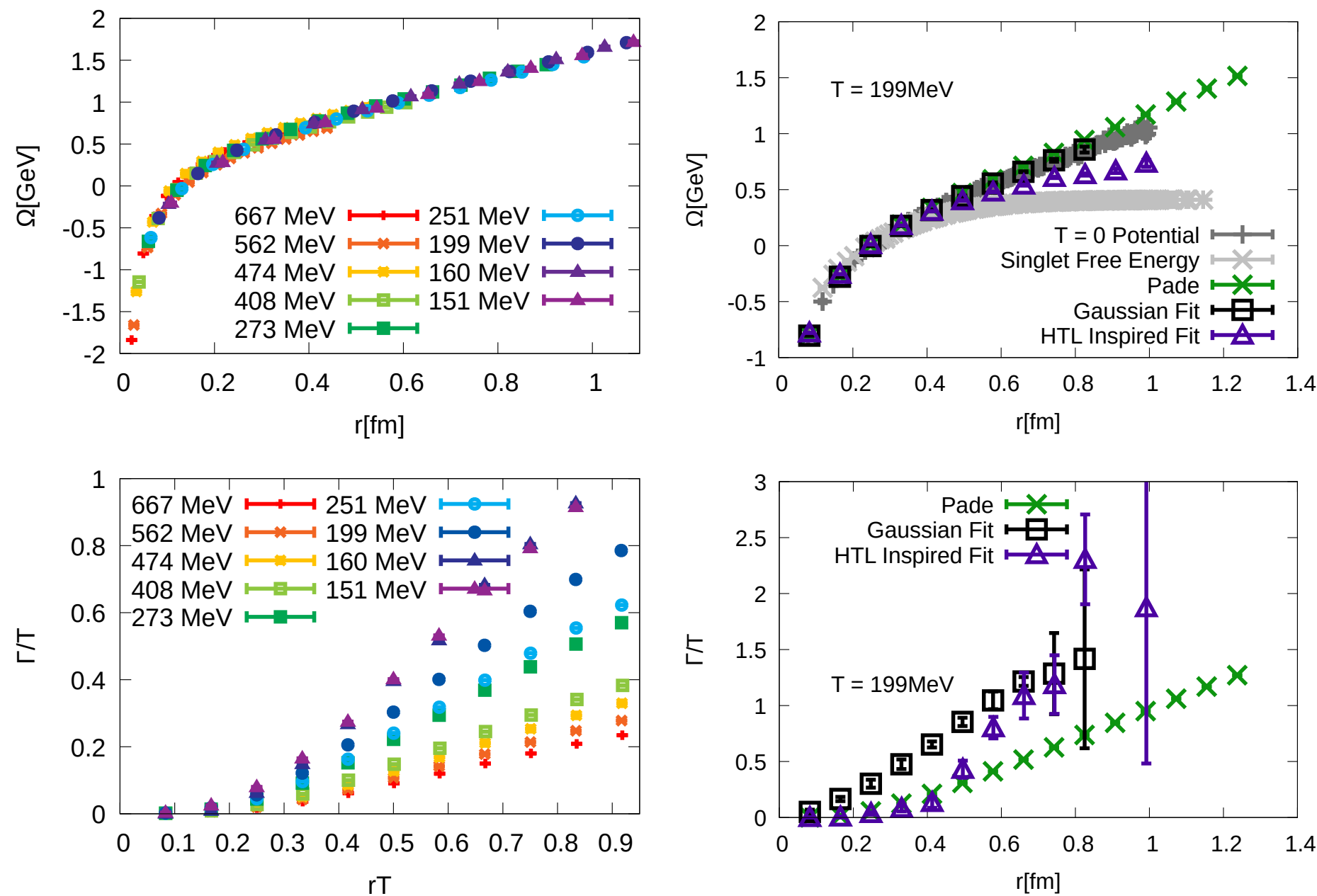
- ▶ Singly-, doubly- and triply-charmed baryons: Spectrum in both parity channels and investigating parity doubling due to the restoration

Chris Allton, Wed 16:30, Ryan Bigneli, Wed 16:50

From the hadronic to the QGP phase: correlators, screening masses, spectral functions

Complex static potential at nonzero T , with $N_f = 2 + 1$ HISQ

- ▶ Wilson line correlators in Coulomb gauge [Bala et al. '22 \(PRD\)](#)
- ▶ Spectral functions with different methods: fits, HTL inspired fit, Padé rational approximation, Bayesian reconstruction, ...
- General qualitative feature: Dominant peak in spectral function
 - Position Ω is $\Re V_S^{(0)}$: It is T -independent, shows no screening
 - Effective width Γ/T is $\Im V_S^{(0)}$: It has strong T dependence



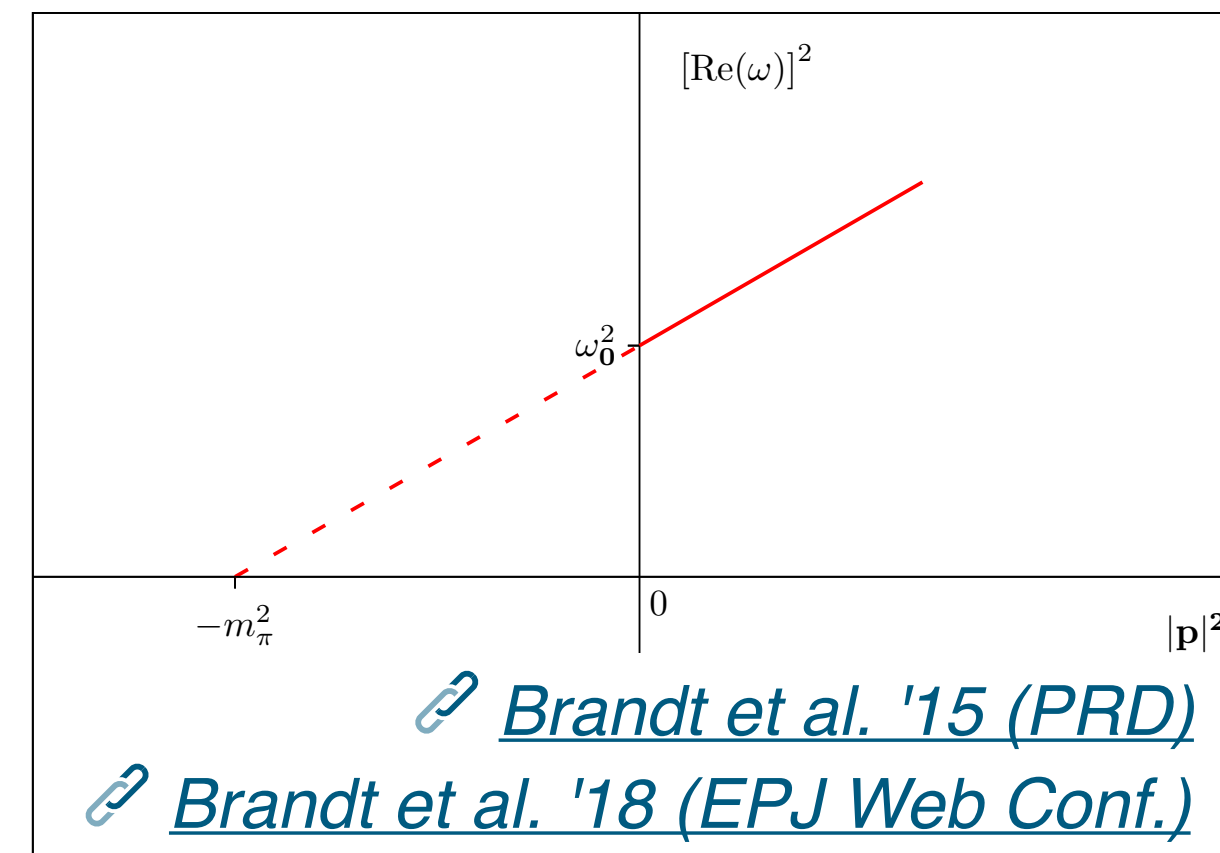
UPDATE: $m_S^{\text{phys.}}$, m_l such that $m_\pi = 310$ MeV on $96^3 \times N_\tau$ lattices with $1/a = 7.1$ GeV and $T \in [127 - 354]$ MeV [Gaurang Parkar, Tue 17:50](#)

Charm and beauty in QGP, with $N_f = 2 + 1$ $\mathcal{O}(a)$ -impr. Wilson on HISQ

Correlators & spectral functions in the PS channel using physical valence quark masses

[Sajid Ali, Wed 15:40](#)

Pion quasiparticle, with $N_f = 2 + 1$ $\mathcal{O}(a)$ -impr. Wilson



$m_\pi(T = 0)$ 'splits' at nonzero T

- ▶ Lower pion quasiparticle mass ω_0 : Real part of pole of $G_R(\omega, |\vec{p}| = 0)$ of the PS density in ω
- ▶ Higher static screening mass (inverse spatial correlation length): Pole of $G_R(\omega = 0, \vec{p})$ of the PS density in $|\vec{p}|$

UPDATE: $N_f = 2 + 1$, physical quark masses, lower $T = 128$ MeV

- ▶ $\omega_0 = 111(3)$ MeV sensibly reduced w.r.t. $m_\pi(T = 0) = 130(1)$ MeV
- ▶ f_π^t changes little w.r.t. $T = 0$ decay constant
- ▶ static screening mass $m_\pi = 143(3)$ MeV increases with T
- ▶ chiral symmetry breaking/restoration via difference of the vector- and axialvector spectral functions

[Ardit Krasniqi, Fri 15:50](#)

From the hadronic to the QGP phase: correlators, screening masses, spectral functions

Exploring QCD up to the electroweak scale

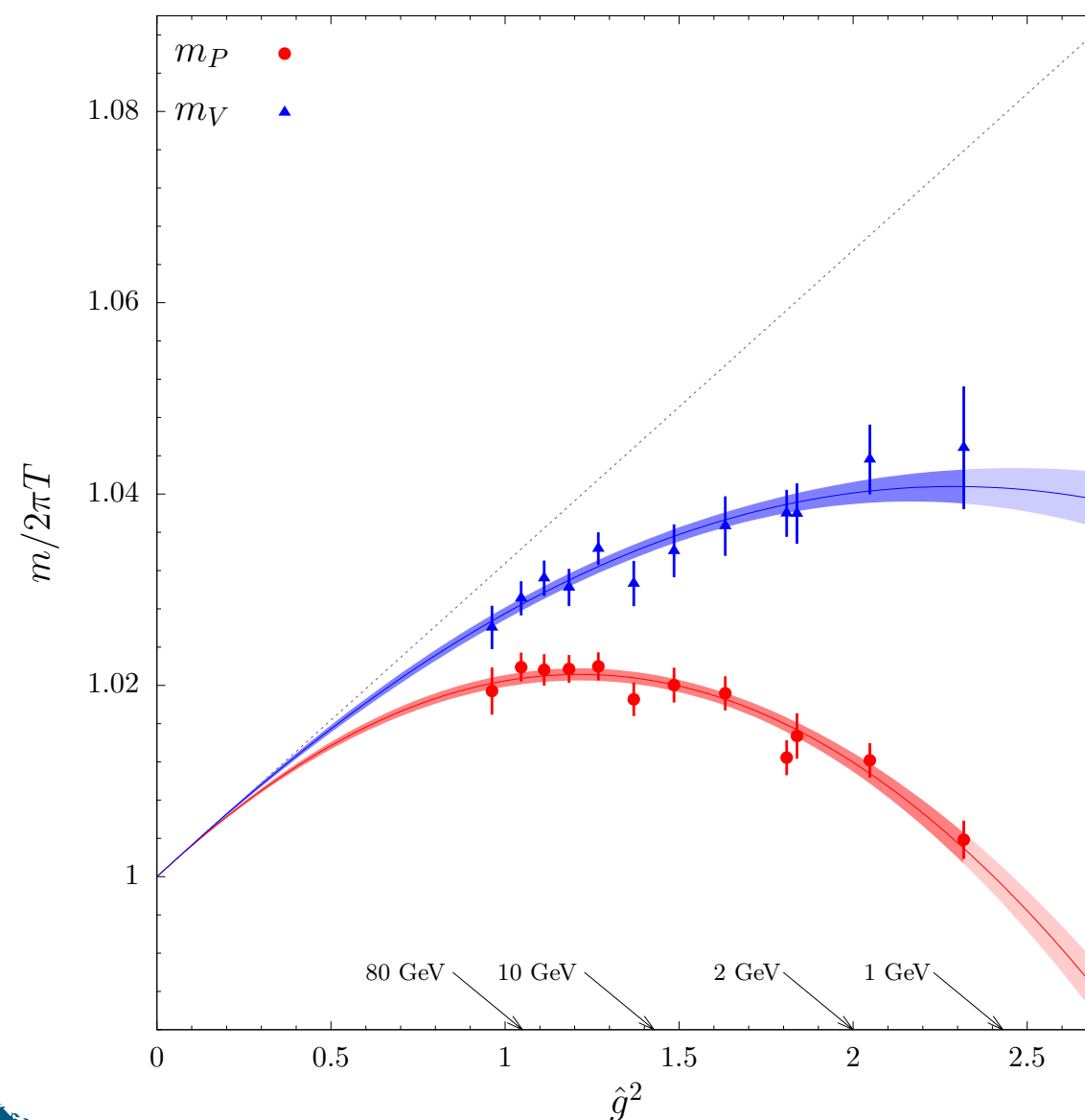
[Dalla Brida et al. '22 \(JHEP\)](#)

QCD non-perturbatively on the lattice even at very high temperatures

- ▶ Large range of temperatures from $T \sim 1$ GeV up to $T \sim 160$ GeV, thanks to scale-setting strategy that
 - Exploits non-perturbative, finite-volume, definition of the strong coupling constant to renormalize the theory
 - Employs step scaling techniques

Enables extended comparison with perturbation theory!

Flavor non-singlet meson screening masses (I)...

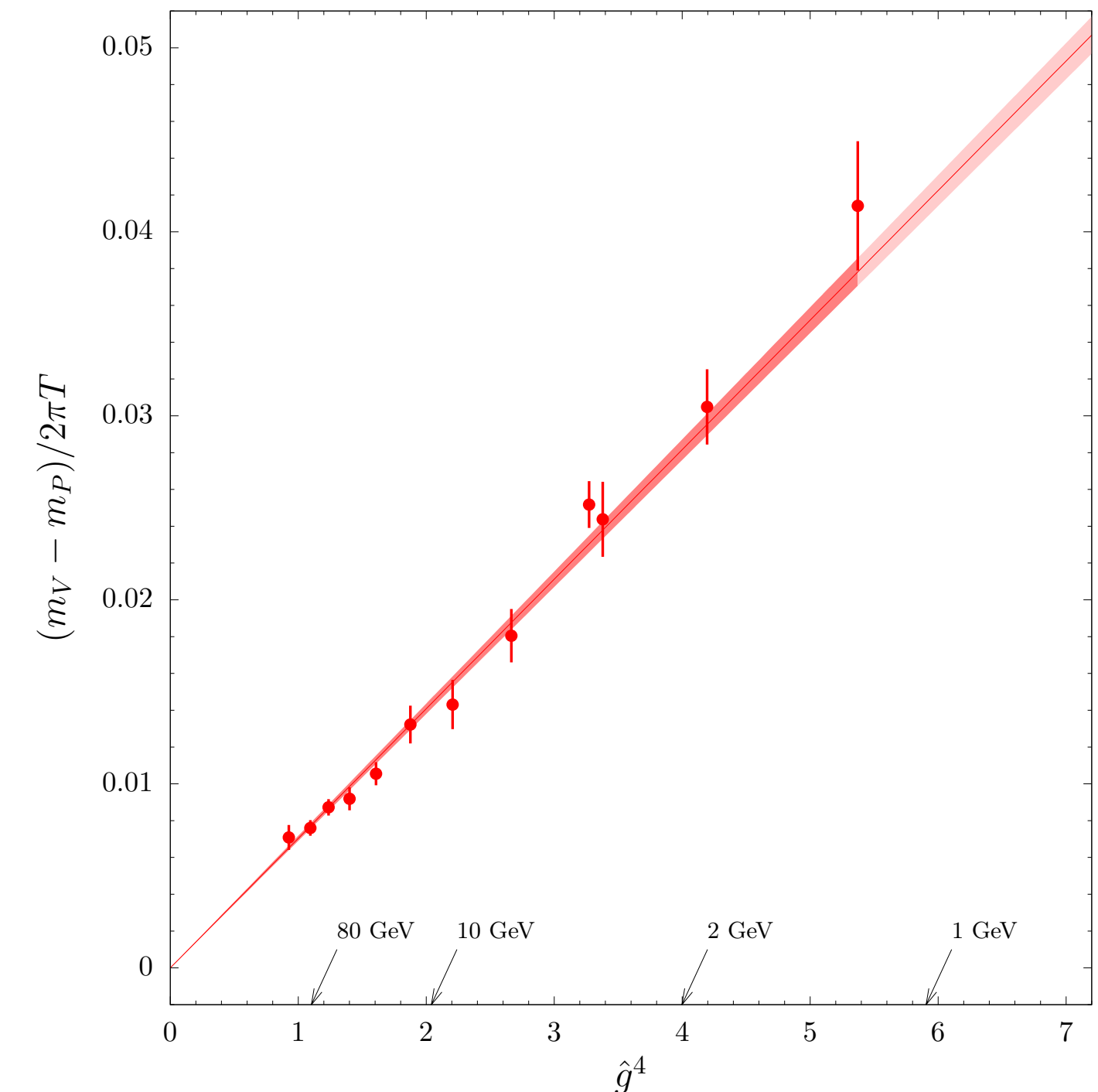


...in QCD with $N_f = 3$ massless quarks, for $T \in [1 - 160]$ GeV

- ▶ T -dependence of PS- and V-screening masses (normalized to their free value) compared to NLO-PT
- Large relative corrections to the perturbative result even at the electroweak scale

Flavor non-singlet meson screening masses (II)...

...in QCD with $N_f = 3$ flavors of massless quarks, for $T \in [1 - 160]$ GeV

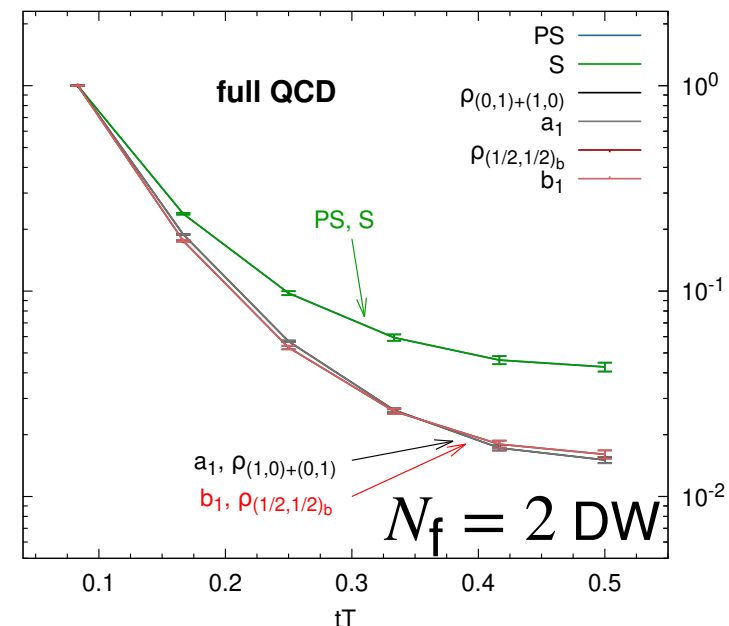


- ▶ Splitting between V and PS screening masses
 - Non-negligible up to EW scale, due to higher order effects not explained by NLO-PT
- ▶ Chiral symmetry restoration, instead, manifests itself through the degeneracy of the PS and the S channels and of the V and the A ones.

From the hadronic to the QGP phase: correlators, screening masses, spectral functions

Emergent chiral spin symmetry and the QCD phase diagram

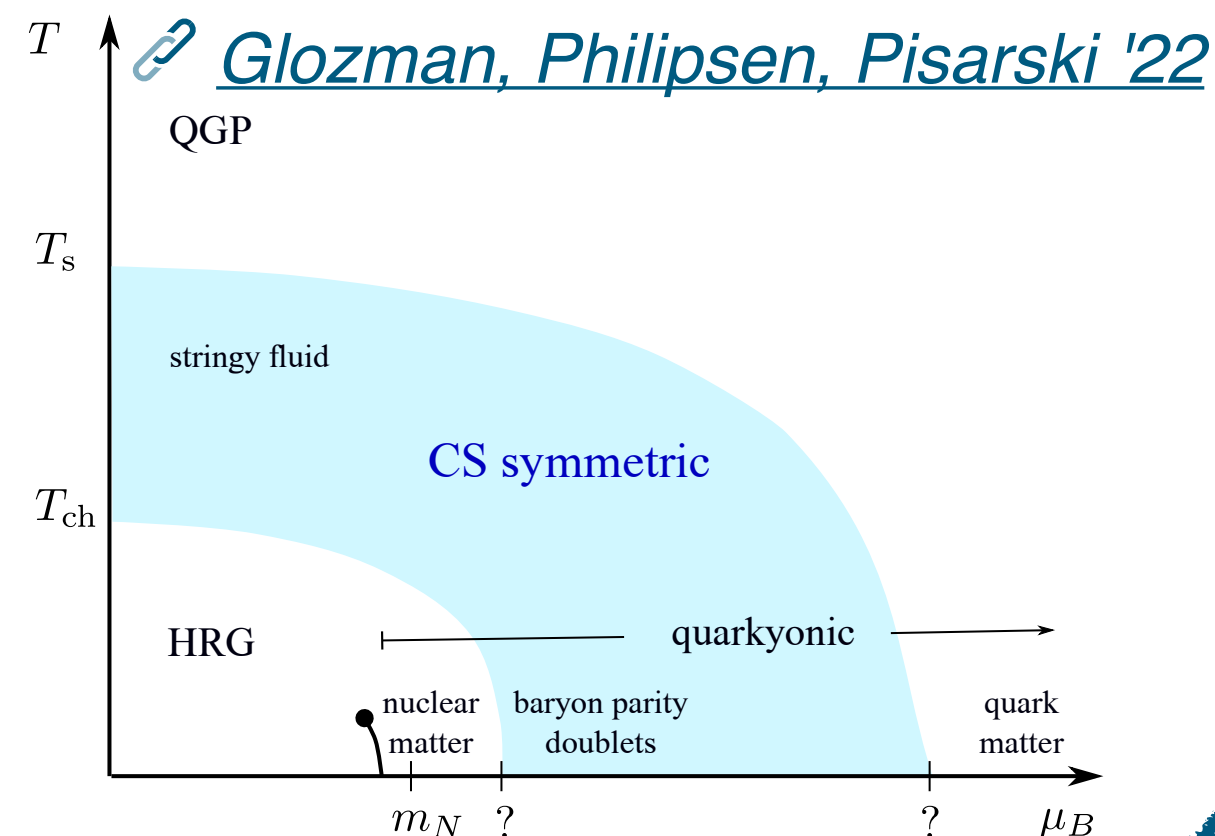
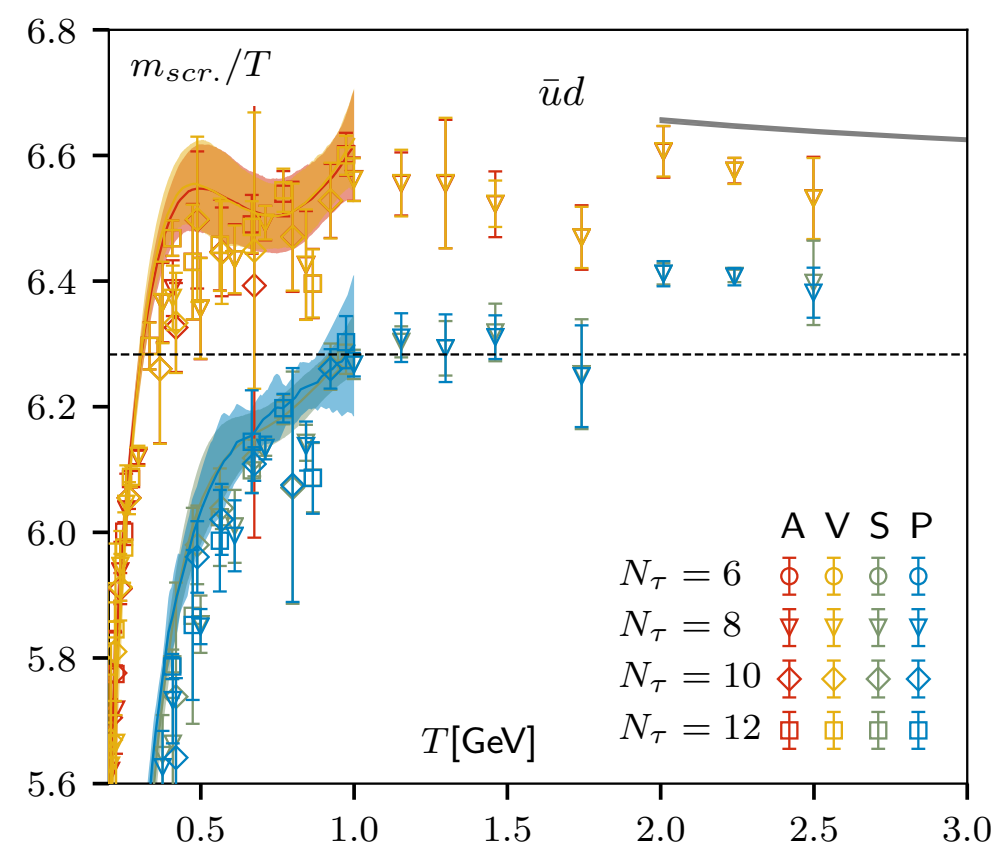
- ▶ $T < T_c$, with spontaneously broken chiral symmetry
- ▶ $T_c \lesssim T \lesssim 3T_c$, with larger approx chiral spin and $SU(2N_f)$ symmetries



- multiplet patterns, of $SU(2)_{CS}$ and $SU(2N_f)$ groups, of meson correlation functions
 - Dominance of color-electric q-g interactions (dof chirally symmetric quarks bound to color singlet objects by color electric field)
- [Rohrhofer, Aoki, Glozman '20 \(PLB\)](#)

- ▶ $T \gtrsim 3T_c$, with screening & usual χ -symmetry recovered via crossover

Additional evidence based on $T \in [0.5 - 0.7]$ GeV meson screening masses: Change of dynamics at the “knee”... [Bazavov et al. '19 \(PRD\)](#)



Pion spectral properties above T_c

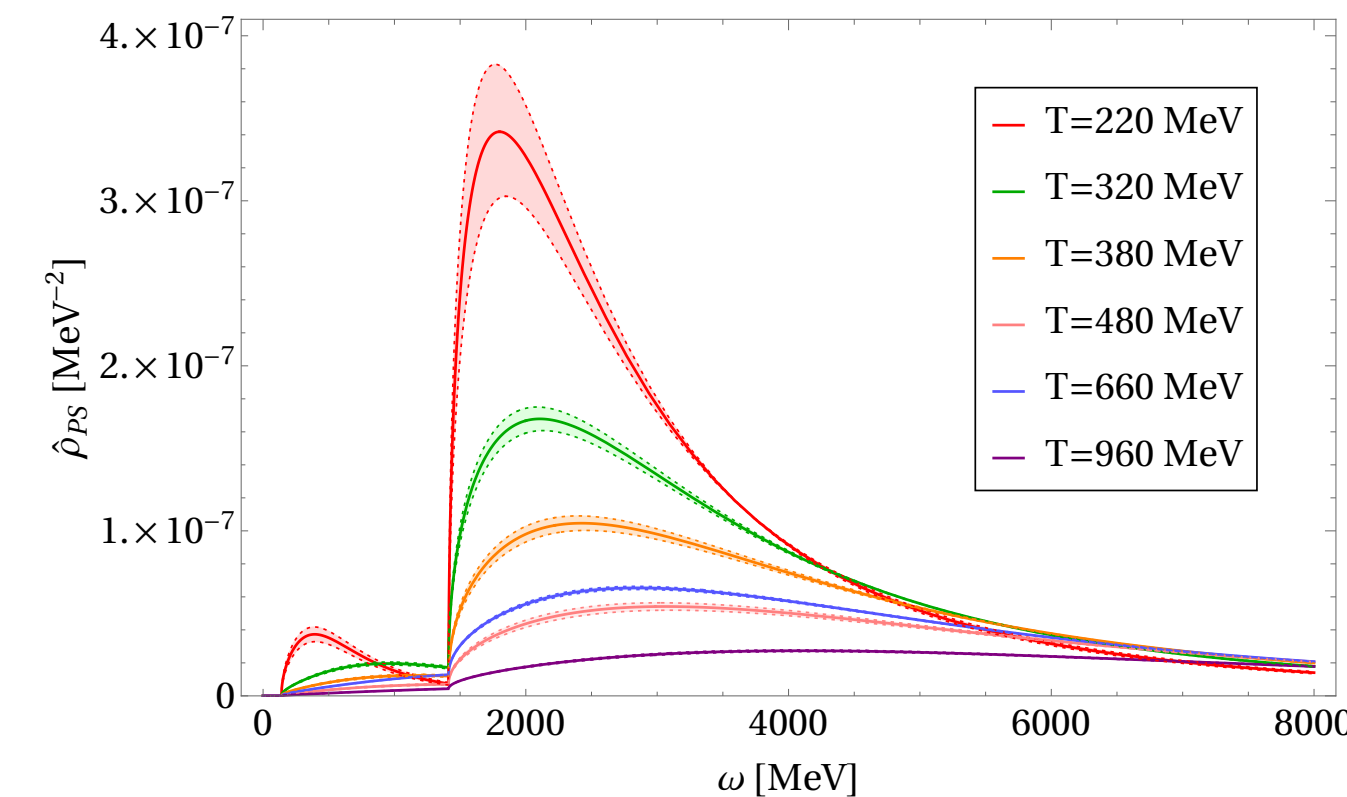
[Lowdon, Philipsen '22](#)

Spectral functions: Key quantities to access the transport coefficients parametrizing the in-medium response of QGP to any perturbations

- ▶ Related by an integral transform to the conserved current Euclidean correlators measured in lattice QCD
- Inversion required to extract spectral functions is an ill-posed problem!

IDEA: Exploit constraints imposed by field locality at finite T:

- ▶ Non perturbative representation of the spectral function generalizing for $T > 0$ the Källén-Lehmann representation and featuring so-called "damping factors" (controlling the thermal broadening of peaks)



- ▶ Fit lattice spatial PS meson correlator for $T \in [220 - 960]$ MeV
→ damping factors
→ analytic spectral function
- ▶ Test: spectral function reproduces temporal correlators @ $T = 220$ MeV

- ▶ Distinct pion state above T_c + contributions from its first excitation + gradual melting as T increases

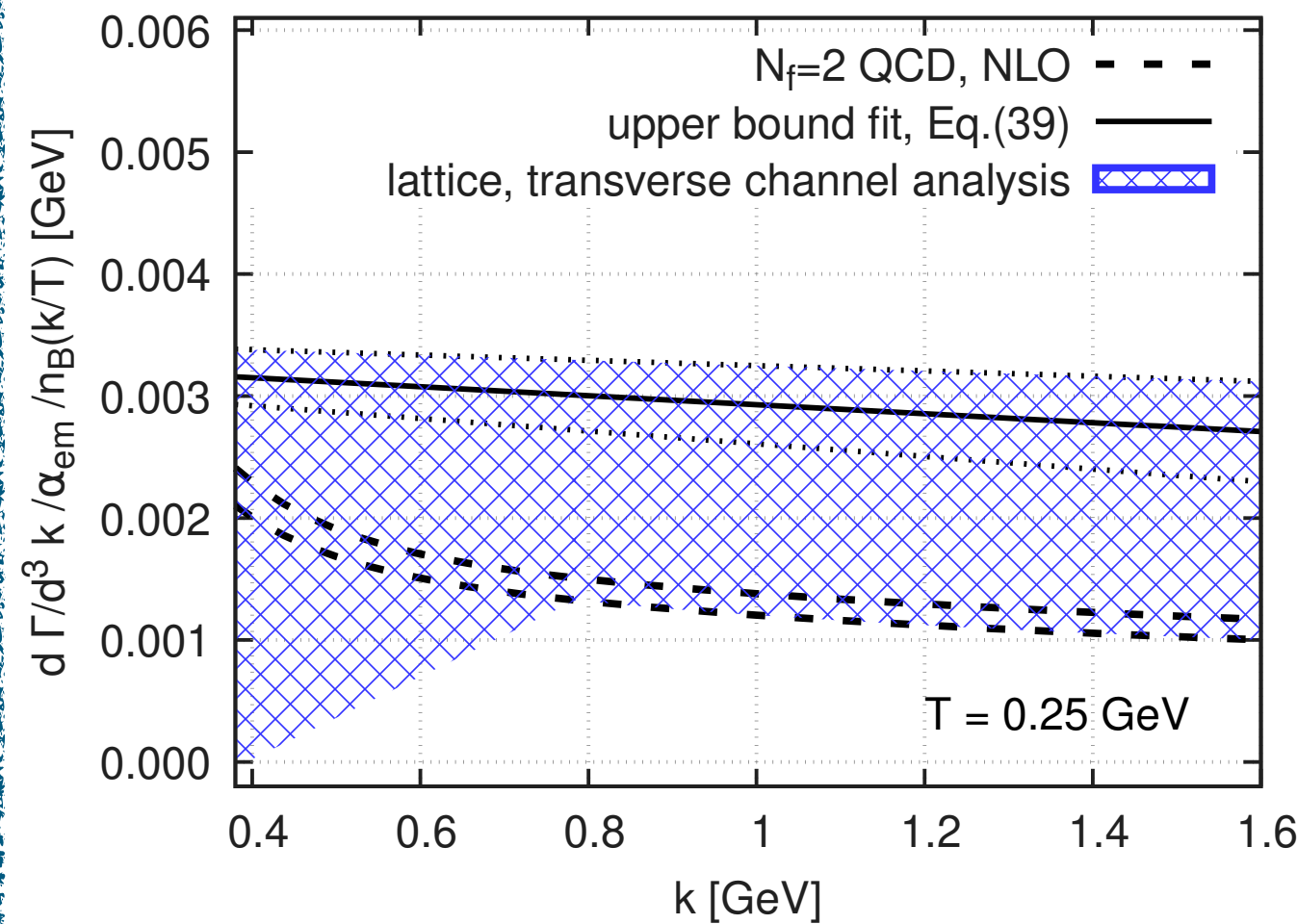
[Owe Philipsen, Tue 14:00](#)

Transport properties - Thermal photons from the QGP

How brightly does the quark-gluon plasma glow?

Photon emissivity of the QGP important input to predict photon yield in heavy-ion collisions

- ▶ Kin. factors \times spectral function associated with 2-point correlator of EM current at light-like kinematics
- ▶ Probes in medium interactions: Differs between weakly & strongly coupled plasma in soft- γ regime

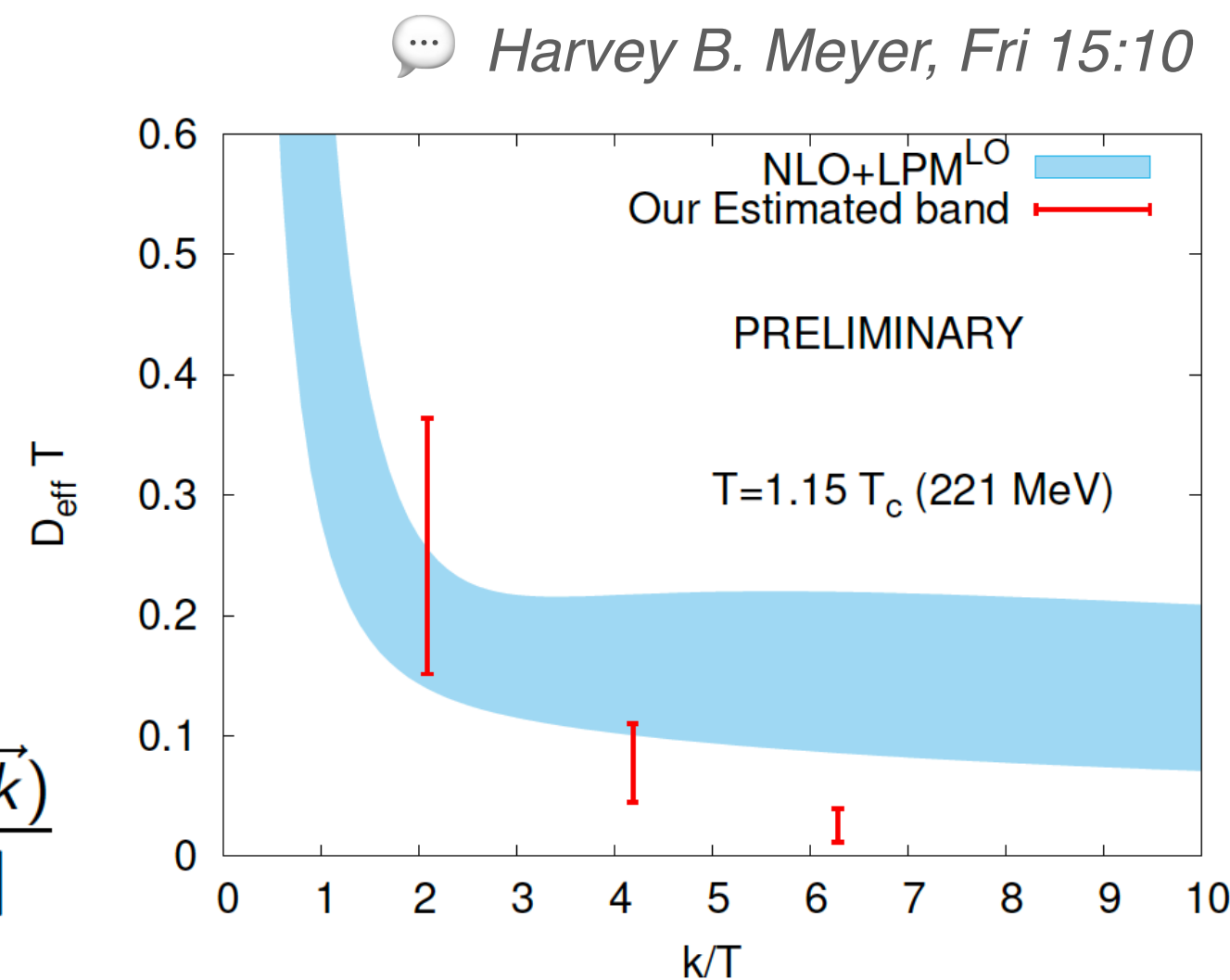


Photon emissivity (and lepton-pair production rate) based on continuum-extrapolated (Euclidean) time-dependent correlators with $N_f=2$ $\mathcal{O}(a)$ -impr. Wilson at $T \sim 1.2T_c$ and $m_\pi \sim 270$ MeV

[Cè et al. '22](#)

$N_f = 2 + 1$ flavor HISQ configurations with $m_l = m_s/5$ corresponding to $m_\pi \sim 310$ MeV, at $T \sim 1.15T_c$

$$\frac{d\Gamma_\gamma}{d^3\vec{k}} = \frac{\alpha_{em} n_b(\omega) \chi_q}{\pi^2} D_{eff}(k) \quad D_{eff}(k) = \frac{\rho_H(|\vec{k}|, \vec{k})}{2\chi_q |\vec{k}|}$$



[Dibyendu Bala, Fri 15:30](#)

Correlators at imaginary spatial momentum

[Cè et al. '22 \(PoS LAT21\)](#)

New perspective circumventing the inverse problem:

- ▶ Dispersion relations at fixed spacelike virtuality, rather than at fixed spatial momentum, to access moments of the spectrum of emitted photons
- ▶ Directly computing the analytic continuation of the retarded correlator at fixed, vanishing virtuality of the photon via calculation of the appropriate Euclidean correlator at imaginary spatial momentum

Test in $N_f = 2$ $\mathcal{O}(a)$ -impr. Wilson fermions at $T \sim 1.2T_c$ with $m_\pi \sim 270$ MeV

[Csaba Török, Tue 17:30](#)

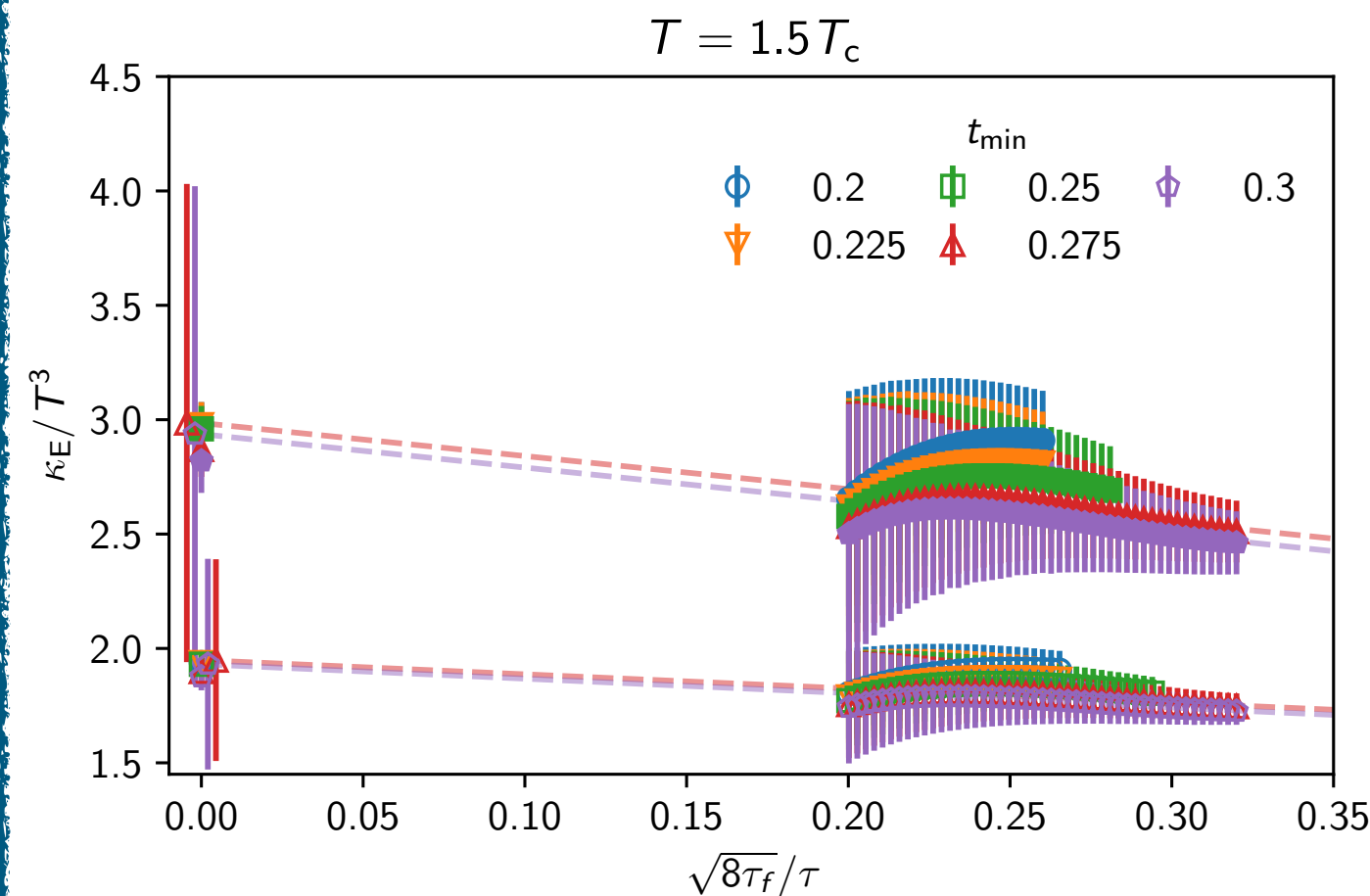
Transport properties - Heavy quarks equilibration time in the QGP

How fast do heavy quarks thermalize in a hot medium?

- Equilibration time \leftrightarrow heavy quark diffusion (Brownian motion) described by Langevin equation depending on three related transport coefficients
 - Heavy quark diffusion coefficient κ related, in thermal equilibrium, to the heavy quark diffusion coefficient D via $D = 2T^2/\kappa$
- $\kappa \leftrightarrow$ Euclidean correlators of field strength tensor components in the heavy quark limit $M \gg \pi T$ (HQET)
 - Correlator of two chromo-electric fields $E \leftrightarrow$ Leading contribution in the T/M expansion κ_E
 - Correlator of two chromo-magnetic fields $B \leftrightarrow T/M$ correction κ_B

Heavy quark diffusion coefficient in SU(3) pure gauge

[Brambilla et al. '22](#)

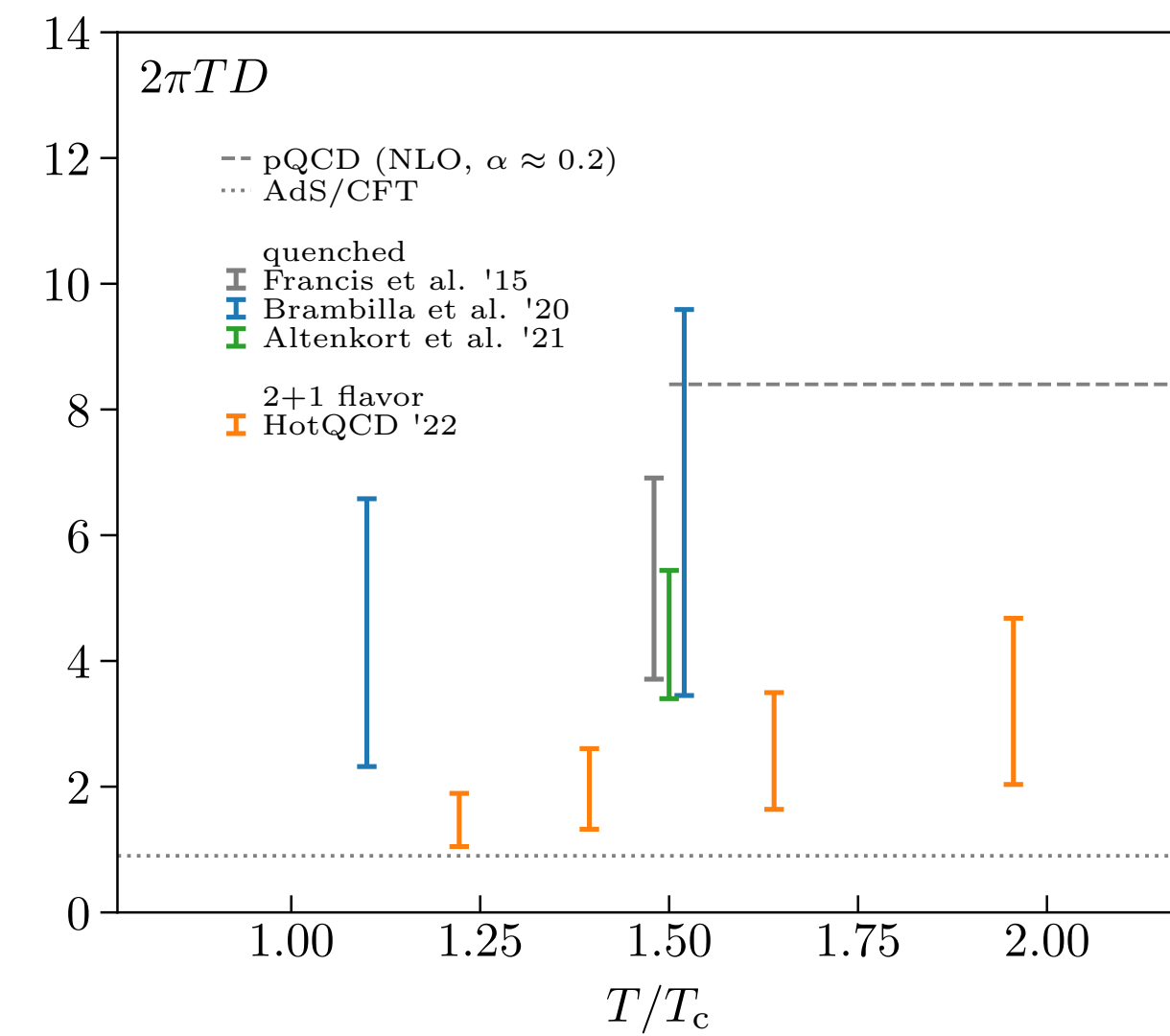


- Chromo- electric & -magnetic correlators
 - $1.70 \leq \kappa_E/T^3 \leq 3.12$
 - $1.23 \leq \kappa_B/T^3 \leq 2.74$
- Mass suppressed effects in the heavy quark diffusion coefficient are 20% for bottom and 34% for charm quark at $T = 1.5T_c$

... Viljami Leino, Wed 15:00

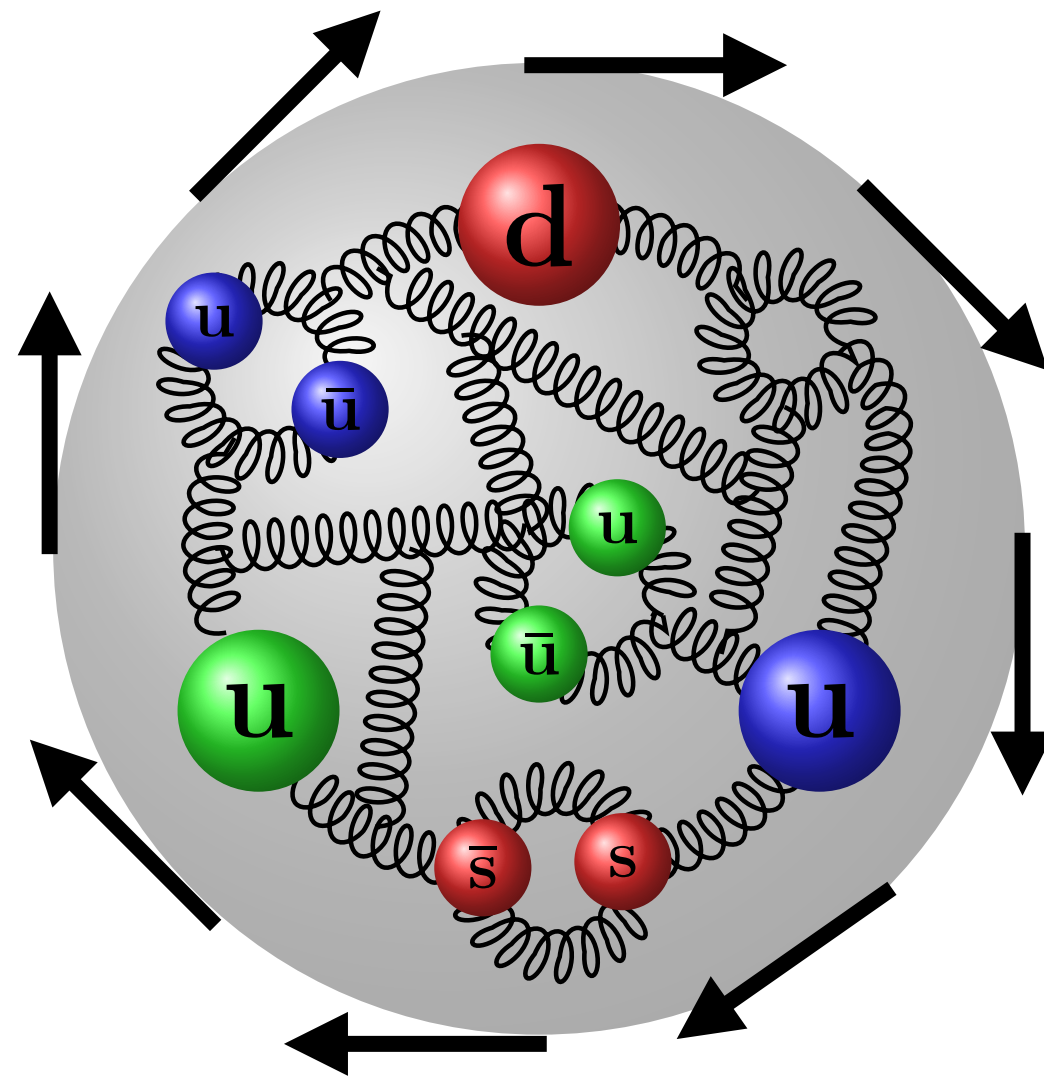
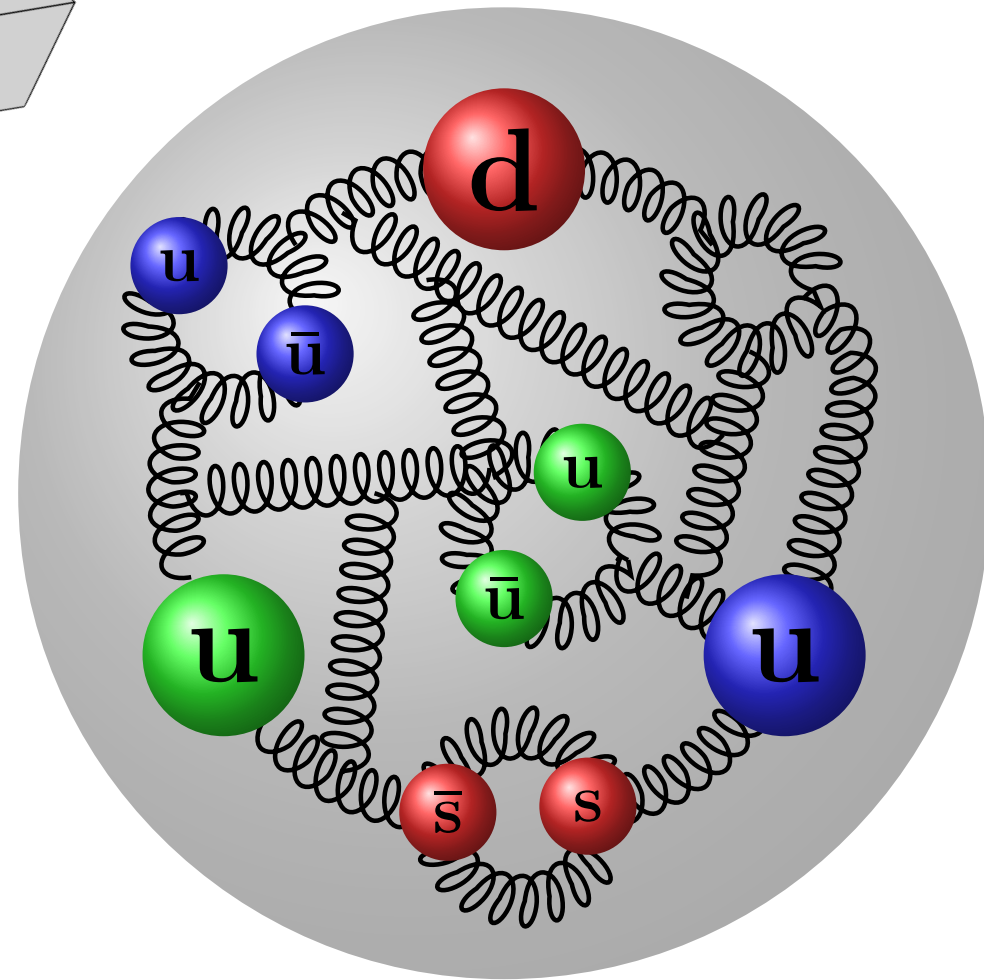
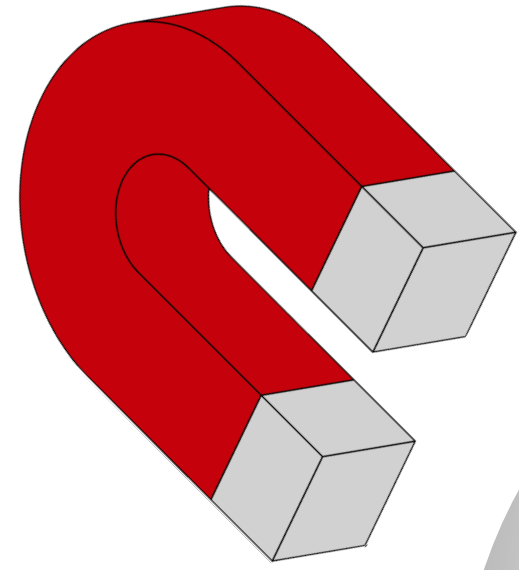
Heavy quark diffusion coefficient, with $N_f = 2 + 1$ HISQ

[Altenkort et al. '22 \(PRD\)](#)



- First study on heavy quark momentum diffusion with dynamic quarks
- Significant decreasing of $2\pi TD$ with dynamical quarks as compared to the quenched case

... Luis Altenkort, Wed 15:20



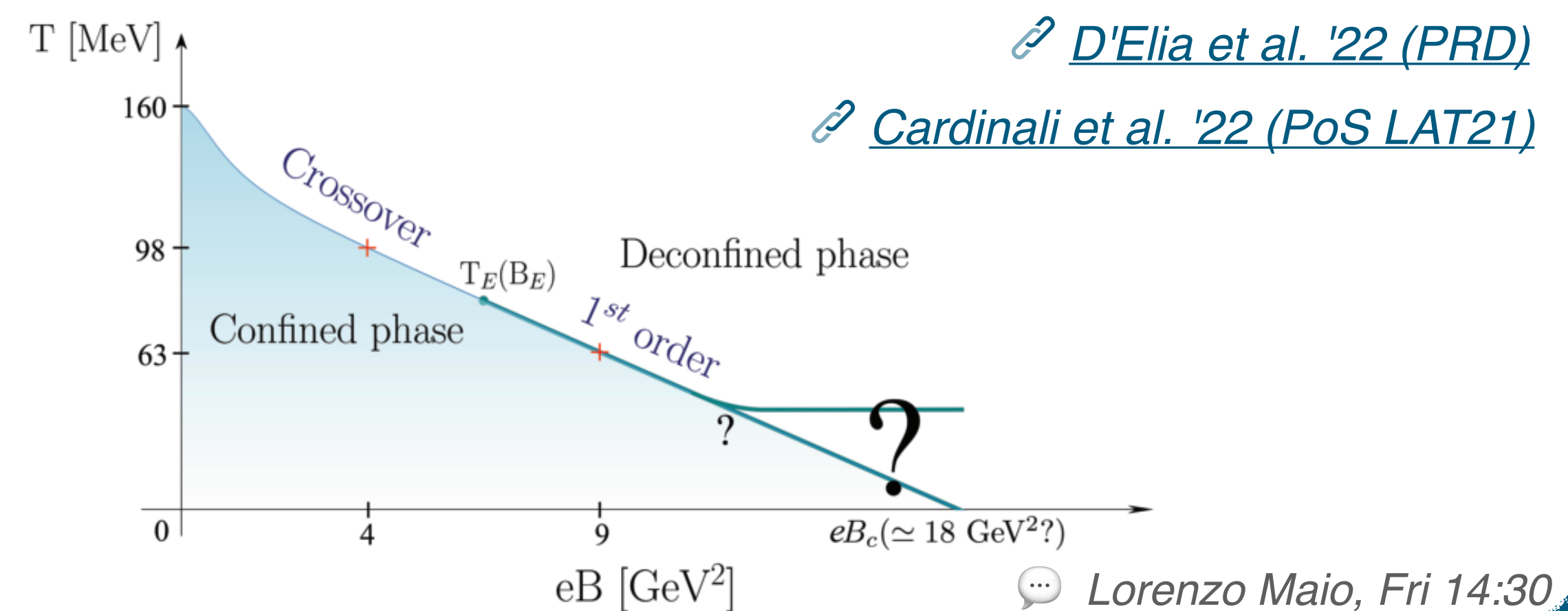
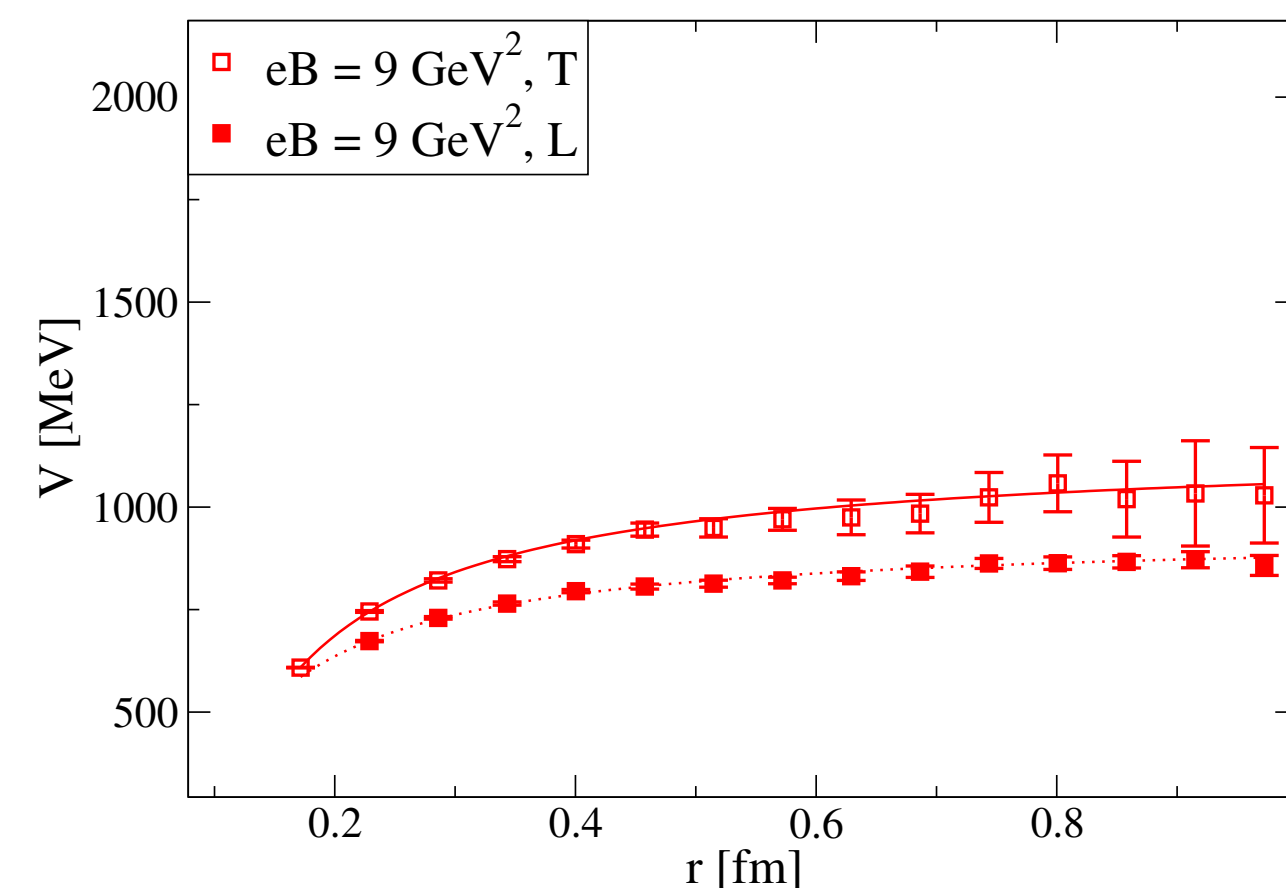
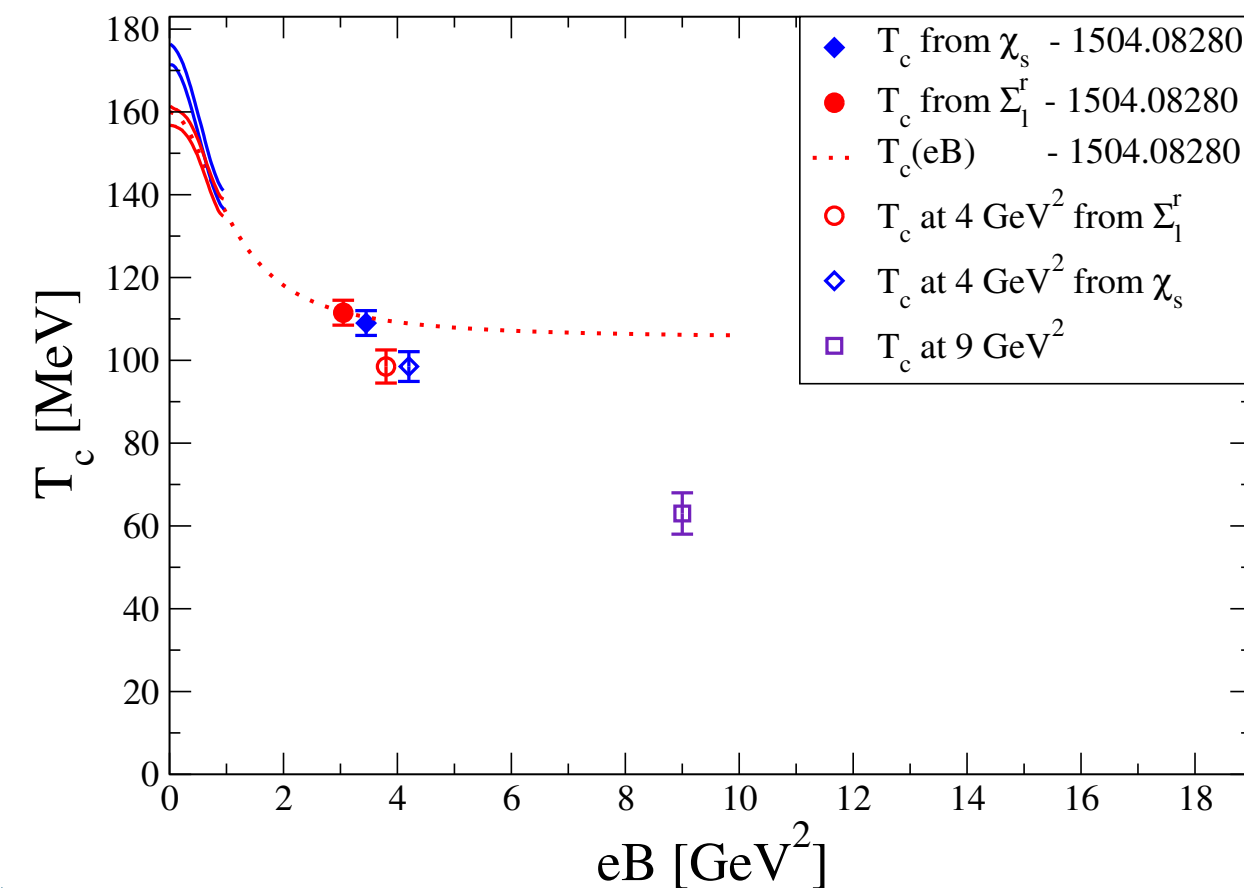
Nonzero EM fields or vorticity

- ▶ Nonzero EM fields
 - Magnetic phase diagram
 - Topological aspects
 - Anomalous transport
 - Inhomogeneous B fields
- ▶ Vorticity

Phase diagram in a magnetic/vortical background & inhomogeneous B fields

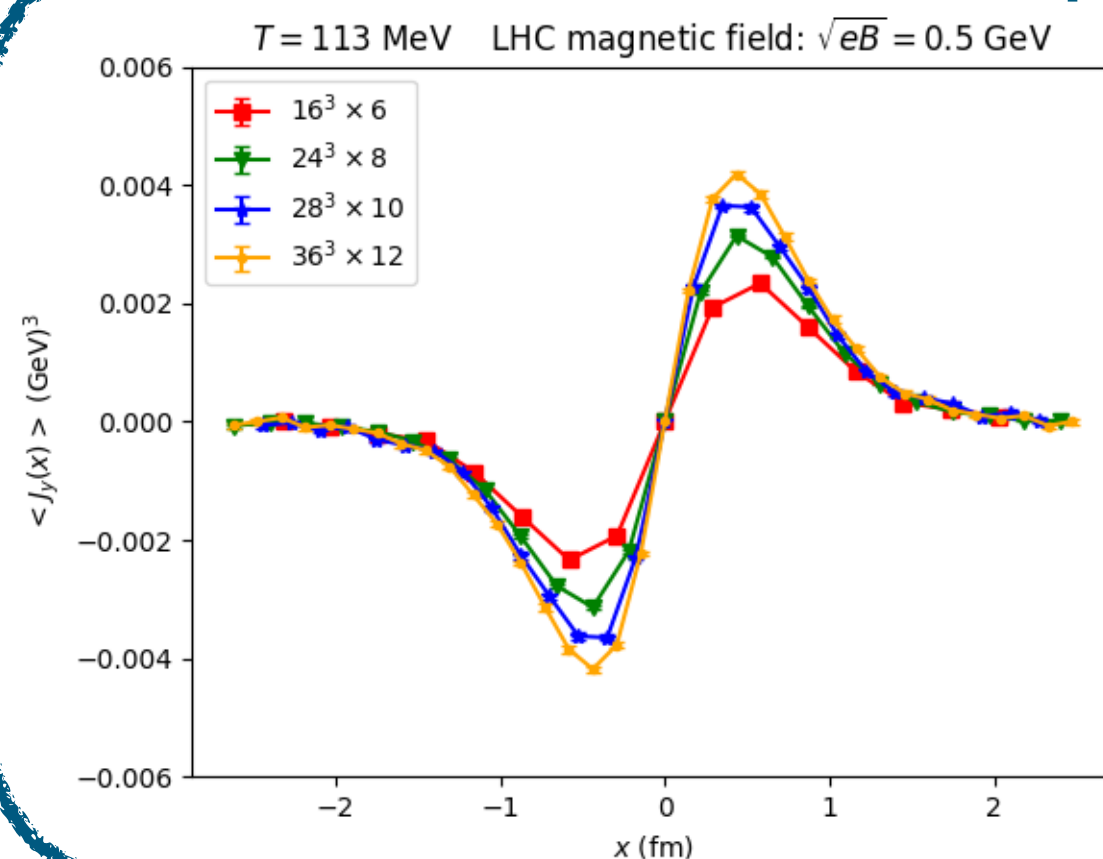
QCD phase diagram in a magnetic background, with $N_f = 2 + 1$ stout-improved staggered quarks at physical quark masses

- ▶ Crossover at $eB = 4 \text{ GeV}^2$ (with $T_c = (98 \pm 3) \text{ MeV}$) and strong 1st order phase transition at $eB = 9 \text{ GeV}^2$ (with $T_c = (63 \pm 5) \text{ MeV}$)
- ▶ Transition from strongly anisotropic confined phase to completely deconfined phase: $\sigma = 0$ in all directions
- ▶ Steady decrease of $T_c \rightarrow$ Will $T_c(B)$ continue its drop until $T_c(B_c) = 0$?



... Lorenzo Maio, Fri 14:30

Inhomogeneous B , with $N_f = 2 + 1$ stout-improved staggered



... Brandt et al. '22 (PoS LAT21)

$$\mathbf{B}(x_1) = B \left(\cosh \frac{x_1 - L_1/2}{\epsilon} \right)^{-2} \hat{\mathbf{z}}$$

- ▶ Prominent steady electric currents at LHC-like B fields

... Adeilton Dean Marques Valois, Fri 14:10

Rotating QCD with $N_f = 2$ dynamical quarks

... Braguta et al. '21 (PRD)

- ▶ Phenomenological effective models predict decrease in T_c in rotating QCD
- ▶ T_c in gluodynamics found to increase due to rotation, with $C_2 > 0$ in $T_c(\Omega)/T_c(0) = 1 + C_2\Omega^2$
- ▶ Rotation of gluons and fermions found to have opposite effect on T_c ...
- ...with some dependence on the pion mass

... Artem Roenko, Fri 17:20

Non-dissipative transport effects and topological aspects

Anomalous transport phenomena: Chiral Separation Effect (CSE)

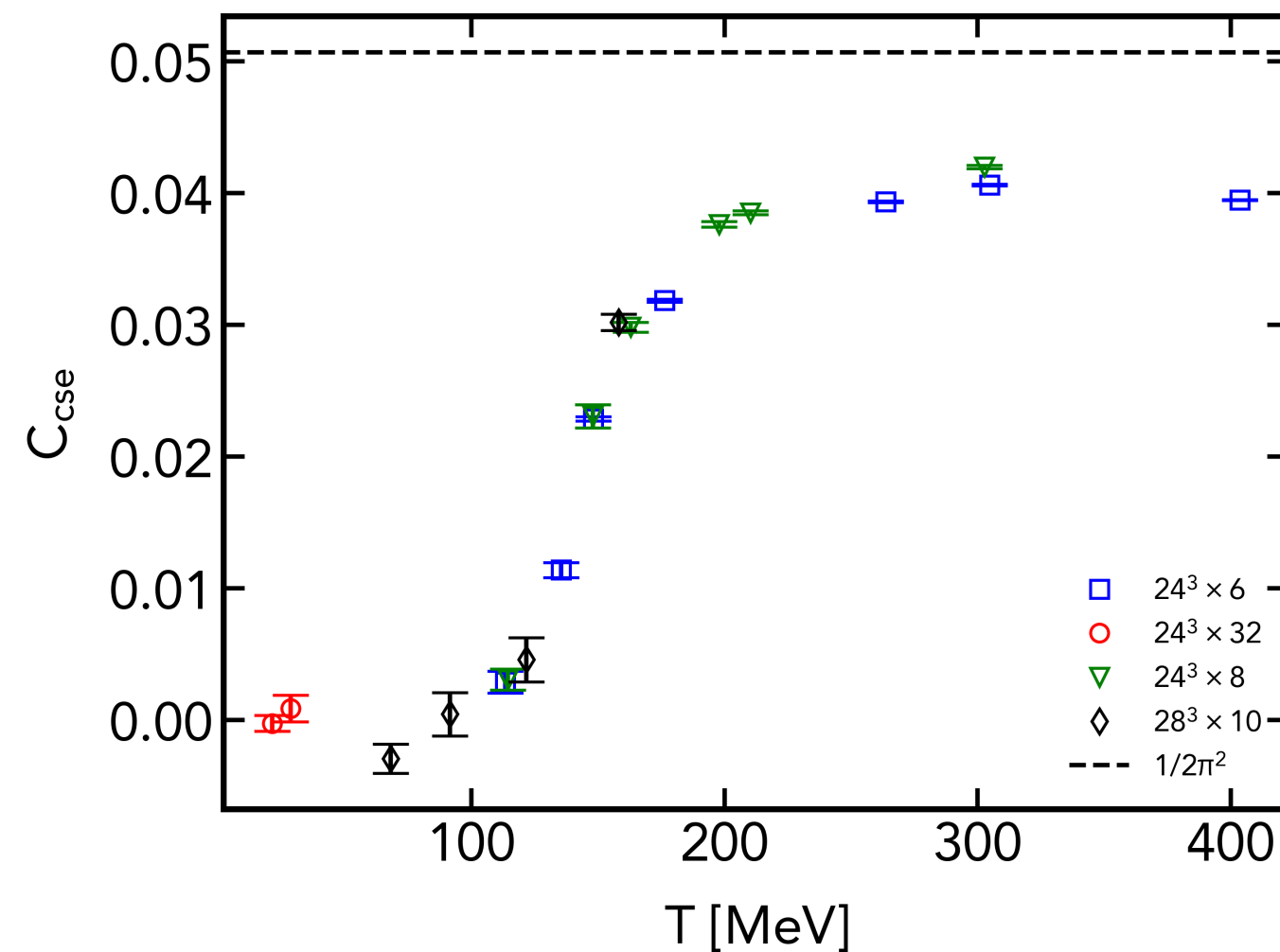
Quantum anomalies + EM fields → non-dissipative transport, e.g. CSE

- ▶ At nonzero μ and (strong) B -field → CP-odd axial current appears

$$j_i^A = C_{\text{cse}} \mu B_i$$

- ▶ On the lattice one can measure, from $\mu = 0$ simulations, at nonzero B_z ,

$$\left. \frac{dj_z^A}{d\mu} \right|_{\mu=0} = C_{\text{cse}} B_z$$



- ▶ Free case: confirmed analytic prediction $C_{\text{cse}} = 1/(2\pi^2)$
- ▶ Interacting case ($N_f = 2+1$ stout-impr. staggered at physical masses):
 - suppression at low T , approach free case value at high T
 - m -dependence to be checked, continuum limit to be taken

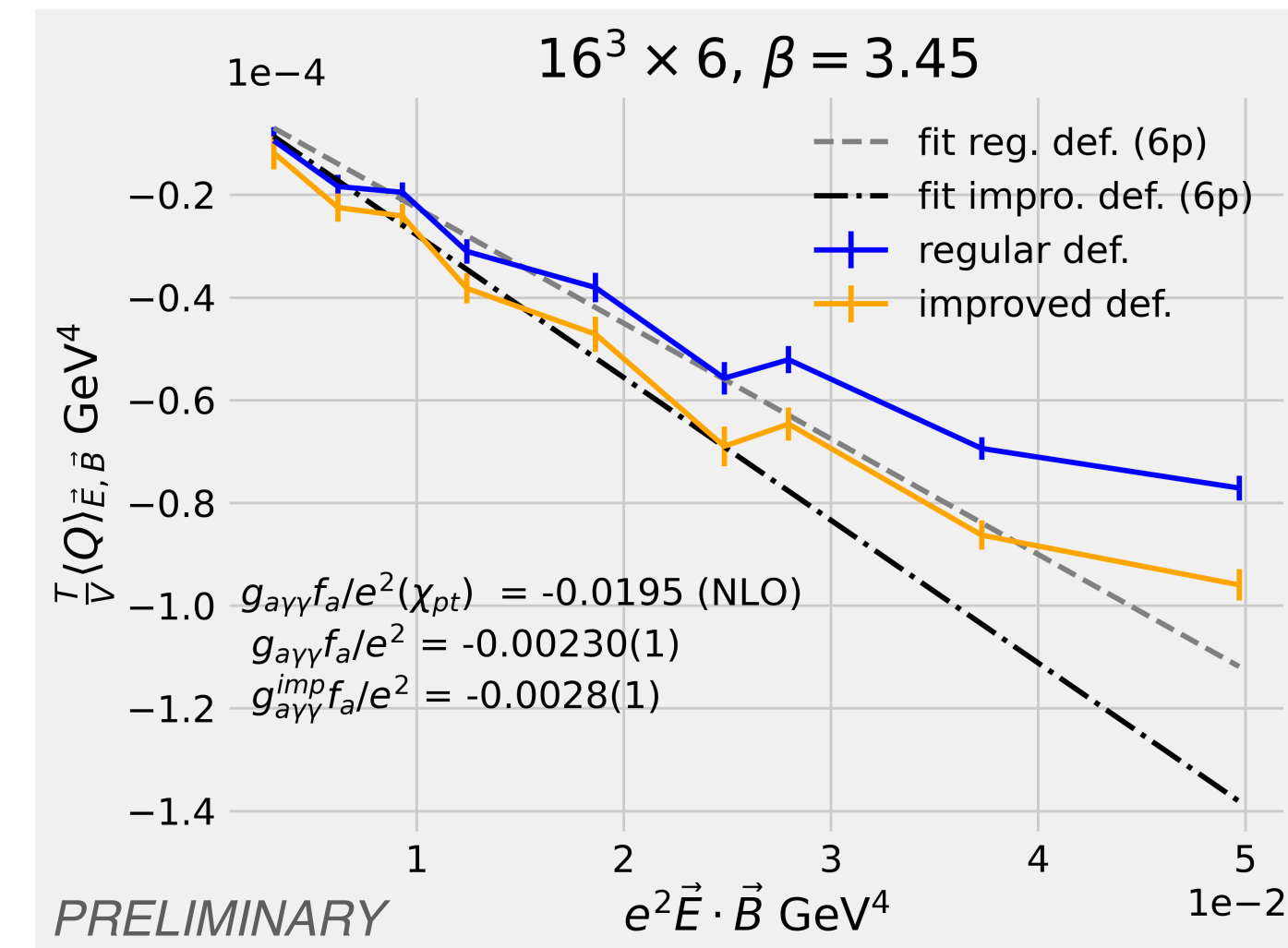
🗨 Eduardo Garnacho Velasco, Wed 17:50

Topology in electromagnetic fields and the axion-photon coupling

- ▶ Direct axion-photon coupling $g_{a\gamma\gamma}^{\text{QCD}}$ by linear response of Q_{top} to weak background EM fields (f_a , energy scale suppressing axion dynamics)

$$\frac{T}{V} \langle Q_{\text{top}} \rangle_{E,B} \approx \frac{g_{a\gamma\gamma}^{\text{QCD}} \cdot f_a}{e^2} e^2 \vec{E} \cdot \vec{B}$$

- $N_f = 2+1$ stout-impr. staggered at physical masses with B and iE
- Weight of topological sectors with non-zero topological charge enhanced

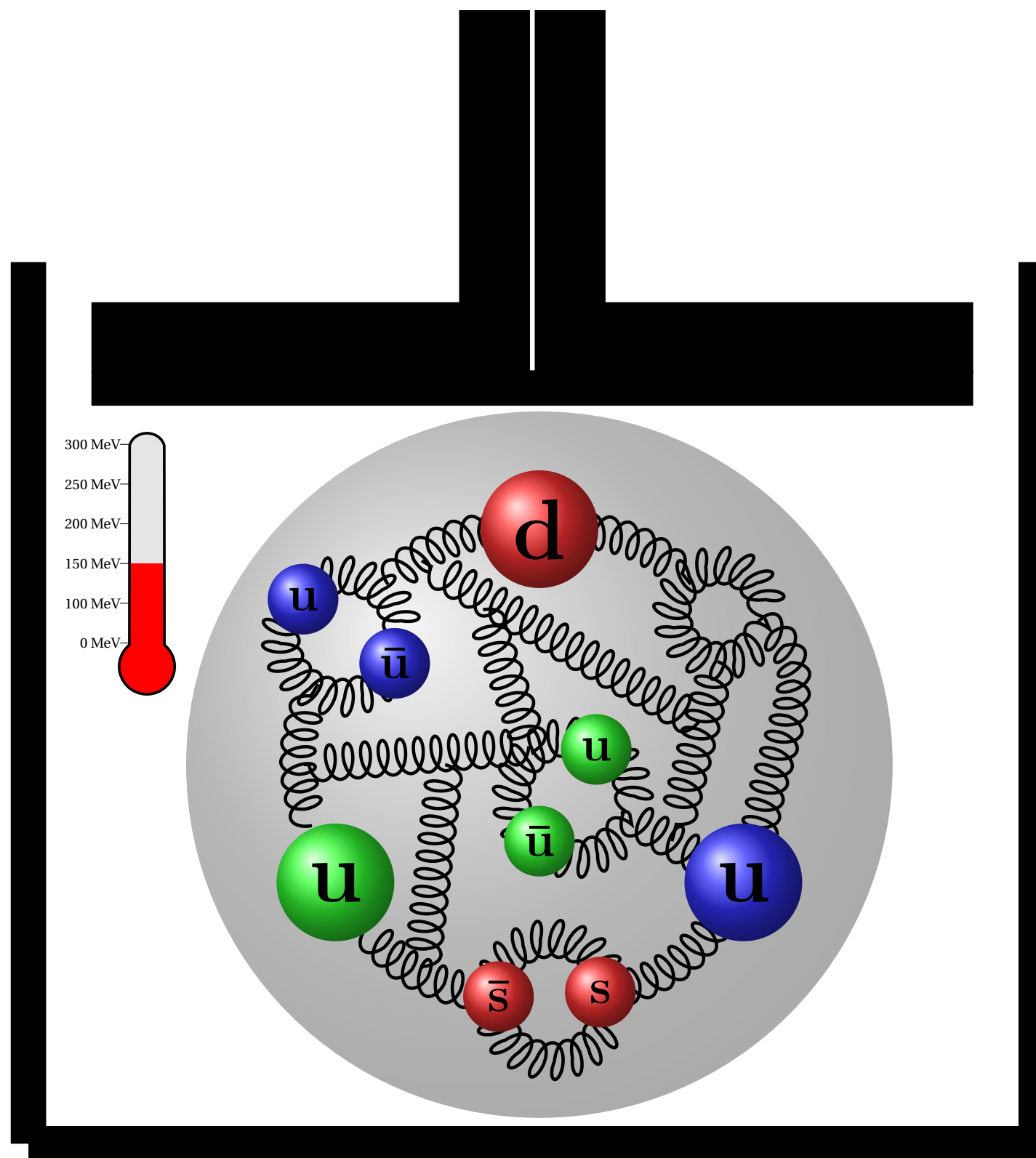


- ▶ Two different lattice discretizations for Q_{top}
- ▶ Fit in the linear region
- ▶ Comparison with chiral perturbation theory prediction

🗨 José Javier Hernández Hernández, Fri 14:50

Nonzero density

- ▶ Phase transitions
- ▶ Fluctuations of conserved charges
- ▶ Equation of State
- ▶ Speed of sound
- ▶ Properties of dense QGP
- ▶ The cold and dense regime



Phase transitions in QCD at nonzero density

Multi-point Padè for the study of phase transitions

[Singh et al. '22 \(PoS LAT21\)](#)

Method to investigate the QCD phase diagram based on

- ▶ Computation of Taylor series coefficients at both $\mu = 0$ and $\mu = i\mu_B$
- ▶ Poles of multi-point Padè approximants for locating Lee Yang edge singularities

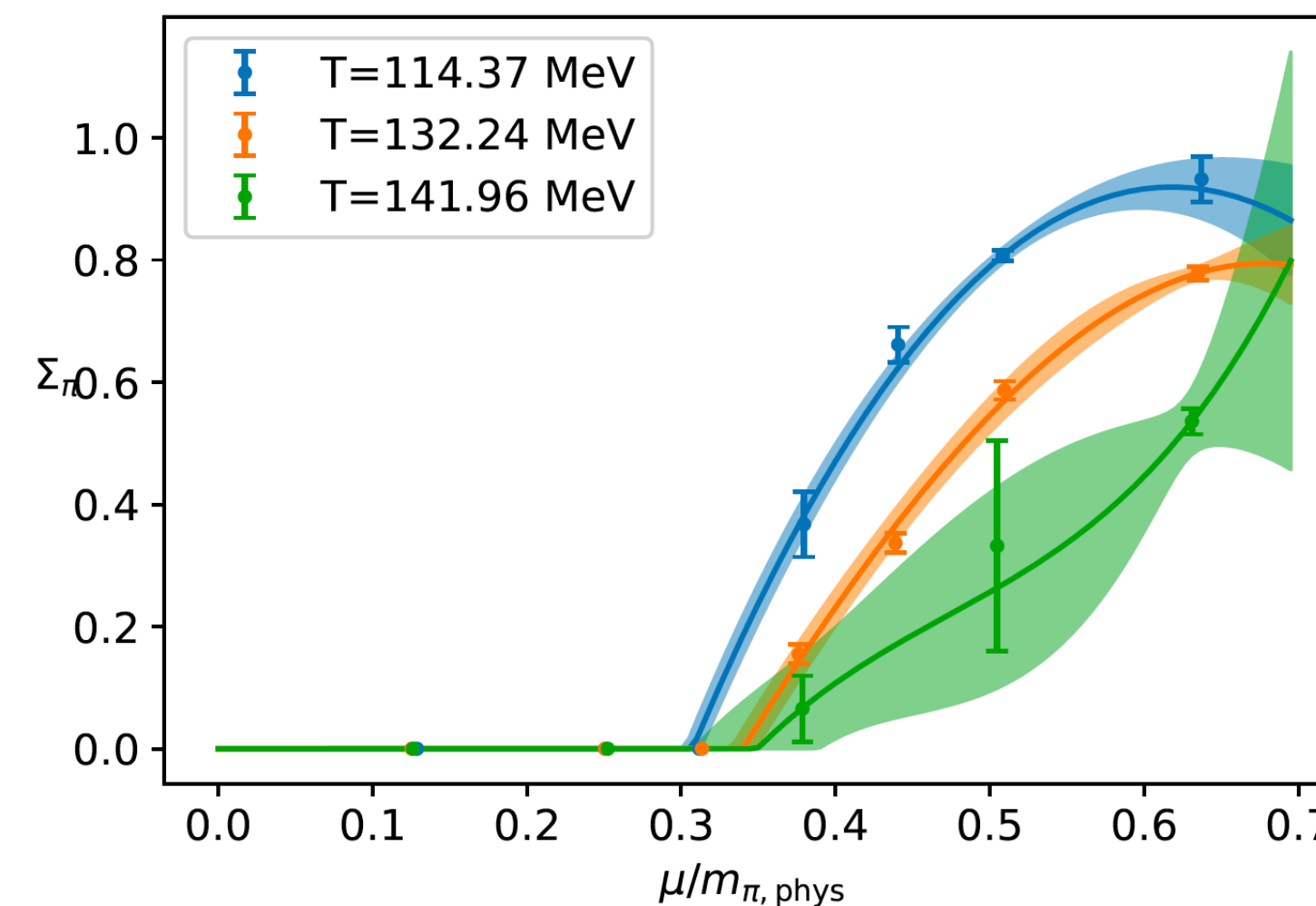
Method applied to:

- ▶ Two-dimensional Ising model 🗨️ Francesco Di Renzo, Mon 14:00
- ▶ $N_f = 2 + 1$ QCD at physical masses, with HISQ 🗨️ Kevin Zambello, Mon 14:20
 - identifying singularities of the net-baryon number density in the complex μ_B plane using conserved charges
 - close to the Roberge-Weiss (RW) transition, the location of the LYE singularities scales according to the 3-d \mathbb{Z}_2 universality class
 - preliminary results for singularities close to the chiral phase transition

Pion condensation at lower than physical quark masses

Isospin imbalance in QCD drives transition to Bose-Einstein Condensation (BEC) phase with condensation of charged pions.

- ▶ Phase diagram affected by the flavor content
 - At the physical point \rightarrow BEC boundary known in large μ_I and T ranges
 - In the chiral limit $\rightarrow T = 0$ condensation at infinitesimally small μ_I
- ▶ $\mu = 0$ chiral transition might be affected, depending on the shape of the BEC boundary, by its proximity!



- ▶ First step towards the chiral limit: simulations of $N_f = 2 + 1$ stout-impr. staggered fermions at half the physical quark masses
- ▶ BEC boundary mapped and compared with the results at physical masses

🗨️ Volodymyr Chelnokov, Mon 16:30

Fluctuations of conserved charges

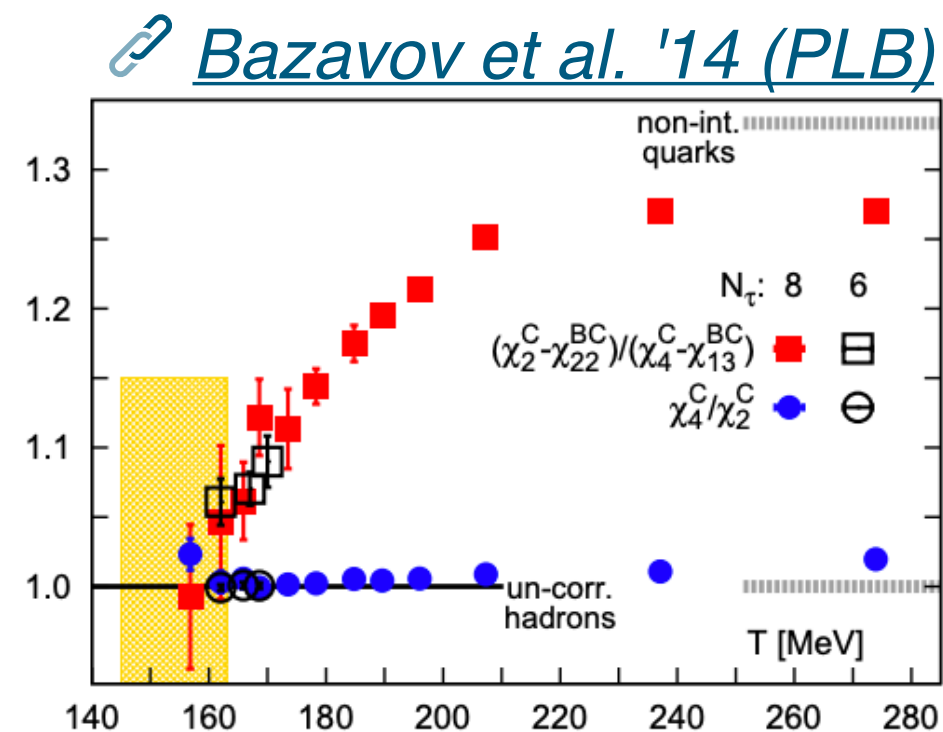
Charm fluctuations - $N_f = 2 + 1$ QCD @high T & physical masses

Measuring dimensionless generalized susceptibilities of conserved charges

$$\chi_{klmn}^{\text{BQSC}} = \frac{\partial^{(k+l+m+n)} [p(\hat{\mu}_B, \hat{\mu}_Q, \hat{\mu}_S, \hat{\mu}_C)/T^4]}{\partial \hat{\mu}_B^k \partial \hat{\mu}_Q^l \partial \hat{\mu}_S^m \partial \hat{\mu}_C^n} \bigg|_{\vec{\mu}=0} \quad \text{for comparison with:}$$

- Confined phase phenomenology by hadron resonance gas model (HRG)
- Ratios of identified particles yields in heavy-ion collisions

Validity range of quark model extended HRG description of open charm sector and dissociation temperature of charmed hadrons by extraction of



- 2nd and 4th order cumulants of charm fluctuations
- Correlations of charm with lighter conserved flavor quantum numbers
- Appropriate combinations of the above

... Sipaz Sharma, Tue 16:30

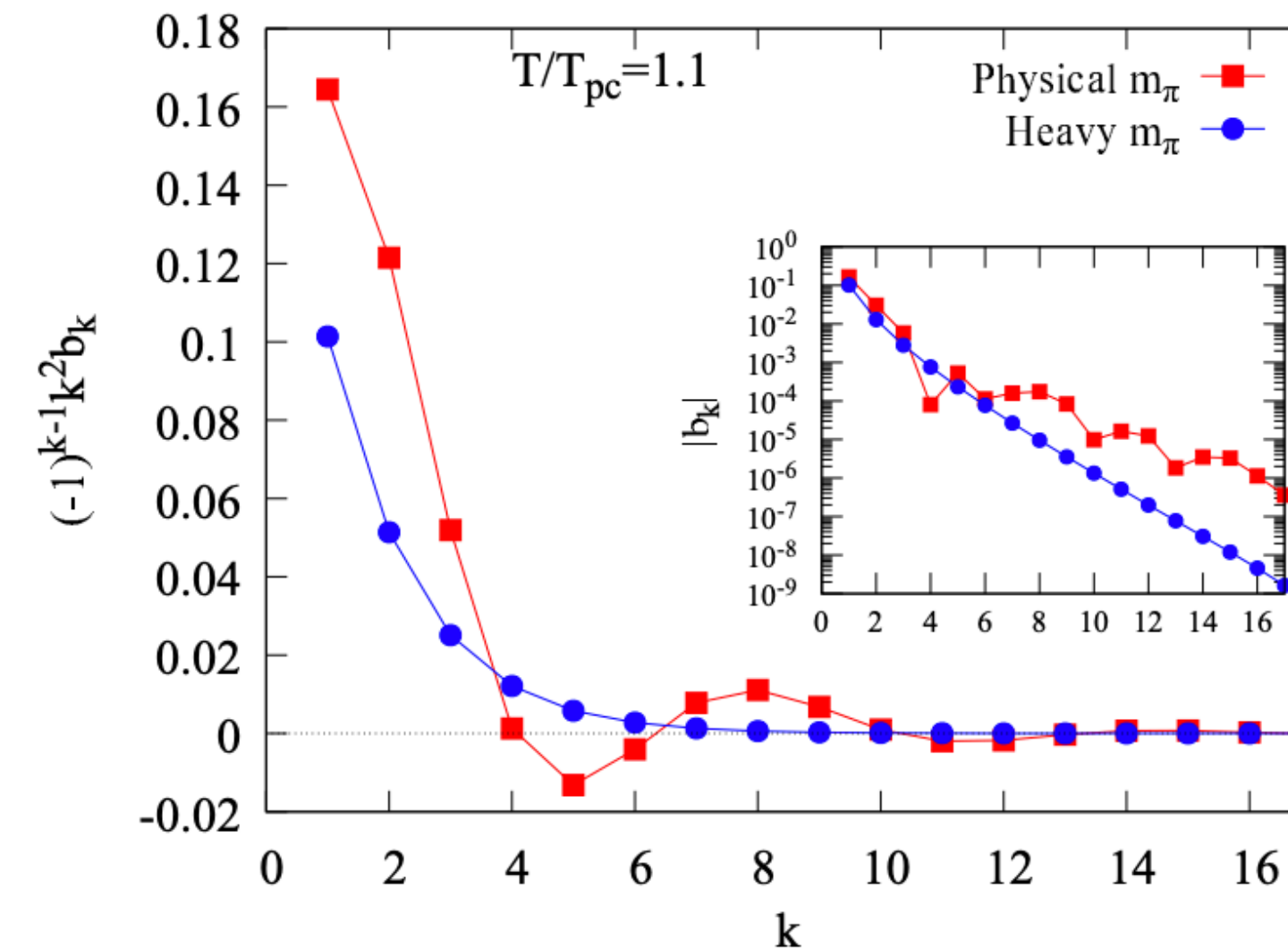
Electric charge fluctuations using 4HEX quarks

- Most severe lattice artefacts among fluctuations ... P. Parotto, Tue 16:50
 - Data with a novel discretization suppressing artefacts
- continuum extrapolated results in T region of chemical freeze-out

Fourier coefficients of net-baryon number as function of $\mu = i\mu_i$

Coefficients' asymptotics at large k governed by singularity structure of \mathcal{Z}_{QCD} in the complex chemical potential plane

- They encode information on phase transitions
- characteristic behavior reflected also in the baryon number fluctuations
- Calculation via asymptotic numerical quadrature designed for highly oscillatory integrals
- Estimate the position of the nearest singularities in the complex μ plane
- Compare:



- Data from simulations of QCD with $N_f = 2 + 1$ HISQ at physical quark masses at imaginary chemical potential on $N_\tau \in \{4, 6, 8\}$ lattices
- Predictions from phenomenological models

... Almasi et al. '19 (PRD)

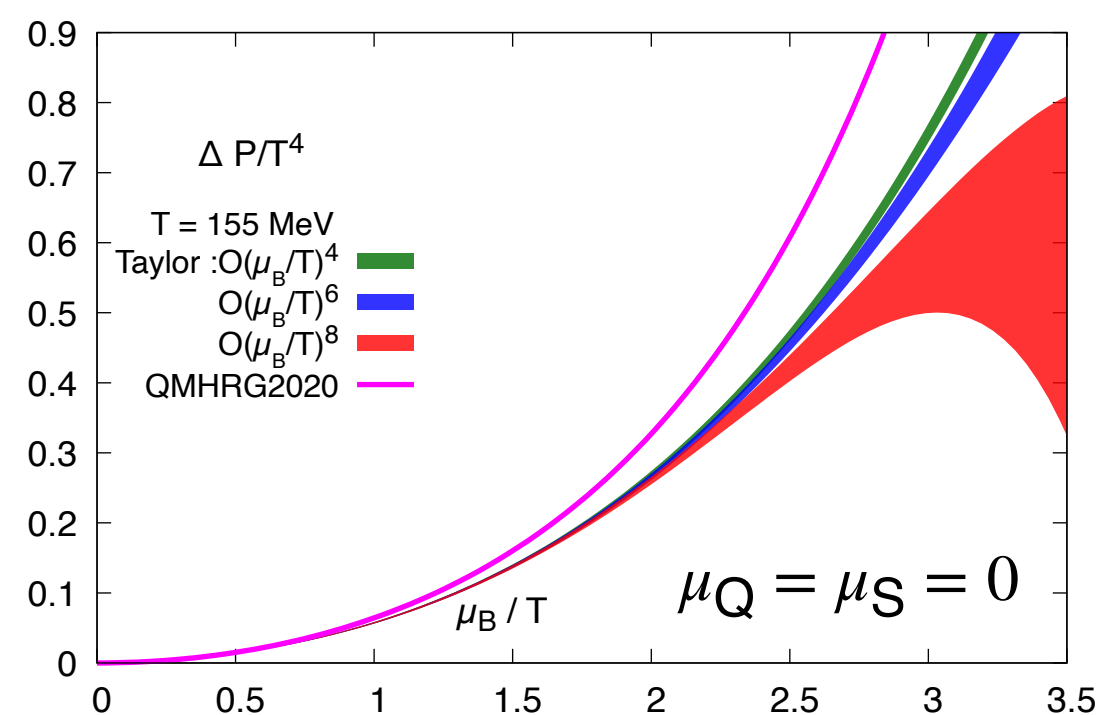
... Christian Schmidt, Mon 14:40

Equation of State (EoS)

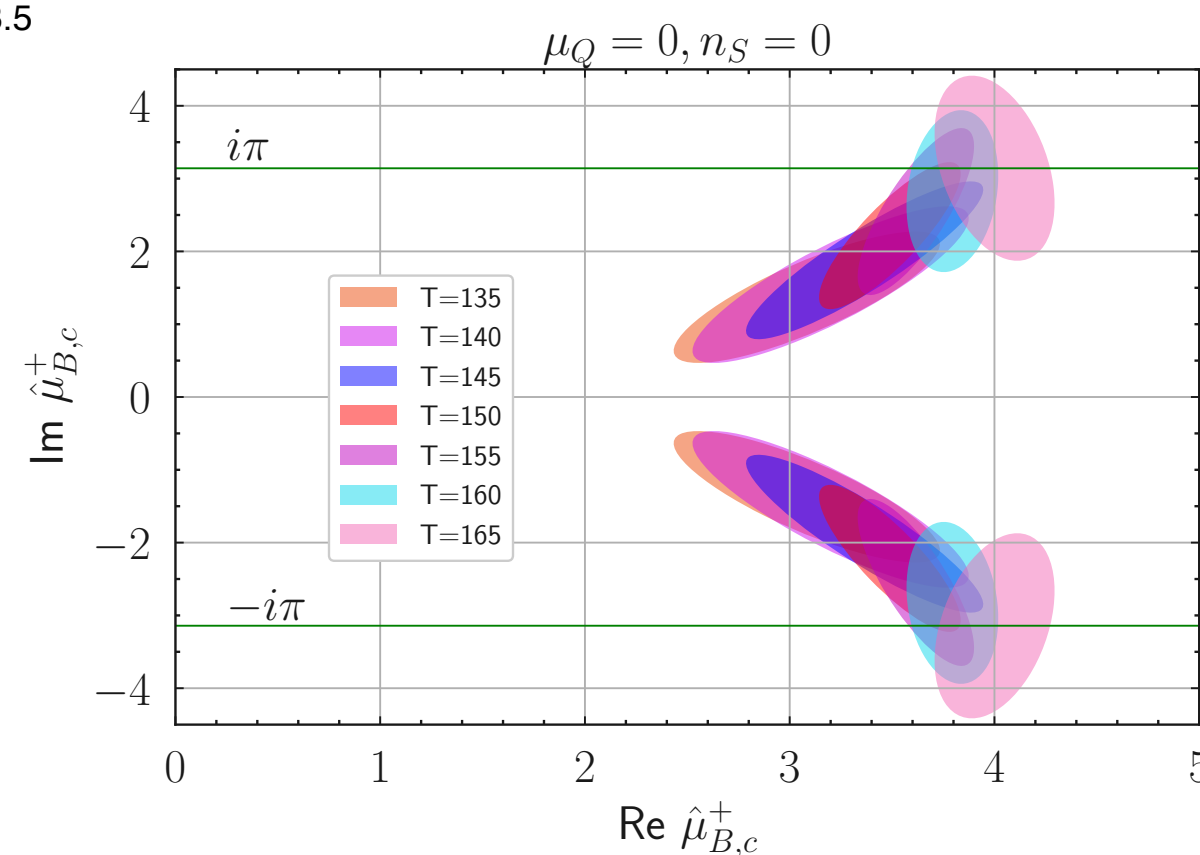
Isentropic equation of state in $N_f = 2 + 1$ QCD

[Bollweg et al. '22 \(PRD\)](#)

Based on high precision Taylor expansion and Padé-resummed expansion



- ▶ Energy density and pressure along lines of constant entropy per net baryon-number density
- ▶ 8th order Taylor series for p ($N_\tau = 8$)
- ▶ Straightforward Taylor series expansion for $\Delta P/T^4$
→ well controlled description up to $\mu_B/T \leq 2.5$



- ▶ Location of singularities in the complex μ_B -plane (influencing convergence of Taylor series)
- ▶ Studied isospin symmetric case $\mu_Q = 0$ at $\mu_S = 0$, and at $n_S = 0$
- ▶ Results compared at low- T with HRG model calculations based on QMHRG2020 hadron list including resonances in relativistic quark models

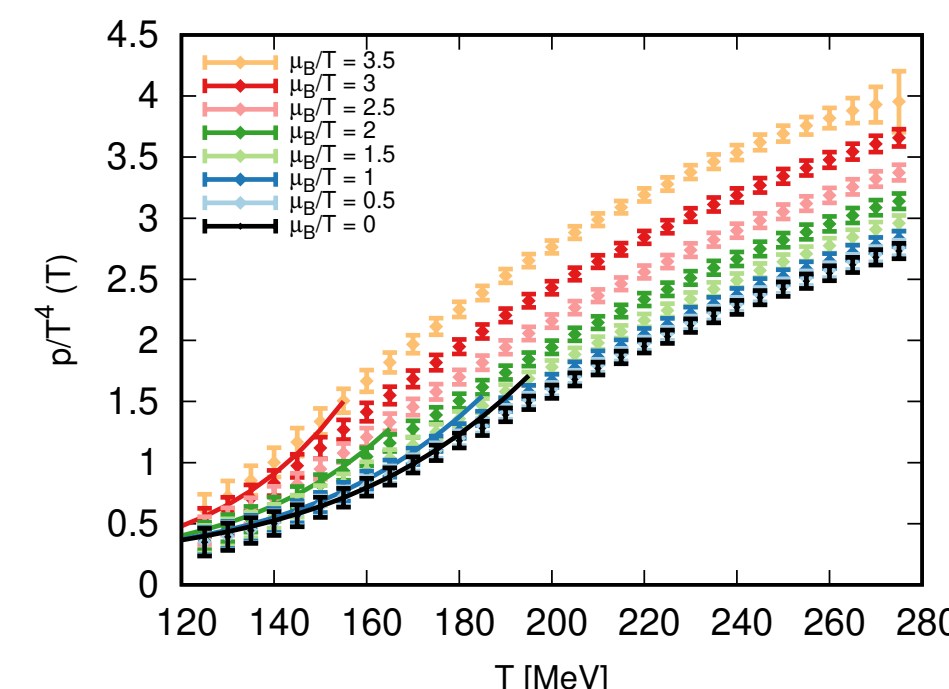
... Jishnu Goswami, Thu 09:40

Resummed equation of state at nonzero baryon density

[Borsanyi et al. '22 \(PRD\)](#)

- ▶ Continuum extrapolated results with extrapolations from imaginary μ using 4stout-impr. staggered fermions with $N_\tau \in \{8, 10, 12, 16\}$
- ▶ Physically motivated extrapolation scheme based on observation, that the main effect of an imaginary μ is parametrized by a shift (F observable of interest, of sigmoid shape in T) [Borsanyi et al. '21 \(PRL\)](#)

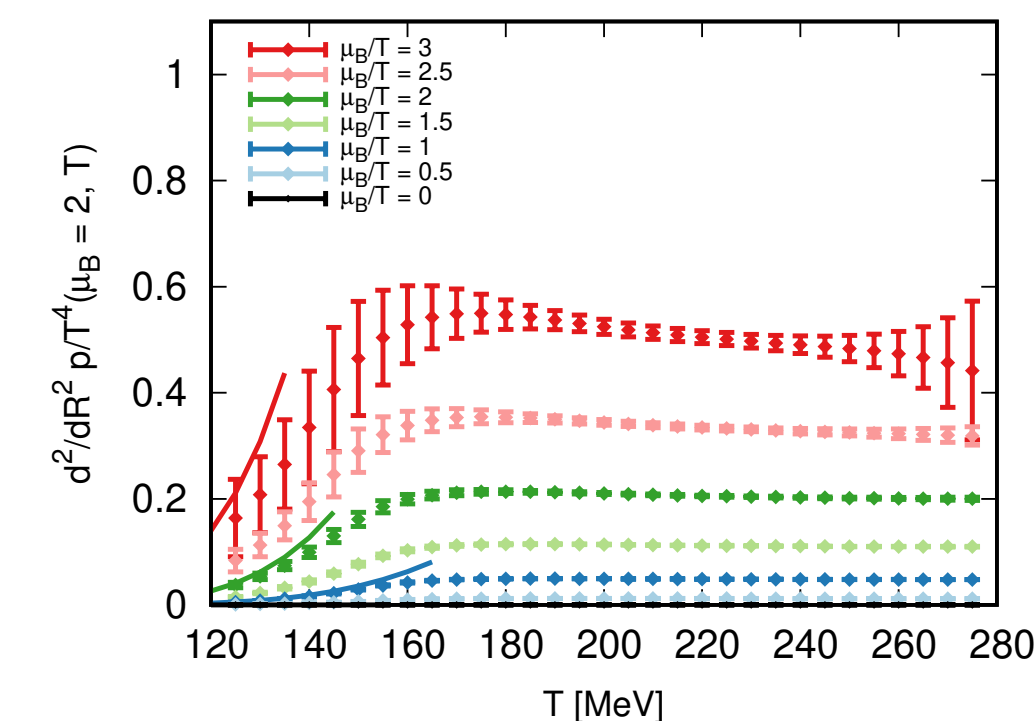
$$\frac{F(T, \hat{\mu}_B)}{FSB(\hat{\mu}_B)} = \frac{F(T_F, 0)}{FSB(0)}, \quad \text{with } T_F = T \left(1 + \kappa_2^F(T) \hat{\mu}_B^2 + \kappa_4^F(T) \hat{\mu}_B^4 + \dots \right)$$



- ▶ Scheme generalized to the case of non-zero μ_S (focusing on $n_S = 0$)
- ▶ Larger T dividing by Stefan-Boltzmann limit
- ▶ Up to $\mu_B/T \leq 3.5$, $T \in [130 - 280]$ MeV

- ▶ Relax $n_S = 0$: Extrapolate to small $R = n_S/n_B$
 - In HIC, only global strangeness neutrality guaranteed with large local charge fluctuations

... Jana N. Guenther, Thu 10:40



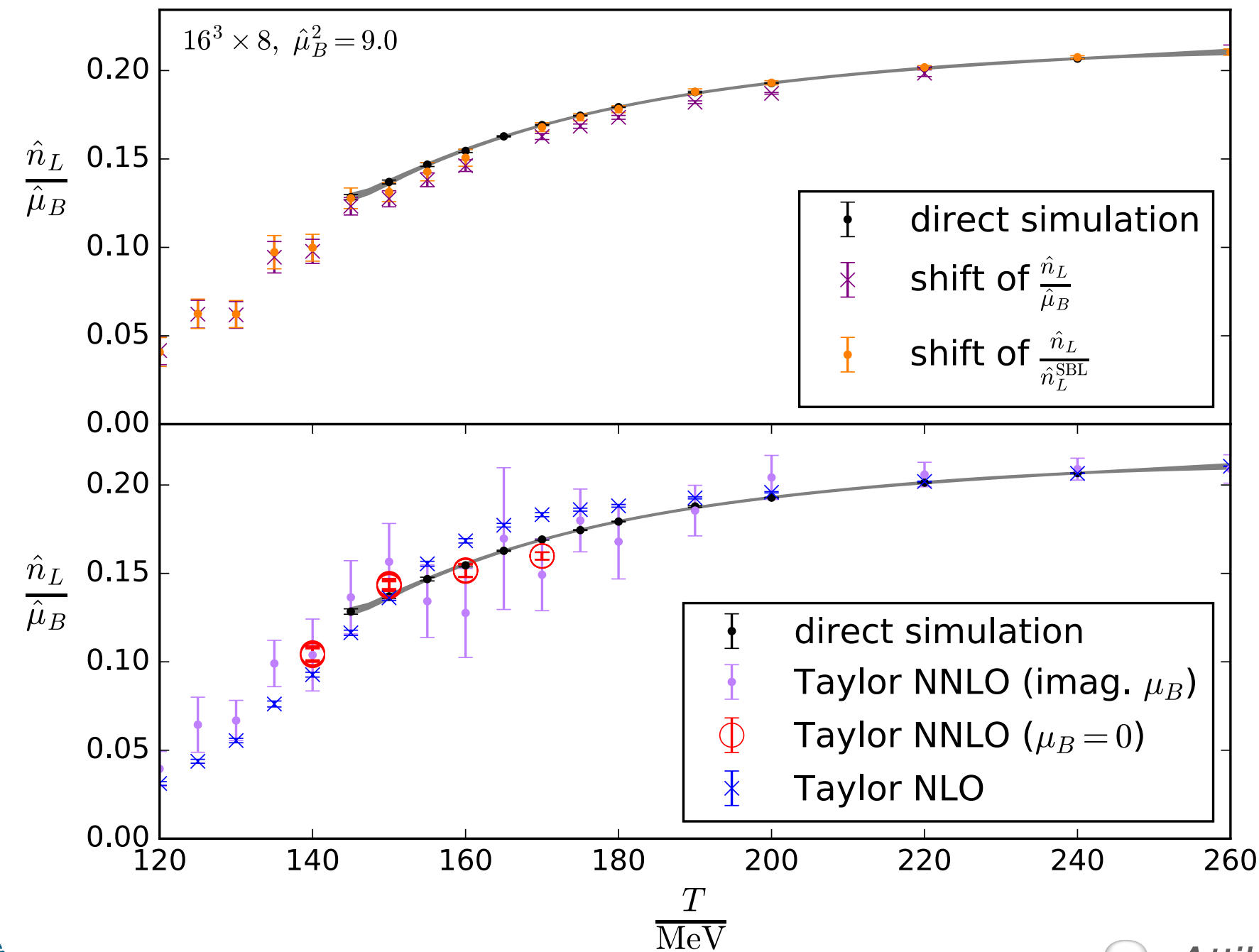
Equation of State (EoS)

Hot & dense QGP EoS: direct results vs. extrapolations

Direct reweighting [Giordano et al. '20 \(JHEP\)](#) [Borsanyi et al. '22 \(PRD\)](#)

2-stout-impr. staggered fermions, with $N_\tau = 8$ and at physical quark masses

- ▶ Results up to $\mu_B/T = 3$ in the QGP phase
- ▶ Comparison with results from different extrapolation procedures:
 - Taylor expansion around zero chemical potential,
 - some of its resummations [Borsanyi et al. '21 \(PRL\)](#)



- ▶ Tension with Taylor up to χ_4^B
- ▶ Large errors with Taylor up to χ_6^B
- ▶ Newer schemes for extrapolation perform better
- ▶ Superiority of direct method

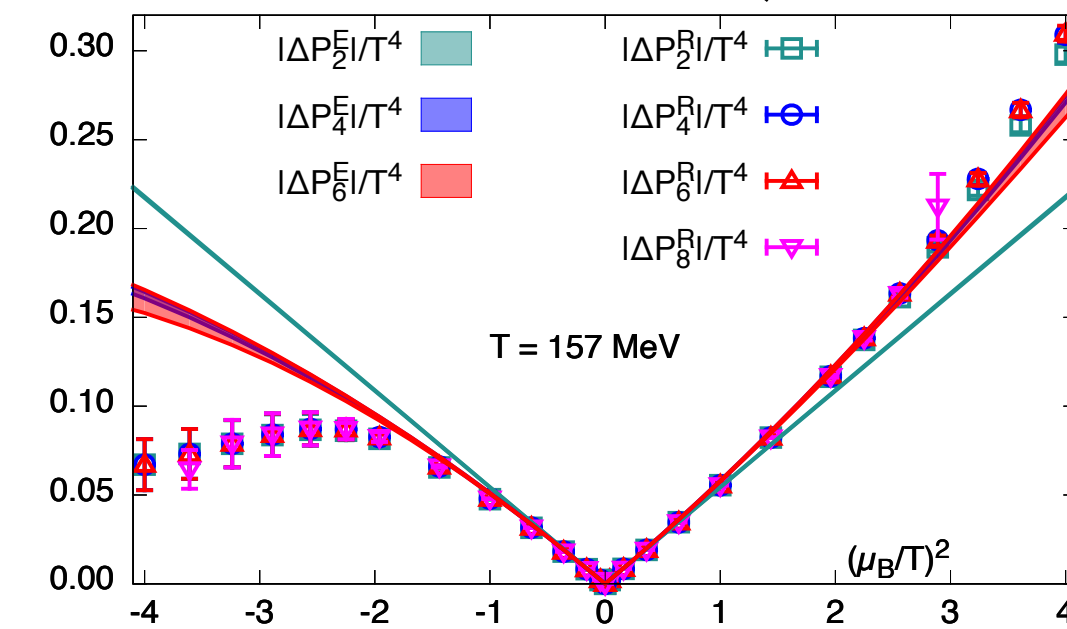
Attila Pasztor, Thu 10:20

Yet another way of extending the QCD EoS to larger μ_B/T

Resummation scheme for the Taylor expansion of the EoS in μ_B based on n -point correlation functions of the conserved (baryon) current D_n

$$\frac{\Delta P_N^E}{T^4} = \sum_{n=1}^N \frac{\chi_n^B}{n!} \left(\frac{\mu_B}{T} \right)^n \longleftrightarrow \frac{\Delta P_N^R}{T^4} = \frac{1}{T^3 V} \ln \left\langle \exp \left[\sum_{n=1}^N \frac{D_n}{n!} \left(\frac{\mu_B}{T} \right)^n \right] \right\rangle$$

resums contributions of the first N correlation function $D_1; \dots; D_N$ to the Taylor expansion of \mathcal{L}_{QCD} to all orders in μ_B

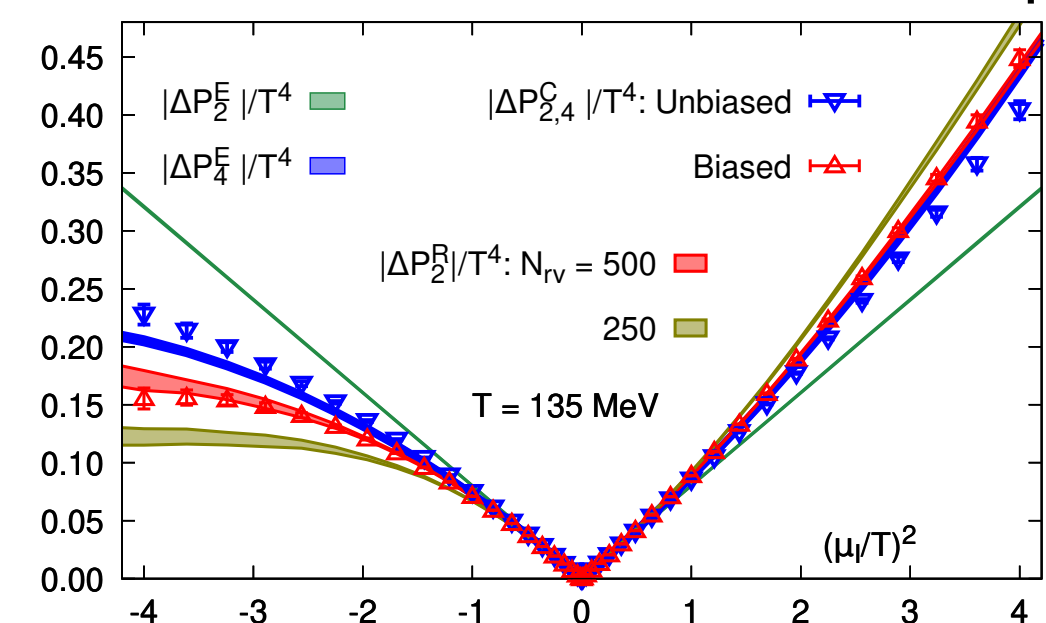


- ▶ Resummed \mathcal{L} , approximation to the reweighted \mathcal{L} at $\mu_B \neq 0$
- ▶ Improved convergence, breakdown reflects singularities of \mathcal{L} & severity of sign problem

[Mondal, Mukherjee, Hegde '22 \(PRL\)](#)

- ▶ D_n calculated stochastically \rightarrow bias in exp factor (esp. @large N, μ_B)

- Resum based on cumulant expansion [Mitra, Hegde, Schmidt '22](#)



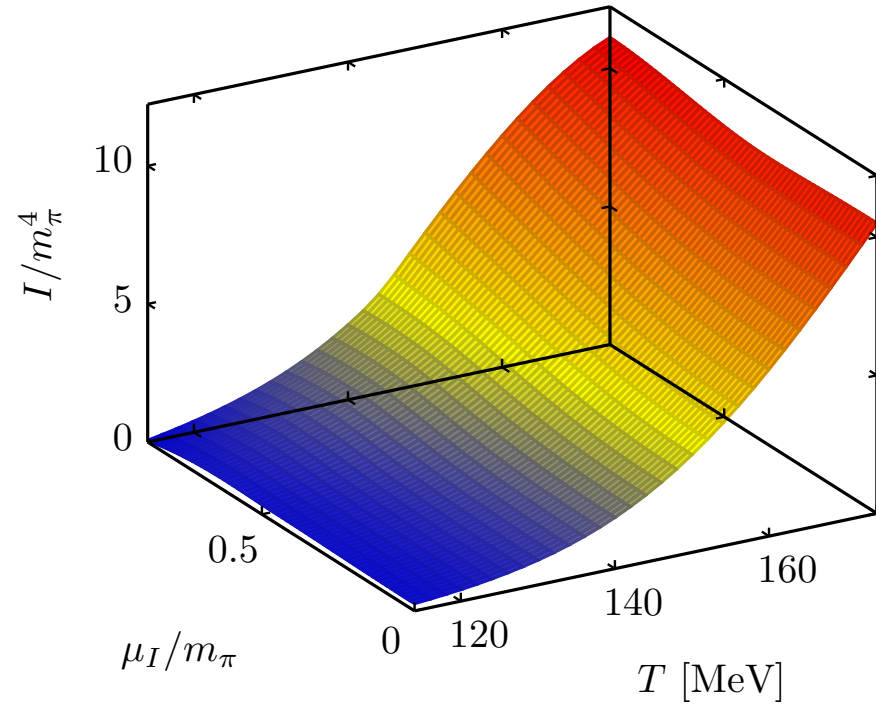
- Each term evaluated using unbiased powers of the operators
- Truncating at max order M , only finite unbiased products of D_n

Sabarnya Mitra, Thu 10:00

Equation of State (EoS) and speed of sound

Equation of state and Taylor expansions at $\mu_I \neq 0$

Brandt et al. '22 (PoS LAT21)



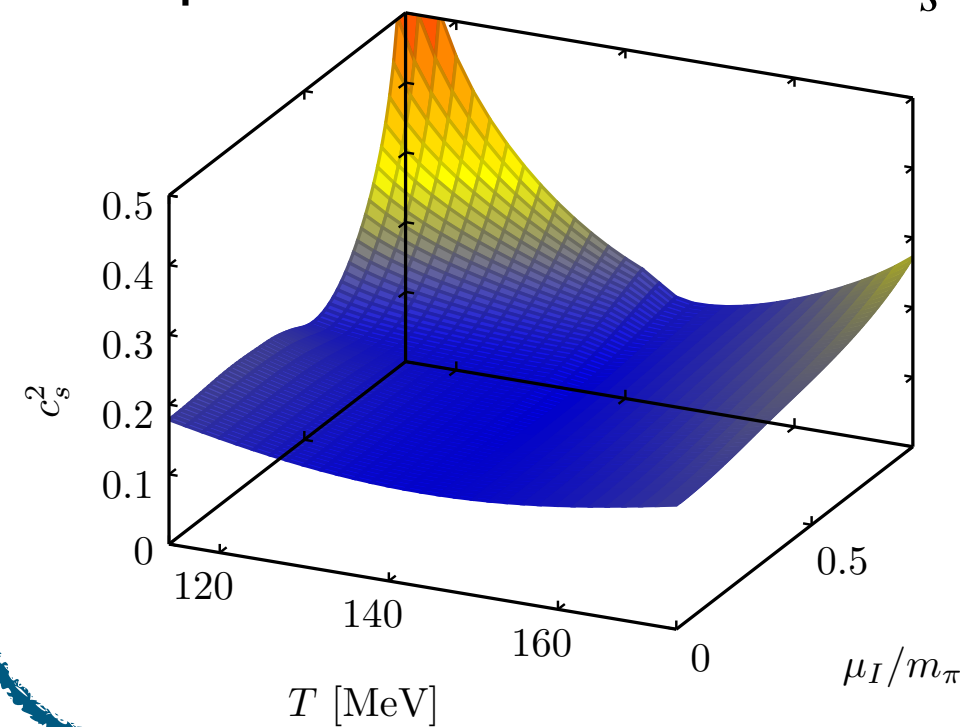
- QCD EoS at $\mu_I \neq 0$ and zero and non-zero T from simulations, with $N_f = 2 + 1$ improved staggered fermions at physical quark masses and $N_\tau \in \{8, 10, 12\}$
- First steps toward extending the EoS to small $\mu_B \neq 0$ via Taylor exp.

Speed of sound.

$$c_s^2 = \frac{\partial p}{\partial \epsilon} \bigg|_{\left[\frac{s}{n_I} = \text{const}; \frac{n_I}{n_L} = \text{const}; \dots \right]}$$

- Violation of holographic bound:
 $T \ll T_c \ \& \ \mu_I \gg m_\pi/2 \longrightarrow c_s^2 > 1/3$
implications for EoS modelling based on neutron star radii & masses

Bastian Brandt, Thu 09:00



Isothermal & isentropic c_s^2 in $N_f = 2 + 1$ QCD at nonzero μ_B

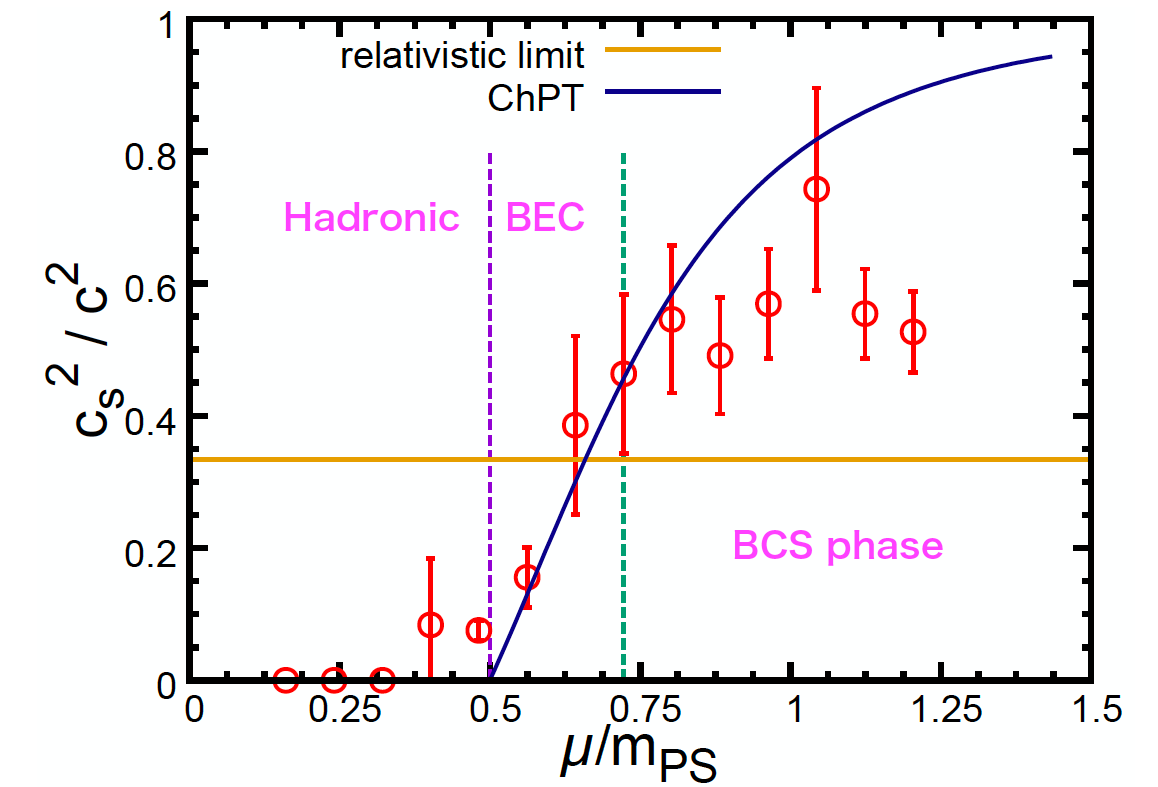
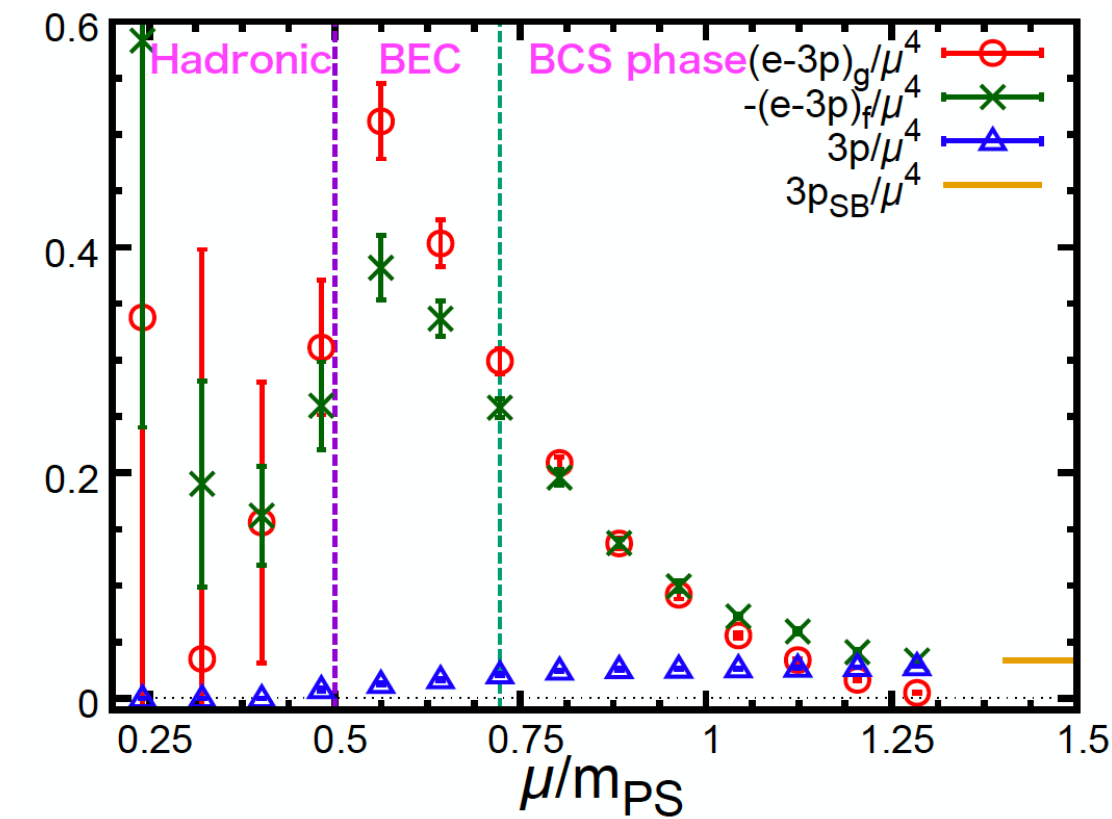
- c_T^2 and c_S^2 & comparison with HRG at low T & vanishing μ_S or n_S
- Imprint of chiral transition on c_T^2 and c_S^2 (sensitive a peak in specific heat, characteristic for critical behavior of 3d, $O(N)$ spin models) at low m_π

David Anthony Clarke, Thu 09:20

Dense 2-color QCD: Bump of sound velocity & hadron masses

Iida, Itou '22

- $p(\epsilon)$ and $\frac{c_s^2}{c^2} = \frac{\partial p}{\partial \epsilon}$ for 2-color QCD at low T and nonzero μ



Chiral Perturbation Theory (ChPT), $c_s^2/c^2 = \frac{1 - \mu_c^4/\mu^4}{1 + 3\mu_c^4/\mu^4}$

In BEC phase, our result is consistent with ChPT.
In high-density, it seems to peak around $\mu \approx m_{PS}$.

in the superfluid phase $c_s^2/c^2 > 1/3$

- Result consistent with results from effective models which have shown the bump of sound velocity.

Etsuko Itou, Thu 12:10

Kotaro Murakami, Thu 12:30

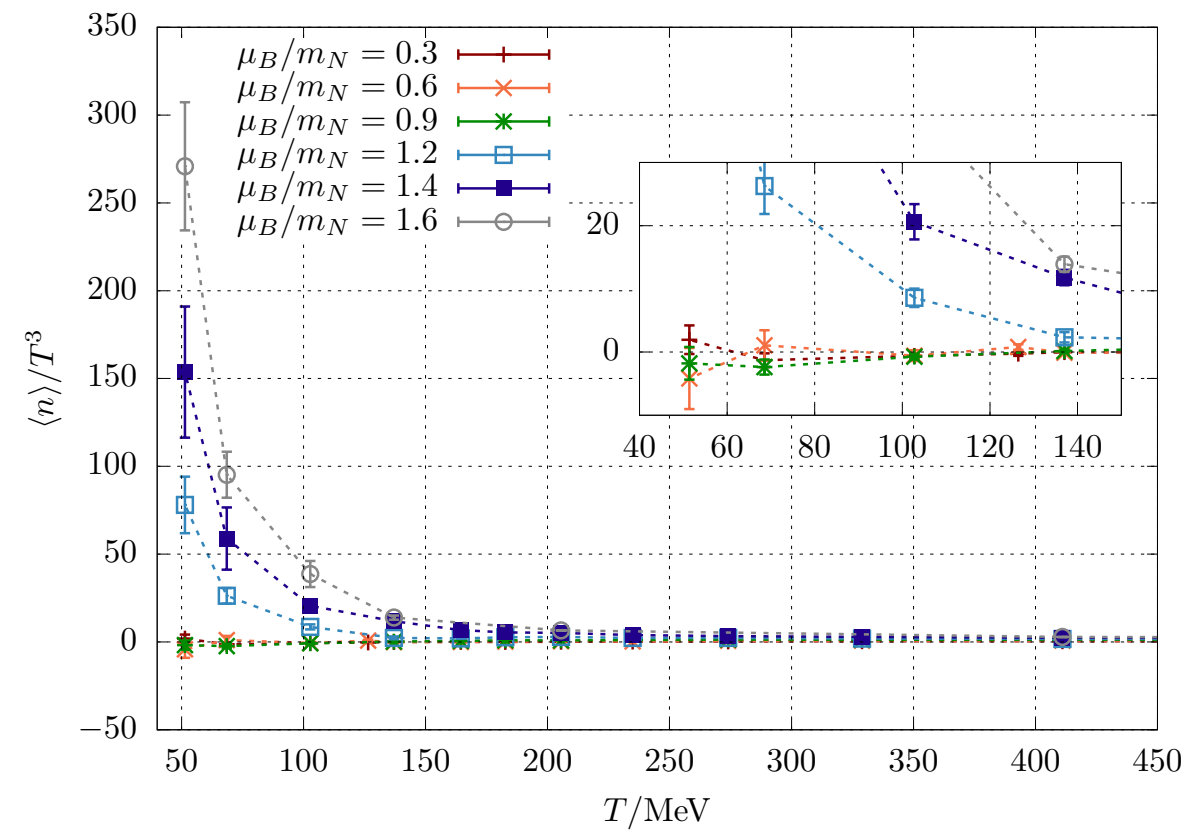
- Flipping of spectral ordering near the transition between the hadronic and superfluid phases of π and ρ meson masses masses ($N_f = 2$)
- 2-point functions for $I = 0$, $J^P = 0^\pm$ consistent with expected mixing (lin. σ model) of meson, diquark, antidiquark states due to $U(1)_B$ breaking in superfluid phase

Equation of State (EoS), EM conductivity and screening masses

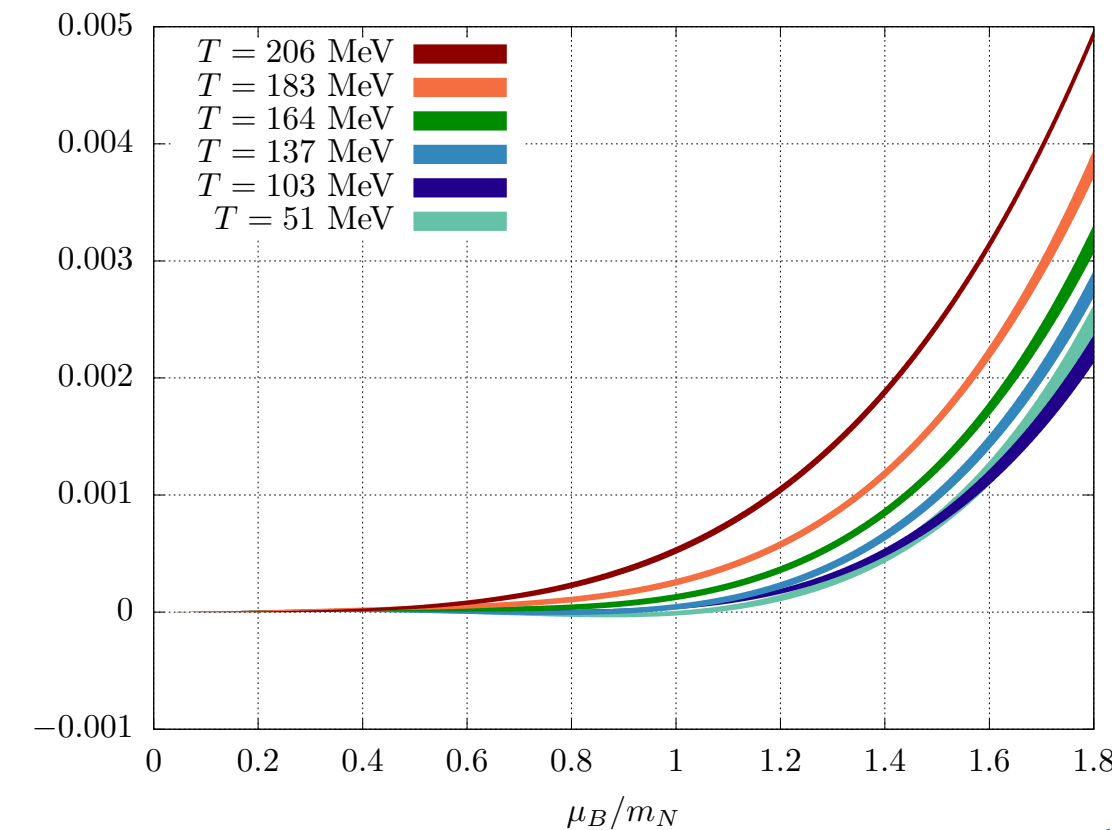
$N_f = 2$ QCD EoS via the complex Langevin method

[Attanasio, Jäger, Ziegler '22](#)

First step towards low T and physical pion mass, with $m_\pi \approx 480$ MeV



- ▶ Silver Blaze phenomenon: vanishing $\langle n \rangle / T^3$, at $T = 0$ for $\mu < m_N/3$



- ▶ Predictions for EoS at $n \sim 15n_0$
- ▶ EoS stiffer at low T : p grows slower
- ▶ Energy & entropy EoS measured

... Felix Ziegler, Thu 11:30

More on complex Langevin & contour deformations

- ▶ Boundary terms in Complex Langevin for full QCD: updates w.r.t. [Sexty et al. '22 \(PoS LAT21\)](#) ... Michael W. Hansen, Thu 11:50
- ▶ Alleviating sign problem in (2+1)d XY model at $\mu \neq 0$ on deformed integration manifolds [Giordano et al. '22](#) ... Zoltan Tulipant, Mon 18:10

QGP electromagnetic conductivity at $\mu_B \neq 0$

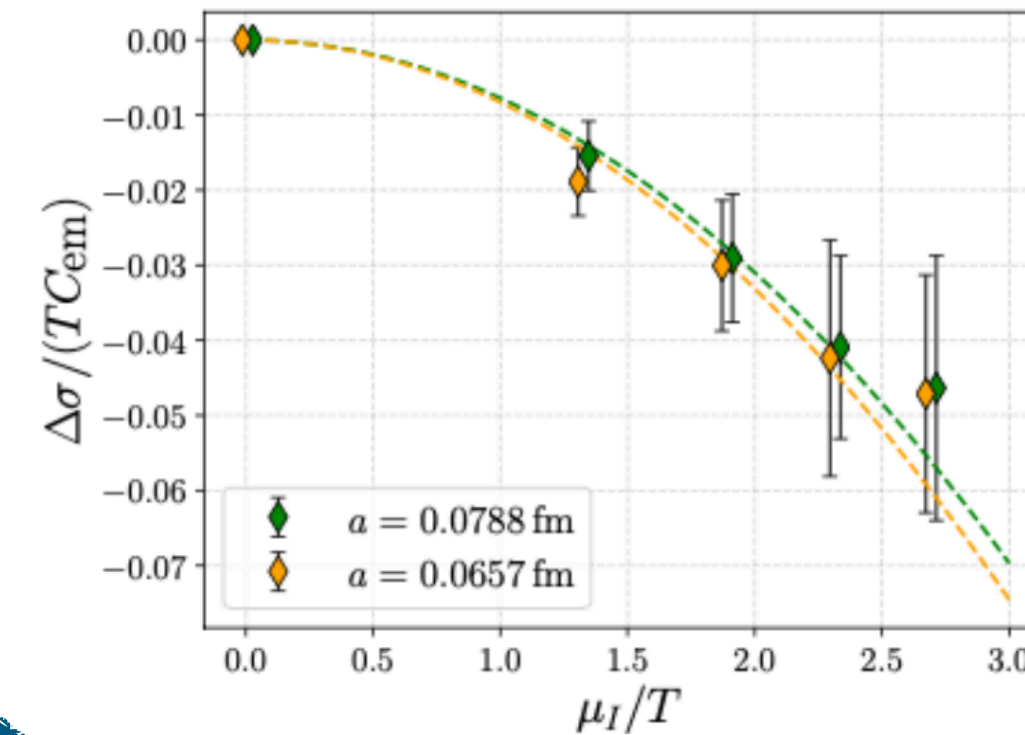
- ▶ $N_f = 2 + 1$ stout improved staggered at the physical point, at $\mu = i\mu_i$

$$C_{ij}^{e,o}(\tau) = \int_0^\infty \frac{d\omega}{\pi} \frac{\cosh[\omega(\tau - \beta/2)]}{\sinh[\omega\beta/2]} \rho_{ij}^{e,o}(\omega), \quad \frac{\sigma_{ij}}{T} = \frac{1}{2T} \lim_{\omega \rightarrow 0} \frac{\rho_{ij}^e(\omega) + \rho_{ij}^o(\omega)}{\omega}$$

- ▶ Conductivity from $J - J$ correlators with modified Backus-Gilbert method [Hansen, Lupo, Tantalo '19 \(PRD\)](#)

$$\frac{\Delta\sigma}{TC_{\text{em}}} = -c(T) \left(\frac{\mu_I}{T} \right)^2, \quad \text{with} \quad C_{\text{em}} = e^2 \sum_f q_f^2, \quad \text{and} \quad \Delta\sigma = \sigma_{\mu_I} - \sigma_{\mu_I=0}$$

well described by quadratic polynomial, analytically continued to real μ_B



- ▶ Electromagnetic conductivity of QGP grows rapidly with real μ_B

... Manuel Naviglio, Mon 15:20

Pseudoscalar meson screening mass at $T \neq 0$ and $\mu_B \neq 0$

[Bazavov et al. '19 \(PRD\)](#)

- ▶ By expanding the screening correlator in a Taylor series in μ_B
 - Results for the second derivative of the screening mass w.r.t. μ_B on $64^3 \times 8$ lattices generated using the $N_f = 2 + 1$ HISQ action

... Rishabh Thakkar, Mon 15:00

The cold and dense regime

Chirally inhomogeneous phases in low-energy models for QCD

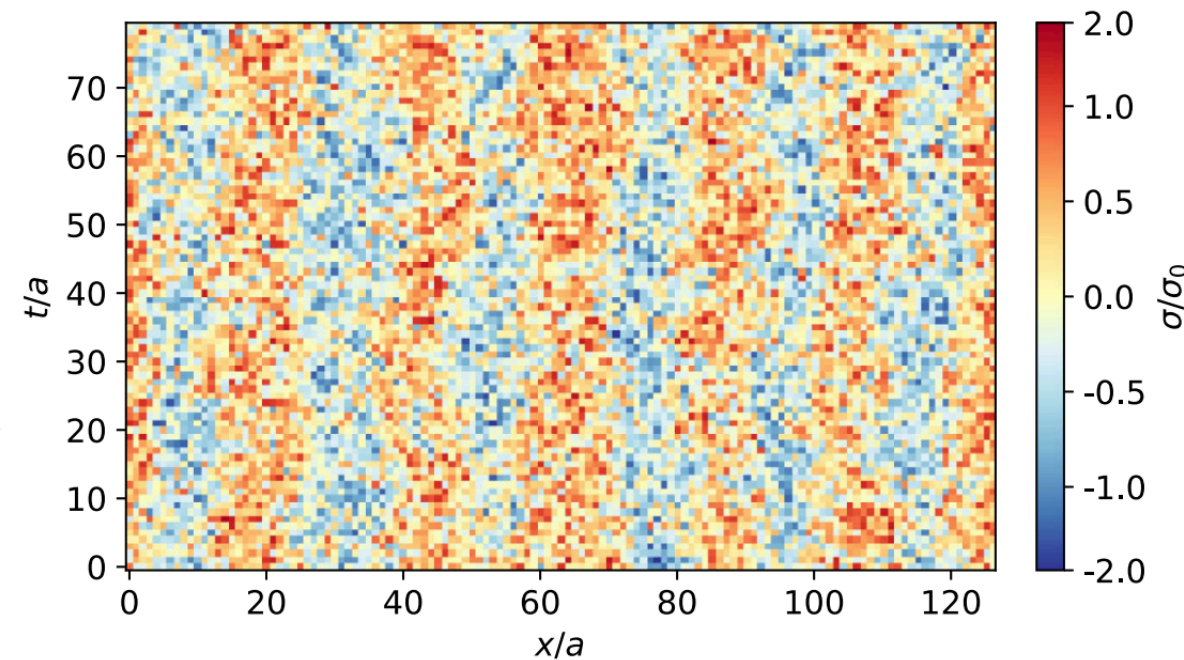
Four-Fermi theories modelling (some) chiral properties of QCD treated analytically by mean-field, or large-N expansions, numerically via MC

- ▶ From 1+3D Nambu-Jona-Lasinio model, prediction of chirally inhomogeneous phase (broken transl. symmetry) at low T & large μ_B

CAVEAT: Non-renormalizable \rightarrow Possible regularization scheme dependence

☞ Laurin Pannullo, Mon 17:50

- ▶ What about lower-d realisations of models with χ -symmetry (breaking)?



- **1+1D** \rightarrow no spontaneous symmetry breaking, quasi-long-range order

- Chiral crystals (consistent with BKT-like algebraically decaying correl. functions) at $N_f \in \{2, 8, 16\}$

☞ [Lenz et al. '20 \(PRD\)](#)

- **1+2D** inhomogeneities shown to be pure cutoff effects in Gross-Neveu model in MF and in a variety of Four-fermion and Yukawa models

☞ Marc Winstel, Tue 17:10

- Constant B -field brings inhomogeneities back?

☞ Michael Mandl, Mon 15:40

- Or quantum-spin liquid phases in all considered cases?

The cold & dense regime from strong coupling

- ▶ Hamiltonian lattice QCD with staggered fermions from continuous time limit of strong coupling lattice QCD based on the dual representation that is obtained when integrating out the gauge links first

- Formalism extended to $N_f = 2$ and, after a resummation, there is no sign problem both for $\mu_B \neq 0$ and for $\mu_I \neq 0$
- progress on implementation of the Quantum Monte Carlo simulations
- Computed baryon and isospin densities in the chiral limit
- Looked at quark mass dependence of baryon mass & nuclear transition

☞ Pratitee Pattanaik, Mon 16:50, ☞ Wolfgang Unger, Mon 17:10

The cold & dense regime from Polyakov loop effective theories

- ▶ For the strong coupling and heavy quark mass regime of QCD
- New set of effective couplings whose T dependence worked out via a method to map correlators of Polyakov loops in the effective theory (high-order expressions using finite-cluster method) to those in full QCD
- Mean-field approximations employed to determine the critical endpoint of the deconfinement transition and the phase diagram at non-zero baryon and iso-spin chemical potential

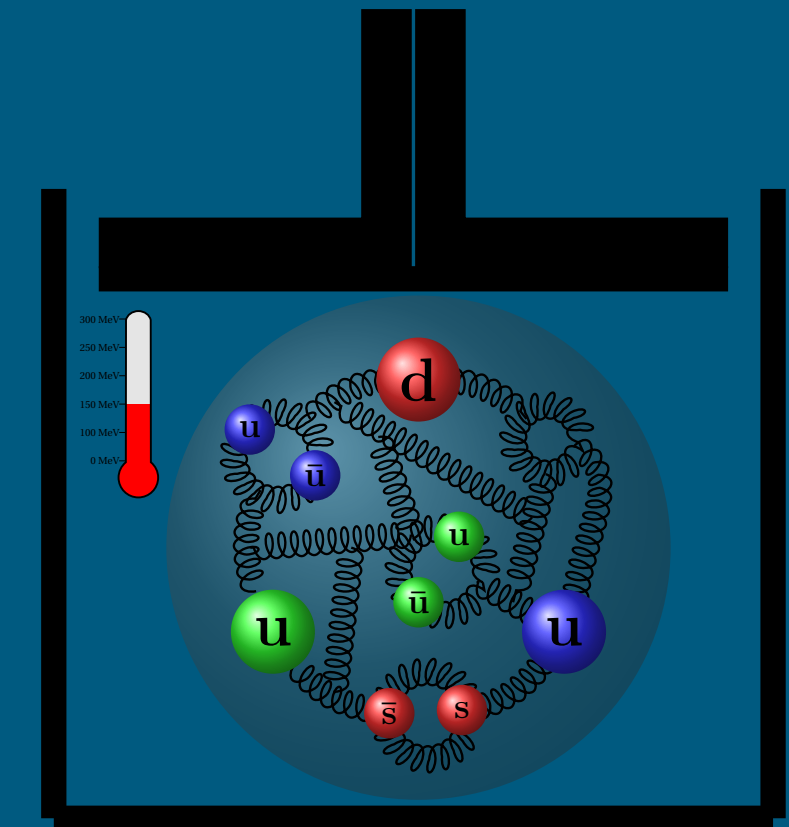
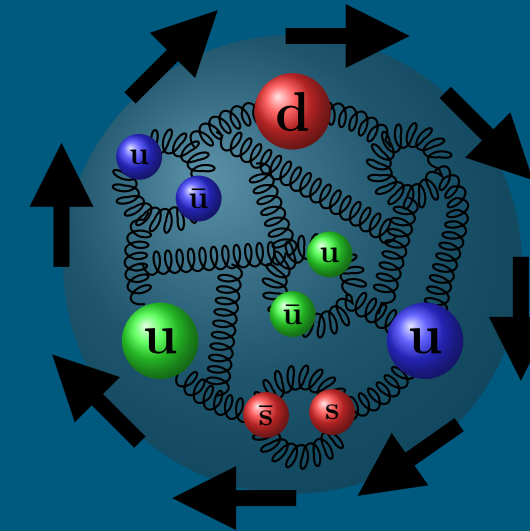
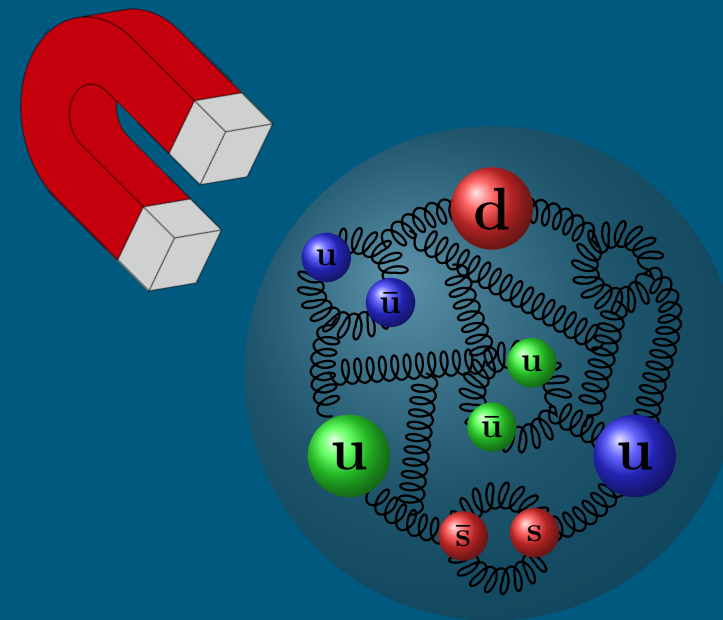
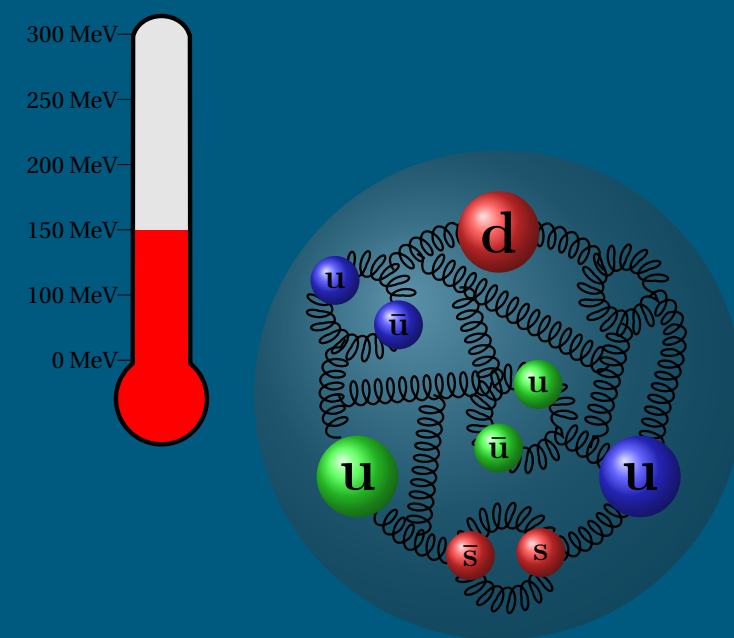
☞ Christopher Winterowd, Fri 17:40

☞ Amine Chabane, Mon 17:30, ☞ Christoph Konrad, Fri 18:00

Thank you for your attention!

Please, drop by at the 55 talks (!!)

In the 'Non-zero Temperature' & 'Non-zero Density' parallel sessions!



A special thank you to those who wrote to me with their results!
[Sorba, Lenz, Laudicina, Günther, Jäger, Bietenholz, Itou, Aarts]